



**Politecnico
di Torino**

Politecnico di Torino

DIPARTIMENTO DI INGEGNERIA MECCANICA E AEROSPAZIALE
Laurea Magistrale in Ingegneria Biomedica

**Design of a passive upper limb exoskeleton with deformable
pneumatic actuators**

Candidato:
Alessia Pizzichillo

Relatore:
Prof. Carlo Ferraresi

Correlatore:
Prof. Carlo De Benedictis
Ph.D Maria Paterna

*Per chi non ha mai mollato, perchè no, anche per chi ha mollato. A voi tutti dedico
questo traguardo!*

Abstract

The shoulder complex is one of the most complex parts of the human body, consisting of four joints: the glenohumeral, sternoclavicular, acromioclavicular and scapulothoracic joints. The glenohumeral joint is commonly referred to as the shoulder joint. When the upper limb is lifted, the contraction of the muscles of the shoulder complex must balance the gravitational torque of the arm segments. Keeping the arm elevated for long periods requires constant work from the muscles, and in the long run can cause excessive stress on the muscles themselves and the surrounding tissues, and can lead to the risk of developing musculoskeletal disorders. This is what happens in an industrial environment where users doing overhead work spend most of their time with their arms in an elevated position, also supporting a load, and thus further increasing the moment generated and thus requiring more force from the muscles.

Thus, to reduce the effort on the shoulder complex muscles, a support device is needed as a wearable device that interacts with the human. Therefore, this thesis aims to present a passive upper limb exoskeleton for the compensation of the gravitational torque during arm lifting, working on a McKibben pneumatic artificial muscle (PAM) as a passive actuator, which, once pressurised, can exert a high force-to-weight ratio by contraction. In the first section, the situation of musculoskeletal disorders is reviewed, followed by an excursus on exoskeletons and their requirements. Then, artificial pneumatic muscles are presented in detail, with the isotonic and isometric characterisation of two FESTO artificial pneumatic muscles. The torque generated by the PAM and that due to gravity are calculated and compared for different values of the angle of elevation of the upper arm, to assess the support provided by the muscles to the user. Next, the design of the exoskeleton in all its components is presented by developing a CAD model and performing the corresponding finite element simulations, choosing materials to make the exoskeleton as light as possible and estimating the total weight of the structure. By analysing the results of the simulations, the prototype will be built.

Contents

1	Musculosekeletal Disorders	8
1.1	The size of the problem	8
1.2	The causes of Musculoskeletal Disorders	11
1.3	Overhead work	14
1.3.1	Task design	15
1.3.2	Fatigue accumulation	16
1.3.3	Bone movement	17
1.3.4	Muscle capacity	18
1.4	The way of prevention	19
2	An innovative solution: exoskeleton	21
2.1	History of exoskeletons	22
2.2	Exoskeletons classification	25
2.2.1	Active exoskeletons	25
2.2.2	Passive exoskeletons	29
2.3	The shoulder complex	31
2.3.1	Shoulder center rotation	34
2.4	Exoskeleton requirements	38
3	Artificial Pneumatic Muscle	41
3.1	The story of the PAM	42
3.1.1	McKibben Muscle and its variants	44
3.2	FESTO actuator	49
4	Original idea of exoskeleton	51
4.1	The cam profile	52

CONTENTS 2

4.2 Project features 53

4.3 PAM characterization 62

 4.3.1 Isometric characterisation 63

 4.3.2 Isotonic characteristic 65

 4.3.3 FESTO DMSP-10 -100N of 350 mm 69

5 Exo design 73

 5.1 Exoskeleton arm 76

 5.2 The back frame 84

6 Simulations and discussion 95

 6.1 Results 100

7 Conclusions and future development 109

Bibliografia 111

List of Figures

1.1	Example of MSDs	8
1.2	Percentage of Musculoskeletal regions affected with musculoskeletal disorders in the Ha'il Region of Saudi Arabia. [4]	9
1.3	Comparison construction with other industries.	10
1.4	Risk factors of MSDs.	11
1.5	The three primary risk factors of MSDs.	13
1.6	The most common symptoms of MSDs	14
1.7	Example of overhead work	15
1.8	Anatomical components of the shoulder.	17
1.9	a) Reduction of subacromial space during humeral elevation b) Angle elevation exceed 90 degree, impingement occurs.	18
2.1	Hardiman exoskeleton.	23
2.2	pHRI exoskeleton.	24
2.3	HAL exoskeleton.	24
2.4	Example of electric actuator and its components.	26
2.5	Example of Pneumatic cylinder and its components.	28
2.6	Example of Pneumatic artificial muscle.	28
2.7	Example of electro-hydraulic actuator and its components.	29
2.8	a) The human upper limb composition. [46] b) Anatomy of the shoulder complex. [47]	32
2.9	DOF of the upper limb	33

2.10	Diagrams of the glenohumeral (GH) joint motion information during humeral raising and lowering movements of five cycles in the sagittal plane: (a) X-direction of the GH joint displacement variable quantity, (b) Y-direction of the GH joint displacement variable quantity, and (c) Z-direction of the GH joint center displacementa. [47]	36
2.11	Diagrams of the glenohumeral (GH) joint motion information during humeral raising and lowering movements of five cycles in the coronal plane: (a) X-direction of the GH joint displacement variable quantity, (b) Y-direction of the GH joint displacement variable quantity, and (c) Z-direction of the GH joint center displacementa. [47]	37
3.1	Biorobotic applications of PAMs. [53]	43
3.2	Medical applications of PAMs. [53]	43
3.3	Types of conventional PAMs:(a) McKibben Muscle/Braided Muscle; (b) Pleated Muscle; (c) PAM reinforced by Kevlar Fiber; (d) Yarlott Netted Muscle; (e) Paynter Hyperboloid Muscle; (f) ROMAC Muscle. [53]	44
3.4	Diagram for structure of a McKibben muscle	45
3.5	(a) Diagram for structure of a multifilament McKibben muscle; (b) with thin muscles arranged in parallel (top) and with thin muscles intertwined.(bottom) [57]	46
3.6	a) Actuator pleated b) Yarlott actuator c) RoMaC actuator c)a)standard version, c) b)miniature version. [53]	48
3.7	Example of a Fluidic Muscle DMSP elongated, at nominal length and contracted and its characteristic at the pressure of 5.5 bar. [60]	50
4.1	Simplified scheme of the shoulder pad, on the left with the upper arm at the elevation angle of 90 degree, on the right instead, 135 degrees.	53
4.2	Shoulder pad CAD model	54
4.3	Continuous camma profile from graphic method.	55
4.4	Development of radius as a function of elevation angle.	56
4.5	PAM shortening for increasing angle values for 30mm FESTO DMSP. The muscle contracts by 1.7%, 6.3%, 11% and 17.4% respectively for theta values of 90, 105, 120 and 135 degrees.	57

4.6	PAM shortening for increasing angle values for 35mm FESTO DMSP. The muscle contracts by 1.7%, 5.7%, 9.7% and 15.1% respectively for theta values of 90, 105, 120 and 135 degrees.	58
4.7	Comparison between gravitational torque and PAM torque for muscle length 30mm.	60
4.8	Comparison between gravitational torque and PAM torque for muscle length 35mm.	61
4.9	Test bench: configuration of isometric test.	64
4.10	Force evolution as a function of pressure for different contraction values. . .	65
4.11	Trend of the pressure as a function of the contraction for different force values with an obvious hysteresis for a low load.	66
4.12	Trend of force as a function of contraction for different pressure values. . .	67
4.13	Comparison between gravitational torque and PAM torque experimentally obtained for muscle length 30mm.	68
4.14	Isotonic characteristic of the muscle.	69
4.15	Trend of force as a function of contraction for different pressure values. . .	70
4.16	Trend of force as a function of contraction for different pressure values. . .	71
5.1	PORTWEST 2 POINT-COMFORT HARNESS a)Frontal view b)Back view	74
5.2	The exoskeleton composed of arm and back frame.	75
5.3	A frontal view of exoskeleton arm.	76
5.4	Rigid strut that runs along the outside of the arm, from the elbow (excluded) to the user's shoulder.	77
5.5	The C bracelet placed at the beginning of the strut through two M4 countersunk screws.	77
5.6	Interior view of strut and bracelet.	78
5.7	PLA filling that defines the arm range of movement at the end of the struct. .	79
5.8	Exploded view of the joint that represents the first degree of freedom. . .	79
5.9	Rounded L-shaped plates with the hing that allows the first arm degree of freedom.	80
5.10	Alluminium filler a) frontal view b) with the M10 pin.	81
5.11	Description of the second joint	82
5.12	Mechanism that allows the two degrees of freedom.	82

5.13	a) Back view and b)frontal view of the cam.	83
5.14	Angular joint that connects the arm to the back frame	83
5.15	Square tubo with square bars, top view	84
5.16	Square tubo with square bars, frotal view	84
5.17	Connection between the back frame and the arm of exo.	85
5.18	Components of the exoskeleton back frame.	86
5.19	Connection between the square tube and the rectangular bar and the C plate for supporting PAMs.	88
5.20	Spherical joint attached to the orizzontal rectangular bar.	89
5.21	Threaded terminal inside telescopic rods.	89
5.22	C-shaped plate where PAM are fixed.	90
5.23	Self-locking pin to block the position of telescopic rods.	90
5.24	U-shaped supports fixed to the inferior rectangular bar where pulleys are attached, with two slots for velcro.	91
5.25	Completed new version of exo with one arm.	92
6.1	Diagram of the forces applied on the back frame reported on the righth side.	96
6.2	Exoskeleton back frame with loads and costraints applied.	98
6.3	Diagram of the forces applied on the exo arm.	99
6.4	Exoskeleton arm with loads and costraints applied.	100
6.5	Von Mises stresses distribution on the washer.	101
6.6	Von Mises stresses distribution on the steel rod.	102
6.7	Visualizzazione of maximum and minimum displacement of the exo arm.	103
6.8	Maximum frame tension at washers M4.	104
6.9	Zoom of the previous picture on the critical region.	105
6.10	Maximum force at the washers M5	105
6.11	Maximum negative displacement on the extremity of the square rod.	106
6.12	Total view of back frame displacement.	107
6.13	Comparison with muscular torque considering the dadditional shortening.	108

List of Tables

- 4.1 Coefficients from theoretical curves of FESTO 10-100N 30mm length. . . . 61
- 4.2 Average percentage errors between gravitational and muscle torque 62
- 4.3 Coefficients from eq. (4.17) for Festo DMSP-10-100N static characteristics 68
- 4.4 Coefficients from eq. (4.17) for Festo DMSP-10-100N of length 350mm
static characteristics 70

- 5.1 Components with square or rectangular section. 93
- 5.2 Components with circular section. 93
- 5.3 Information about commercial components. 94

Chapter 1

Musculoskeletal Disorders

1.1 The size of the problem

According to the World Health Organization [1], a Musculoskeletal Disorder (MSD) is a condition affecting the muscles, tendons, peripheral nerves, or vascular system and it does not result directly from a sudden or acute event such as slips or falls.

These disorders are believed to be work-related when job performance and the work environment contribute significantly to their development, although they are only one of many factors that cause the multifactorial disease. [1]

Repetitive Stress Injury, Repetitive Motion Injury, and Overuse Injury are just a few of the other terms used to describe MSDs. Despite the variations in terminology, Musculoskeletal Disorder indicates repetition and stress as the primary causes of the damage. [2]

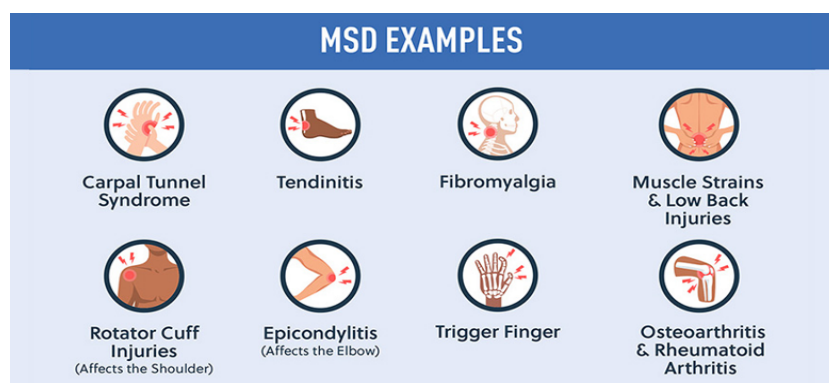


Figure 1.1: Example of MSDs

<https://www.neumannbros.com/>

[national-safety-month-ergonomics-and-musculoskeletal-disorders/](#)

In 1997, the National Institute for Occupational Safety and Health (NIOSH), a part of the Centers for Disease Control and Prevention (CDC), released a review of evidence on work-related MSDs.

Routine lifting of heavy objects, regular exposure to whole-body vibration, performing repetitive forceful tasks, overhead work, neck flexion, are some work conditions that may lead to MSDs. The report showed a positive correlation between work conditions and MSDs of the neck, shoulder, elbow, hand and wrist, and back. [3]

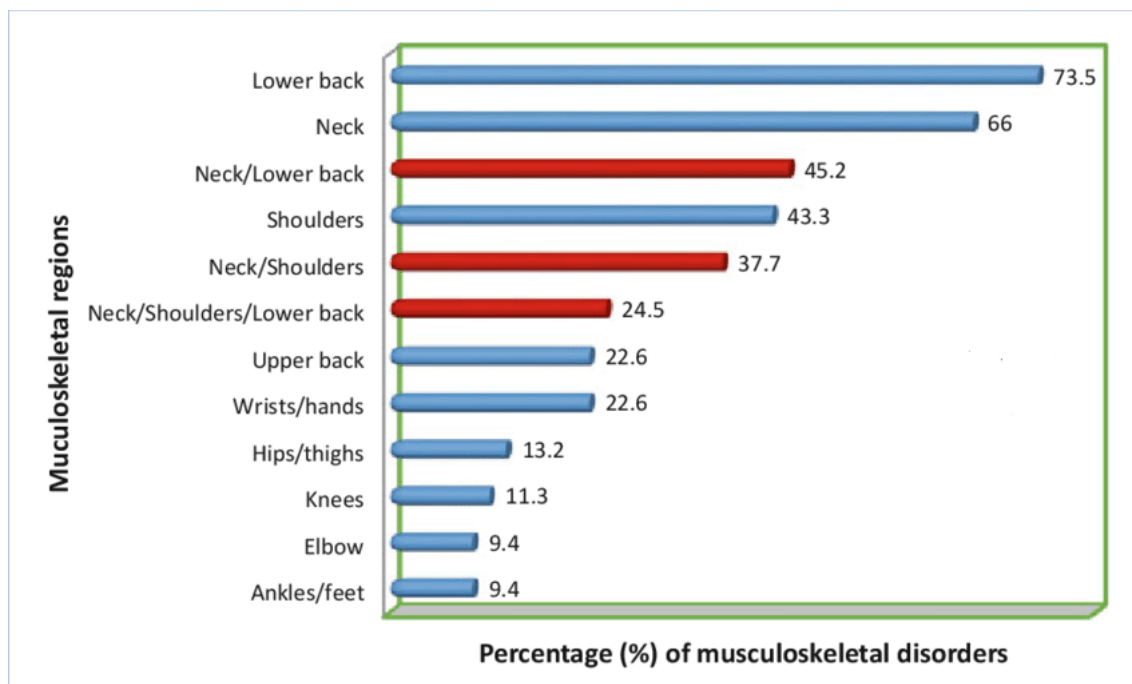


Figure 1.2: Percentage of Musculoskeletal regions affected with musculoskeletal disorders in the Ha'il Region of Saudi Arabia. [4]

As shown in the Figure 1.2, the most affected body regions are lower back, neck and shoulders, suggesting that musculoskeletal disorders are largely due to overloading of the spinal regions.

Neck pain may be mainly due to prolonged static loading from sustained muscle activity in the sternocleidomastoid or trapezius muscles. The origin of the high prevalence of shoulder pain, on the other hand, may be due to overloading of the shoulders during prolonged periods of arm elevation and forward bending in sitting or standing. [4]

Absenteeism, lost productivity, increased health care costs, disability, and workers' compensation result in high costs for employers. [5]

MSDs cases are more severe than the average nonfatal injury or illness:

- In 2001, an average number of days lost to work was calculated, comparing MSDs with all cases of nonfatal accidents and injuries: eight day for MSDs compared to six for others; [5]
- The construction and agriculture industry sectors together accounted for about half of all MSD cases; [5]
- Musculoskeletal disorders account for nearly 70 million physician office visits in the United States annually, and an estimated 130 million total health care encounters including outpatient, hospital, and emergency room visits. [6]
- In 1999, nearly 1 million people absent from work to treat and recover from work-related musculoskeletal pain or impairment of function in the low back or upper extremities. [6]

Musculoskeletal disorders

Construction compared to industries with similar work activities (rate per 100,000 workers)

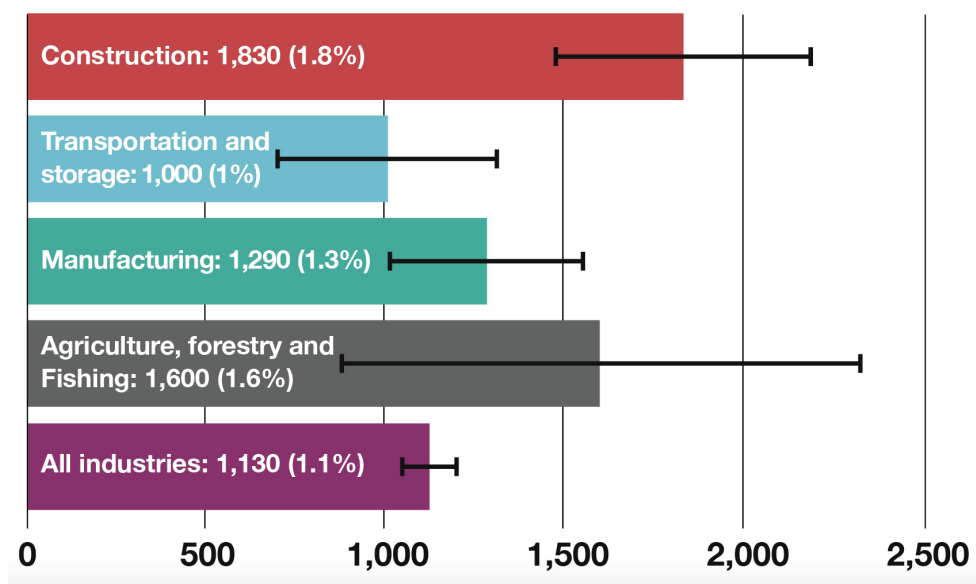


Figure 1.3: Comparison construction with other industries.

<https://projectsafetyjournal.com/>

[musculoskeletal-disorders-top-ill-health-issues-in-construction/](#)

The largest workers' compensation insurance provider in the United States, Liberty Mutual, affirms overexertion injuries as lifting, pushing, pulling, holding, carrying or throwing an object, cost employers 13.4 billion every year.[6]

1.2 The causes of Musculoskeletal Disorders

MSD primary causes are attributed to the exposure of individuals to risk factors that exceed their body's ability to recover, leading to musculoskeletal imbalance and eventually a disorder development.

These risk factors often work in combination and include three main categories: physical and biomechanical, organizational and psychosocial, and individual factors. [7]

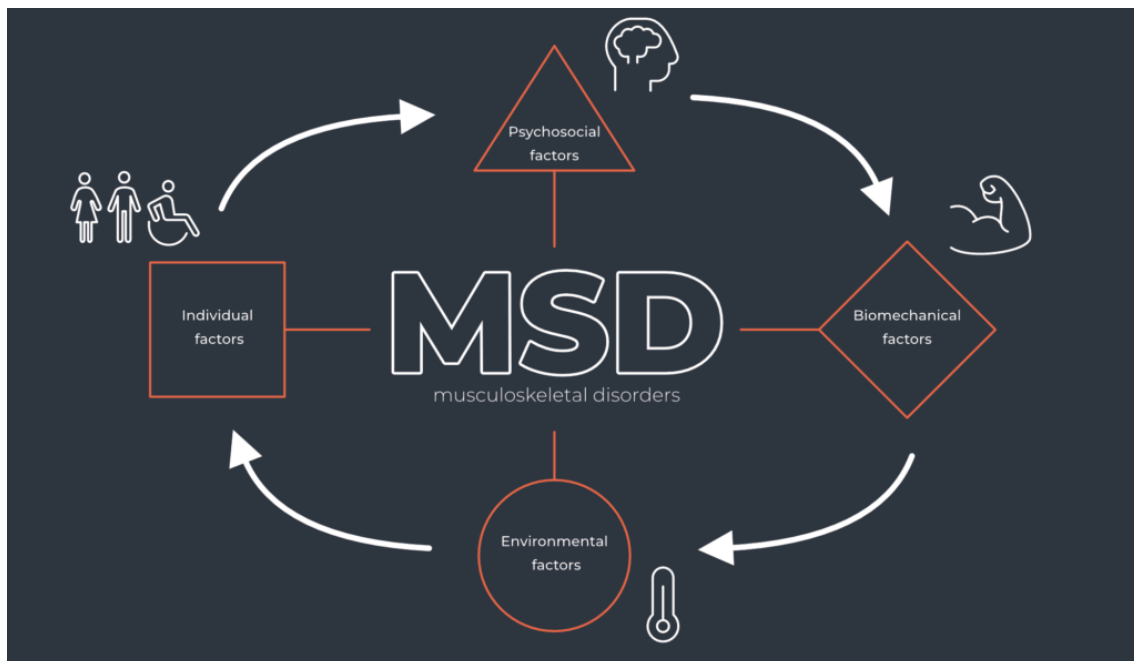


Figure 1.4: Risk factors of MSDs.

<https://nawo-solution.com/the-musculoskeletal-disorders-msd/>

Physical and biomechanical risk factors may include [7]:

- Handling loads, especially when bending and twisting;
- Repetitive or forceful movements;
- Awkward and static postures;

- Vibration, poor lighting or cold working environments;
- Fast-paced work;
- Prolonged sitting or standing in the same position.

It is well known that uncomfortable postures can be harmful. These impose excessive force on joints and tend to overload muscles and tendons.

The efficiency of the joint depends mainly on its closest middle range of motion. When these are made to work repeatedly outside the middle range without providing adequate recovery time, the risk of MSD increases.

Workers exposed to such strains, repetitive tasks and prolonged awkward postures become fatigued and the body is unable to recover. The resulting musculoskeletal imbalance ultimately leads to MSDs. [2]

Organisational and psychosocial risk factors can be: [7]

- Low autonomy and high work demand;
- Lack of breaks or opportunities to change working postures;
- Working at high speed, including as a consequence of introducing new technologies;
- Working long hours or on shifts.

In general, all psychosocial and organizational factors, when combined especially with physical hazards, can lead to stress, fatigue, anxiety or other reactions, which in turn enhance the risk of MSDs. [7]

Individual risk factors may involve: [7]

- Prior medical history;
- Physical capacity;
- Lifestyle and habits as smoking and lack of exercise.



Figure 1.5: The three primary risk factors of MSDs.

<https://www.pshsa.ca/training/free-training/>

5-steps-musculoskeletal-disorder-msd-prevention

As shown in Figure 1.5, work-related risk factors could be divided into three principals areas: [8]

1. High task repetition;
2. Forceful exertions;
3. Awkward postures.

These are considered as primary causes of MSDs.

On the other hand, analysing symptoms of MSDs, the most common are: [2]

- Weakness, stiffness and pain – all of them often persistent;
- Decreased range of motion – limiting mobility, dexterity and functional abilities;
- Noises in the joints – joint deformity may be visualised where early diagnosis and treatment are not available;
- Inflammation – in addiction to pain and impaired function, there is redness, swelling and warmth in the overlying skin area.



Figure 1.6: The most common symptoms of MSDs

<https://www.neumannbros.com/>

[national-safety-month-ergonomics-and-musculoskeletal-disorders/](https://www.neumannbros.com/national-safety-month-ergonomics-and-musculoskeletal-disorders/)

Therefore MSDs can affect joints, spine, muscles and bones developing a large number of pathologies such as osteoarthritis, psoriatic arthritis, gout, rheumatoid arthritis, ankylosing spondylitis for joints, an intense back and neck pain, sarcopenia for muscles and osteoporosis, fragility fractures, traumatic fractures for bones. [8]

1.3 Overhead work

Overhead work is classified as working with the hands above shoulder height.

This type of work is strongly correlated with the development of shoulder injury and pain; jobs requiring arm elevation of 90 degrees or more, for more than ten percent of the shift, can double the risk of developing a shoulder injury [9]. In addition, advancing age and increased exposure to elevated work for long periods of life are strongly correlated with increased risk of shoulder lesion. [10]

Throughout the scientific literature, overhead work is associated with numerous negative side effects, including increased intramuscular pressure, impaired circulation, increased muscle activity, and development of fatigue. [11]

Workplaces have attempted to ergonomically improve and avoid exposure to elevated work. However, where it is strictly necessary, careful job design and evaluation can help reduce the risk of associated MSD. [12]

Four main factors [9] have been proposed that may increase or decrease the risk of MSD during overhead work, and consequently influence the risk of injury. These include: [8]

1. Task design;

2. Fatigue accumulation;
3. Bone movement;
4. Muscle capacity.

1.3.1 Task design

When performing overhead work, six factors cause changes in the demands on the muscles surrounding the shoulder:[8]

1. Direction of the force applied to the hand;
2. Vertical extension distance;
3. Horizontal extension distance;
4. Amount of arm elevation;
5. Amount of force applied to the hand;
6. Accuracy required to complete the task.

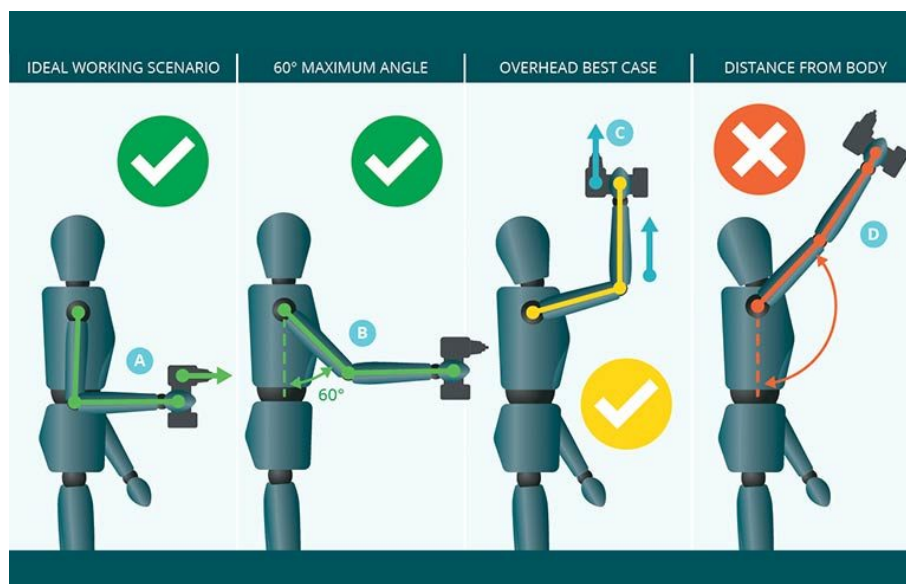


Figure 1.7: Example of overhead work

<https://www.safetyandhealthmagazine.com/articles/>

21184-reducing-the-risk-of-msds-from-overhead-work-new-resources

Of all six factors, the direction of force applied to the hand is the most influential factor in reducing the risk of injury during overhead work. The application of forces in line with gravity, in a vertical and downward direction, results in the least muscular effort. The maximum force that can be produced is also greater in this same vertical and downward direction, in fact you are stronger in the latter. [13]

Therefore, changing the direction of force applied to the hand can be used as a method to reduce the risk of injury when overhead tasks must be performed. Also, decreasing any of the above factors in combination with the direction of force applied to the hand would reduce the risk of injury such as by decreasing the horizontal reach distance or the amount of force applied to the hand required to complete a task. [14]

1.3.2 Fatigue accumulation

Numerous scientific studies [15, 16] have demonstrated that arm elevation increases fatigue of the shoulder complex. In addition, the increased hand force required to complete a task, the use of heavy tools, and high-precision tasks such as electrical wiring further, increase the accumulation of shoulder fatigue during overhead work. [15]

In the field of ergonomics, the work cycle is a significant measure for highlighting precautionary considerations for repetitive work tasks. The duty cycle determines the portion of an activity cycle during which effort is exerted, with 1.0 representing one hundred percent of the cycle. For instance, if a task requires holding a tool for 5 seconds in a cycle that repeats every ten seconds, the work cycle would be 0.5. [16]

General guidelines have been developed to suggest that tool masses greater than 1.25 kg and duty cycles greater than fifty percent should be avoided for two-hour shifts involving overhead work. [15]

Moreover, there is evidence [17] indicating that the manner in which a task is performed can affect the accumulation rate of fatigue in the shoulder. Endurance times for overhead work can be extended by up to twentyfive percent by employing shorter cycle times. For example, for a repetitive work task that takes a total of two minutes, with 1 minute devoted to overhead work, it might be beneficial to divide that minute of overhead work into multiple parts over the two-minute period rather than completing it all at once.

Overall, reducing hand force or tool mass, work cycle, or overall cycle time during overhead work are all techniques that can be used to decrease the risk of shoulder MSDs when

performing overhead work activities. [16]

1.3.3 Bone movement

During overhead work, the humerus shifts upward. As a result, the subacromial space (i.e., the humerus-acromion distance) decreases, increasing the risk of catching tendons. [18]

It is an important consideration because the supraspinatus tendon, which represents part of the rotator cuff muscle, must pass through this space. The site of most initial rotator cuff injuries, including tears and tendinitis, is this tendon.[18, 19]

The subacromial space decreases with arm elevation and is minimal when the arm is raised between 60-90 degrees of elevation. Impingement or crushing of the tendon between the bones is a common consequence of overhead work, especially between 95-106 degrees of elevation. Therefore, it is recommended to keep the upper arm below 60 degrees of elevation. [19]

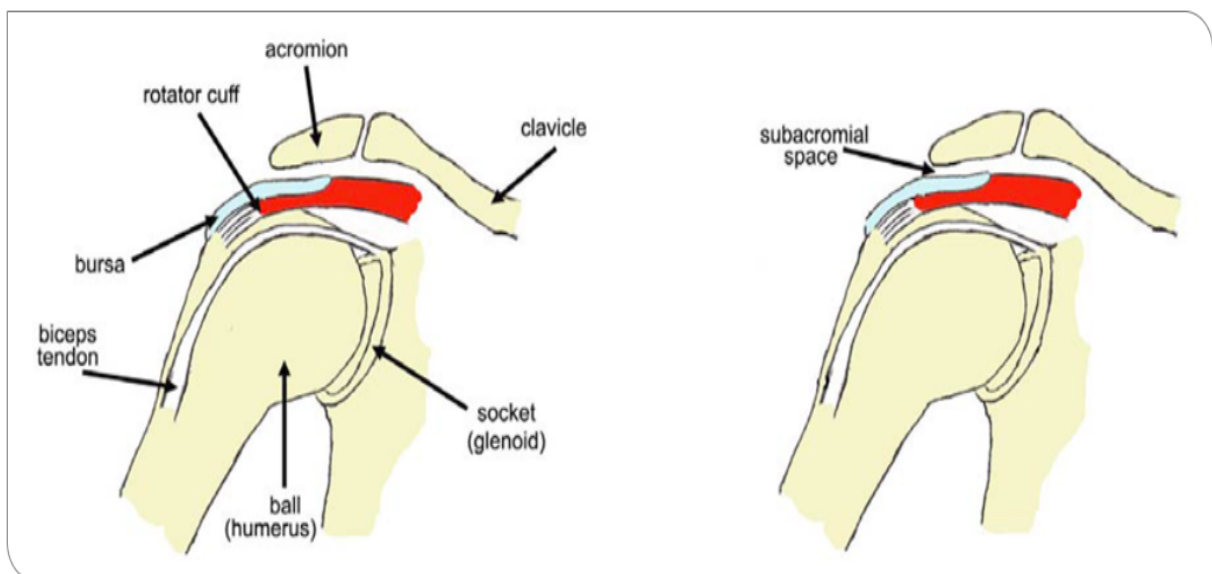


Figure 1.8: Anatomical components of the shoulder.

[https://www.kneehipandshoulder.com/conditions/shoulder-problems/
shoulder-impingement-syndrome/](https://www.kneehipandshoulder.com/conditions/shoulder-problems/shoulder-impingement-syndrome/)

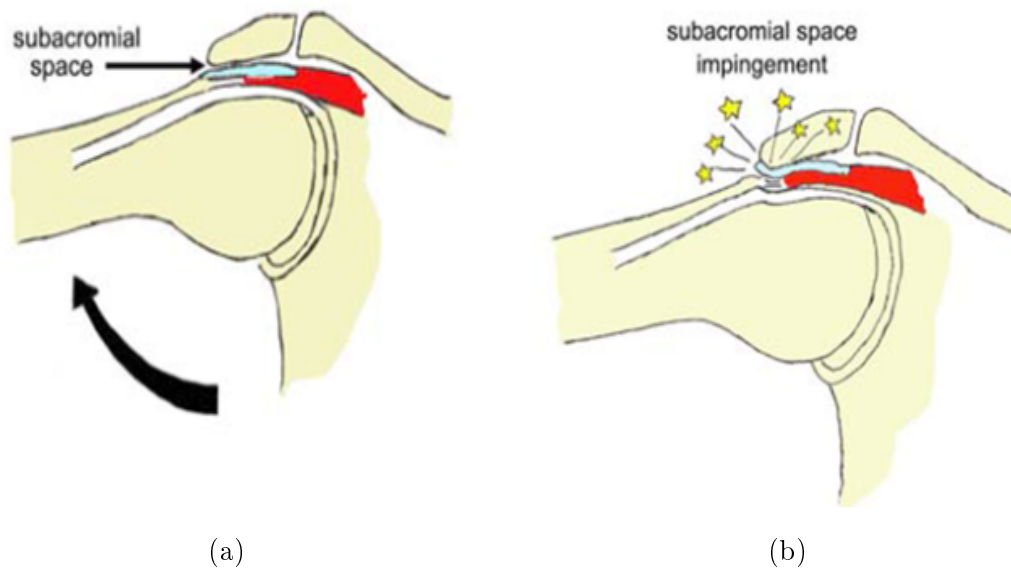


Figure 1.9: a) Reduction of subacromial space during humeral elevation b) Angle elevation exceed 90 degree, impingement occurs.

<https://www.kneehipandshoulder.com/conditions/shoulder-problems/shoulder-impingement-syndrome/>

1.3.4 Muscle capacity

Regardless of the structure of the task, the shoulder muscles are fatigued much more quickly by overhead work than by non-overhead work. In general, when arm elevation exceeds 60 degrees the muscles surrounding the shoulder complex are less effective. [20] Therefore, engaging in an overhead activity requires greater muscular effort compared to a similar activity performed at a lower height. Consequently, this heightened exertion can contribute to the accelerated onset of muscle fatigue. [20]

The shoulder heavily relies on muscular support to maintain joint stability, and when muscles become fatigued, it can negatively impact work performance, compromise joint stability, and increase the susceptibility to musculoskeletal disorders. Specifically, fatigued shoulder muscles, including the rotator cuff muscles, are less capable of sustaining the proper alignment of the upper arm bone within the joint causing the impingement mentioned above. [21]

Hence, it is recommended to incorporate regular rest periods when engaging in overhead work activities to allow the muscles surrounding the shoulder complex sufficient time for recovery. [21]

In particular, when performing overhead work, it is important to have certain cautions as minimizing arms away from the body, ensuring that the upper arm remains below an elevation of 60 degrees, avoiding high-precision tasks, applying forces in line with vertical movement, and incorporating regular rest periods. [22]

1.4 The way of prevention

The design of a workplace is a vital factor in the development of Musculoskeletal Disorders. When individuals exceed their body's limits and abilities while working, they put their musculoskeletal system at risk. An unbiased evaluation of the workstation will offer us valuable insights into whether the individual's recovery system can cope with the fatigue associated with the job. [43]

After completing the risk assessment, a prioritized list of measures should be drawn up and workers and their representatives should be involved in their implementation.

To minimize the severity of any injuries, one must focus on primary prevention by ensuring that all workers have the correct information, proper education and training in occupational health and safety, in order to avoid specific hazards and risks.

Measures can include the following areas:

- Workplace structure: adapt the structure to enhance work postures;
- Equipment: make sure it is ergonomically designed and suitable for the tasks to be completed;
- Tasks: modify work methods or tools;
- Management: plan work to avoid repetitive or prolonged work in poor postures so as to schedule rest breaks, rotate tasks or redistribute work;
- Organizational factors: develop a policy on MSDs to improve work organization and the psychosocial environment in the workplace and promote musculoskeletal health.

Prevention actions must also take into account the technological changes in equipment and digitization of work processes to which it is inevitable to be subjected, and related changes in the way work is organized. It must also be considered in the management

approach to MSDs monitoring and health promotion, rehabilitation and reintegration of workers already suffering from MSDs. [6]

The rising rate of MSDs in recent years calls for a solution. Exoskeletons are one of the most promising solutions to reduce MSDs. These devices facilitate assistance to specific anatomical areas that receive increased biomechanical load. The use of exoskeletons is particularly useful for employees who perform activities that require holding their arms in an elevated position at an angle greater than 90 degrees or for more than five minutes. These prolonged or uncomfortable positions can subject the musculoskeletal system to significant stress and increase the risk of suffering from musculoskeletal disorders. By providing additional support to the arms and back, exoskeletons can help workers avoid these MSDs and reduce the risk of workplace injuries while also increasing their productivity. It is therefore important for employers to consider implementing ergonomic solutions, including exoskeletons, in their workplace design to ensure the health and safety of their employees. [3]

Chapter 2

An innovative solution: exoskeleton

The exoskeleton is one solution that has recently attracted attention in the scientific and industrial world.[23] The latest trend in automation and data exchange in the manufacturing industry is Industry 4.0. The concept involves cyber-physical systems monitoring the physical processes of a factory and making decentralised decisions as a 'smart factory', which has been classified as the fourth industrial revolution. Technical assistance, where systems have the ability to assist humans with difficult or unsafe tasks, is one of the philosophies of Industry 4.0. There are many manual tasks that could be automated, but many others are difficult to perform because they require human precision, skill, decision-making, flexibility and mobility. [24]

A further evolution of Industry 4.0 is Operator 4.0, which is a consideration of the technology-enhanced worker. One such augmentation could be the use of exoskeletons, which can help reduce the trade-off between automation and manual tasks that require human skills. An exoskeleton is a wearable technology designed to augment and assist human movement, thereby reducing the physical wear, which in turn should reduce the risk of developing MSDs. [25]

The main application of exoskeletons to date has been in the medical and rehabilitation field, where the purpose of the device is to be of assistance and/or support to people with physically weak, disabled or injured people in activities of daily living (ADL) or rehabilitation exercises. [23]

A small number of exoskeletons have been developed for military applications, to increase the muscular strength of soldiers or to increase their carrying capacity. [23] In terms of

industrial applications, the concept is relatively new and, as such, research and development is still in its infancy, with many concepts yet to be tested beyond the laboratory. Most industrial exoskeletons can be categorised as either trunk exoskeletons, which assist with trunk flexion/support to prevent back injuries, or upper body exoskeletons, which assist the upper limbs in lifting or provide postural support. An upper body exoskeleton could be beneficial in assisting with static overhead work. [26]

2.1 History of exoskeletons

The early idea of the exoskeleton can be traced back to the end of the 19th century, but the first successful prototype called the Hardiman, appeared in the 1960s. [27] Hardiman was initially developed for military purposes to increase the strength and performance of the wearer. It operated in a master-slave configuration with multiple hydraulic actuators. This configuration implemented two overlapping exoskeletons, the inner exoskeleton was designed to follow the human movement, which could eventually be used to drive the hydraulic actuators of the outer exoskeleton. The device remained at the prototype level due to its relatively high weight and complexity. [28]

Subsequently, an upper limb exoskeleton with the idea of physical human-robot interaction (pHRI) was presented by Kazerooni et al. pHRI allows the direct transfer of mechanical power without using a master-slave system. This kind of exoskeleton is also called *Extender* because is a class of robot manipulators which will extend the strength of the human arm while maintaining human supervisory control of the task. The commands given to the Extender by the human operator are taken directly from the interacting force between the human and the Extender. This interaction force is also used to help the extender manipulate an object, i.e. the force and information signals are transmitted simultaneously. The extender's controller translates the interaction force signals into a motion command for the extender. This allows the human to give tracking commands to the extender in a natural way. [29]

Meanwhile, the University of Tsukuba started to develop a hybrid assistive limb (HAL), which was later commercialised. HAL was initially developed to assist disabled people with ADL, but later versions were also developed for industrial applications. [27]

The HAL for Care Support is composed of an exoskeletal frame, power units, and lumbar and thigh molds. The exoskeletal frame is equipped by fixing the lumbar and thigh molds which is important to control the lumbar movement. A triaxial accelerometer embedded in the exoskeletal frame measures the absolute angle of the trunk. The power supply units are located bilaterally on the carrier's large trochanters and contain angular sensors for measuring the angle of the hip joint and potentiometers for measuring relative angles of the knee and hip. [30] Actuators within the power units produce the torque transmitted from HAL for Care Support to the wearer through the frame. Electrodes on the wearer's skin surface over the lumbar musculus erector spinae detect nerve and muscle action potentials as bio-electrical signals (BES) to sense the wearer's intention of performing a lifting motion. Because of this mechanism, the HAL for Care Support can coordinate the level and timing of the torque to assist the motion of the hip joint. [30]



Figure 2.1: Hardiman exoskeleton.

[https://cyberneticzoo.com/man-amplifiers/
1966-69-g-e-hardiman-i-ralph-mosher-american/](https://cyberneticzoo.com/man-amplifiers/1966-69-g-e-hardiman-i-ralph-mosher-american/)

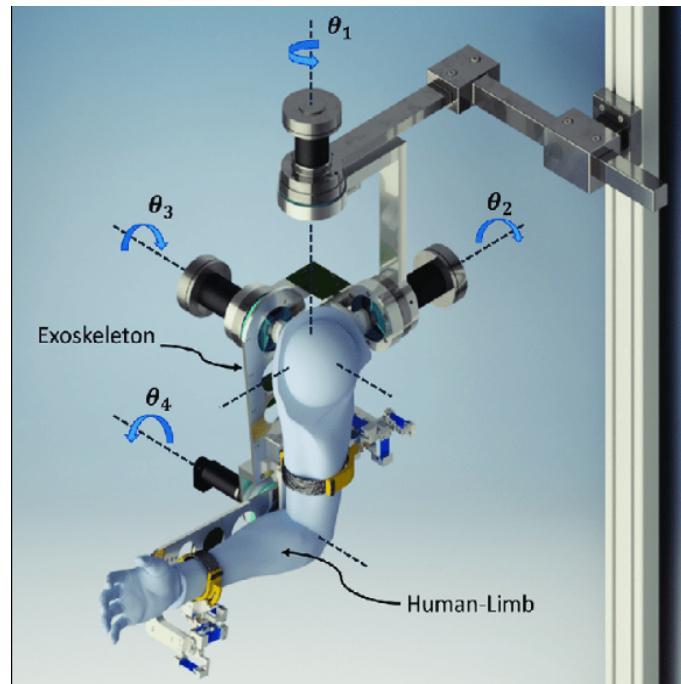


Figure 2.2: pHRI exoskeleton.

DisturbanceObserverbasedDynamicLoadTorqueCompensatorforAssistiveExoskeletonsAugust2018

78-93DOI:10.1016/j.mechatronics.2018.07.003



Figure 2.3: HAL exoskeleton.

<https://robofit.com.au/meet-hal/>

2.2 Exoskeletons classification

Within the category of industrial-use exoskeletons, there are various classifications aimed at which part of the body or on their actuating devices, which can be lower or upper extremity, back, full body or electric, pneumatic, hydraulic and hybrid. [31] All of these different types of exoskeletons can be divided into three broad sub-categories based on the way the assistance is generated:

1. Active exoskeletons, require an external power source in order to supply and control the actuation system to augment human performance; [32]
2. Passive systems use material compliance to offset gravity and/or elastic elements to store and release energy during movement to help workers perform physical movements; [32]
3. Semi-active or adaptive exoskeletons, with both active and passive components, or operating modes integrated in the design of the exoskeleton where the systems use an external energy source to adapt the inherently passive support characteristics to the changing demands of varying activities. [33]

2.2.1 Active exoskeletons

Active exoskeletons use power systems such as motors, hydraulic systems or pneumatic systems to increase human power or reduce the body's energy consumption. They consist of one or more actuators (e.g. electric motors) that actively add power to the human body. In active control mode, the robotic exoskeleton provides all the necessary motion to the limb. [34] The main drive systems of active exoskeletons are described below:

1. Electric actuators: One advantage of electric motors over pneumatic and hydraulic systems is the accuracy of position control and ease of programming; they are equipped with sufficient bandwidth, but have a lower power/weight ratio and reduced load capacity due to power consumption and battery life. In addition, they are expensive, large and heavy and can overheat.

Electric motors can provide a constant force throughout the rotation of the joint, whereas an artificial pneumatic muscle provides a higher force at the beginning of the stroke and a lower force at the end of the stroke. Most of the existing active

exoskeletons use brushless DC motors because they have a better power-to-weight ratio than others, high torque to weight ratio, low noise and reliability. [35]

Electric motors are usually coupled to a gearbox to increase torque and reduce speed, but the gearbox can be heavier than the motor itself and certainly increases the weight of the drive unit. Therefore, the efficiency and weight of reduction systems for a given reduction ratio will vary depending on the type of reduction system. Some exoskeletons use mass-coupled motors on the structure to drive each rotating joint. However, placing the actuator at the user's joints increases both the inertia of the exoskeleton and the size of the motors, as well as introducing misalignment. In addition, the actuator at one joint would have to carry the load of the actuator at the next joint, and so on. One method of solving these problems was to use cable transmission systems. This approach uses cables to transmit movement and forces, allowing the actuators to be mounted away from the couplings on a fixed base, resulting in low weight, reduction in motor size and their cost. [36]

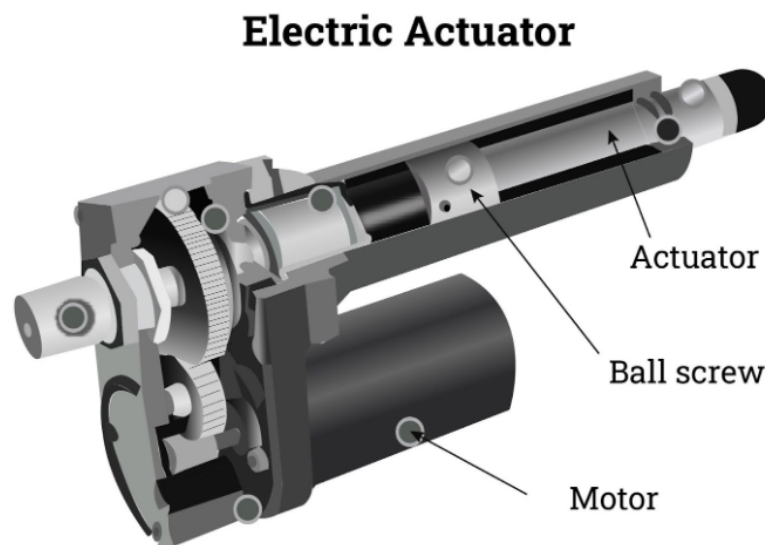


Figure 2.4: Example of electric actuator and its components.

[https:](https://www.iqsdirectory.com/articles/linear-actuator/electric-actuators.html)

[//www.iqsdirectory.com/articles/linear-actuator/electric-actuators.html](https://www.iqsdirectory.com/articles/linear-actuator/electric-actuators.html)

2. Pneumatic actuators: Two types of pneumatic actuators have been developed to date: pneumatic cylinders and artificial pneumatic muscles (PAMs or PMs). Pneumatic cylinders are a simple, low-cost actuation source that has been used for many years in mechanical and prosthetic applications, and they are well suited to

simple, repetitive tasks that require a very limited amount of system control. [37] However, they have not been widely used in advanced robotics because of some key problems due to the compressibility of the fluid, such as low accuracy, difficulty of control and compliance, i.e. the position of the piston is significantly affected by changes in load. Although they can provide good force control, they cannot provide precision in motion control. Instead, their compactness, high power-to-weight ratio and safety are good advantages to be exploited in robotic applications. However, the cylindrical shape of the actuators and the fact that the force is transmitted by a piston make the load and the variable supply pressure affect the positional accuracy of the system. [37]

For this reason, pneumatic muscle actuators have been introduced to overcome these problems, thanks to their elastic material that forms a seal to limit and control the expansion of the air and control the movement of the actuator. This is how the idea of a braided pneumatic muscle, the McKibben muscle, was developed for prosthetic applications in the 1960s. [38]

Due to their intrinsic deformability and similarity to human muscles, Pneumatic Artificial Muscles (PAMs) have been used in human-interactive systems, offering safety, compliant behaviour and a higher power-to-weight ratio than electric motors. The main drawbacks of this technology are reduced stroke, highly non-linear behaviour requiring sophisticated control, bulky air supply and unidirectional pulling force. Mainly to improve the stroke of these deformable actuators and to overcome the limitations in the direction of the applied force, several architectures have been developed to transmit the motion between the PAM and the end effector. Due to their passive properties when inflated with pressurised air, PAMs can also be used as passive elements within the structure of an exoskeleton to provide support for the user, similar to spring-based systems that use elastic components to compensate for the effects of gravity, reducing weight and volume compared to active solutions. For industrial applications, the goal is typically to assist workers in load handling, repetitive movements, overhead manipulation of objects, and to relieve excessive physical fatigue in manual tasks, while always ensuring the user's movements and allowing a relatively high shoulder flexion angle. Because of their advantages, passive devices are usually used. In particular, they often include passive spring mechanisms

and levers to provide assistive torque at the shoulder. [39]

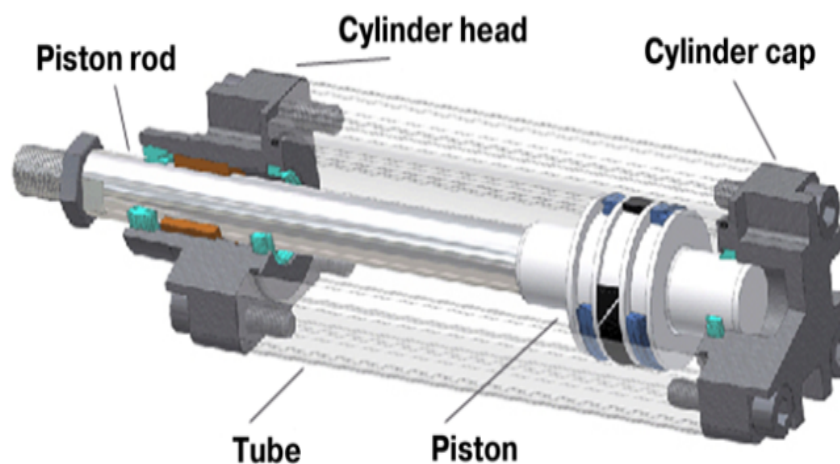


Figure 2.5: Example of Pneumatic cilinder and its components.

<https://www.maconresearch.com/>

grasso-lubrificante-per-cilindro-pneumatico-e-valvola-pneumatica



Figure 2.6: Example of Pneumatic artificial muscle.

[https://www.instructables.com/How-to-make-air-muscles!/?](https://www.instructables.com/How-to-make-air-muscles!/)

3. Hydraulic actuators: A hydraulic actuator applies a lot of force while compressing liquids, which is almost seldom the case, showing a larger torque than other actuators, and good precision. They have high output, but they are bulky and have problems with low energy efficiency. Despite this, they are heavy, and require pumps and valves to operate, besides suffering from fluid linkage. According to

the hydraulic actuator's operating concept, liquid pressure rather than instrument air pressure is used to exert pressure on the diaphragm, which subsequently moves the valve actuator and the position valve's stem. Almost all varieties of hydraulic actuators convert liquid pressure into mechanical power using a piston rather than a diaphragm. [40]

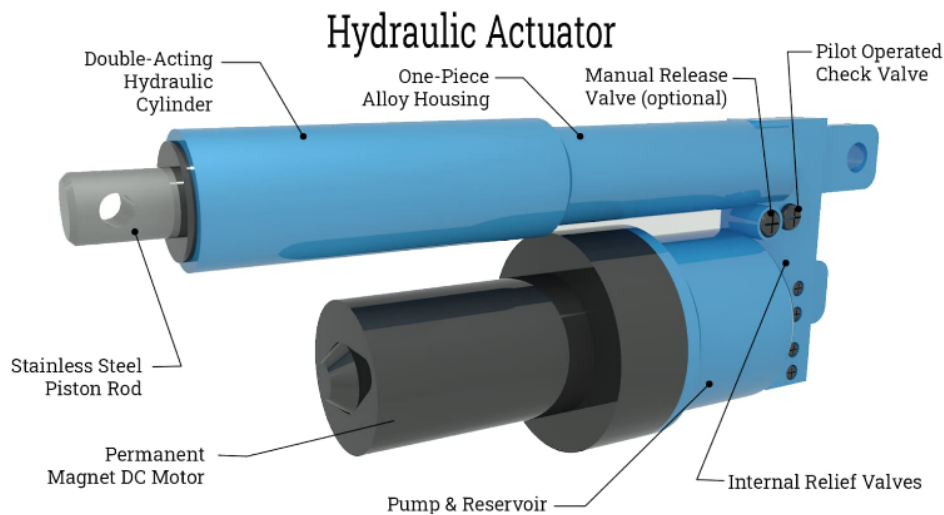


Figure 2.7: Example of electro-hydraulic actuator and its components.

<https://www.hydrauliccylindermanufacturers.net/hydraulic-actuators/>

However, to overcome these weaknesses, it could be possible to consider a hydraulic system operated by electrical power to control the exoskeleton through an electro-hydraulic actuator (EHA). The pump-controlled EHA is a more flexible system than the valve-controlled conventional hydraulic pump system. [40]

2.2.2 Passive exoskeletons

Passive exoskeleton systems are potentially less effective than active exoskeleton systems, but they are lighter and simpler because there is no control, providing a high power-to-weight ratio. Passive exoskeletons cannot actively support movement, so they are limited to generating resistive forces and compensating for gravity, e.g. they are used to compensate for the gravitational potential of the human arm.

Springs and dampers are often used as 'passive actuators' to provide a resistive force to augment human power by storing energy and releasing it when needed and/or transferring force from one part of the body to another without adding inertia. These systems

also have the advantage of not requiring electrical power, which reduces the weight and volume of the exoskeleton. [41]

In a review by de Looze et al. (2016), it is evident that commercially developed exoskeletons are mainly passive in nature with a focus on reducing physical strain during dynamic lifting and static bending. In theory, a passive exoskeleton would counterbalance gravity, arm weight and the load being handled, thus decreasing the risks of MSDs. [42]

The benefits of exoskeletons in reducing physical load have been demonstrated in laboratory settings. Barrett and Fathallah (2001) reported that the PLAD, HappyBack, and Bendezy passive trunk exoskeletons reduced erector spinae muscle activity by 21-31% during static bending while holding a load. [44]

In terms of active systems, Huysamen et al. (2018) investigated the effect of an active trunk exoskeleton for dynamic lifting and reported a significant decrease in reduction in muscle activity of the erector spinae, from 55 to 45% MVC a 27% reduction and biceps femoris from 24 to 19% MVC, a 20% reduction.

Several passive upper arm devices have been developed in recent years, including the Levitate exoskeleton. In a study by Spada et al. (2017b), this exoskeleton showed a positive effect on activities involving a raised-arm posture, with an average increase in 30% and fatigue was perceived to be less when wearing the exoskeleton than when not. However, little is known about the potential benefits of these exoskeletons for the biomechanical strains associated with manual handling tasks.

Theurel et al. (2018) investigated the physiological consequences of using a passive upper limb exoskeleton (EXHAUSS Stronger®) during manual handling tasks and concluded that the exoskeleton effectively reduced the workload on the shoulder flexor muscles during manual lifting/lowering and stacking/unstacking tasks.

Previous studies and developments have shown that it is a challenge to realise technically feasible exoskeletons with a user-centered design. Research has shown that prototyping exoskeletons do not always lead to the intended outcomes, because the exoskeletons do not meet the needs of the end-users or stakeholders, for example, the physical strain is not reduced or the acceptance of the device is low (Almenara et al, 2017). In other cases, the main objectives were achieved by reducing the load on the targeted muscle groups,

but other parts of the body experienced increased load and high local discomfort due to the forces exerted on the body by the exoskeleton.(de Looze et al, 2016).

For example, the EXHAUSS Stronger® passive upper limb exoskeleton increased upper arm antagonistic muscle activity, postural tension, cardiovascular demands and even changes in upper limb kinematics. (Theurel et al., 2018). In addition, the three passive trunk exoskeletons mentioned above increased the muscle activity of one or more leg muscles (Barrett and Fathallah, 2001). [44]

In order to look more closely at the requirements that an exoskeleton must have, it is better to start by analysing the anatomy of the shoulder complex.

2.3 The shoulder complex

The goal of an exoskeleton is to imitate the kinematics and dynamics of the human musculoskeletal system to support the movement of the limbs, which is difficult with existing mechanisms and operating modes. Because of the complex anatomical structure, there is no coherent kinematic pattern for the human upper limb in the biomechanical literature to help us conceive exoskeletons. In addition, the design parameters of the exoskeleton depend heavily on the expected application. It is therefore necessary to analyze the anatomy of the human upper limb in order to conceive the exoskeleton taking into account the application of the end user. [45]

The human upper limb consists of a complex skeletal structure, as shown in Figure 2.2a, which includes the shoulder complex, elbow complex, wrist and fingers, which have multiple joints. The shoulder complex consists of three bones: the clavicle, the scapula and the humerus, and four joints shown in Figure 2.2b:

1. The glenohumeral joint (GH);
2. The acromioclavicular joint (AC);
3. The sternoclavicular joint (SC);
4. The scapulothoracic joint (ST).

The four joints with the thorax providing a stable base. The glenohumeral joint is commonly referred to as the shoulder joint. The sternoclavicular joint is a single joint that

connects the shoulder complex to axial skeleton. The acromioclavicular joint is formed by the lateral end of the clavicle and the acromion of the shoulder blade. The sternoclavicular joint is a compound joint with two compartments separated by articular discs and it is made up of the clavicle, the sternum and the cartilage of the first rib. The scapulothoracic joint is not a joint because it is a bone-muscle-bone articulation that is not synovial. It is formed by the female surface of the shoulder blade and the male surface of the rib cage. However, it is considered a joint when describing the movement of the scapula over the thorax.

In principle, the shoulder complex can be modelled as a ball and socket joint. It is formed by the proximal part of the upper arm bone (humeral head) and the female part of the shoulder blade (glenoid) and the GH joint has three degrees of freedom (DOFs) with axes intersecting perpendicularly in the GH joint center. However, the position of the centre of rotation of the shoulder joint changes with the movements of the upper arm. [46]

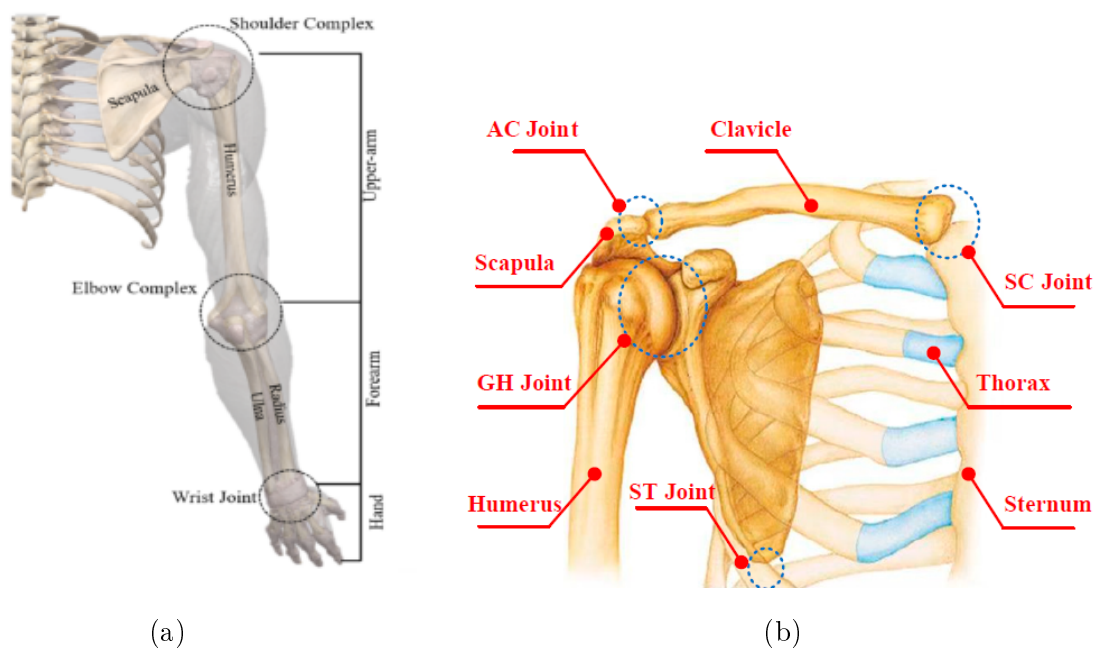


Figure 2.8: a) The human upper limb composition. [46] b) Anatomy of the shoulder complex. [47]

The main movements of the shoulder complex, presented in the Figure 2.3, are performed by the glenohumeral are shoulder flexion/extension (motion in the sagittal plane), shoulder abduction/adduction (motion in the frontal plane) and internal/external rotation (motion in the transversal plane).

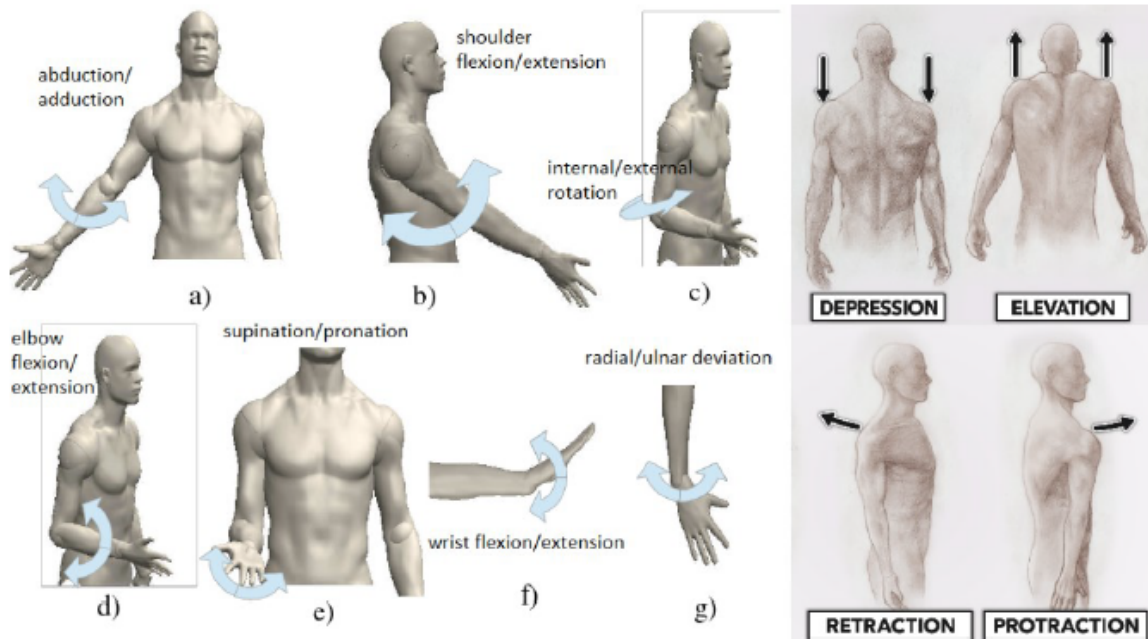


Figure 2.9: DOF of the upper limb

State-of-the-Art Assistive Powered Upper Limb Exoskeletons for Elderly Akim Kapsalyamov¹,
Shahid Hussain,¹ and Prashant K. Jamwal^{2,3}, Senior Member, IEEE.

The sternoclavicular joint has two degrees of freedom (DOF), commonly known as shoulder elevation/depression and abduction/protraction, which cause the glenohumeral joint to move transiently. This gives the shoulder a total of five DOF.

The elbow complex has two DOFs, elbow flexion/extension and forearm pronation/supination, while the wrist has two DOFs, wrist flexion/extension and radial/ulnar deviation. The rotational axes of both wrist DOFs pass through the capitate carpal bone.

The movement of the shoulder girdle (clavicle and scapula) is more important than the movement of the arm below the shoulder during arm elevation. As the arm elevates, the ratio of scapular rotation (rotation of the shoulder blade relative to the trunk) to humeral rotation (rotation of the humerus relative to the shoulder blade) generally rises. If the movement of the shoulder girdle is restricted, the arm cannot be raised beyond a certain position. Therefore, translation of the glenohumeral joint is essential to allow the arm to be raised. If the translational movement is restricted by external forces, the range of motion (ROM) of the shoulder joint will be limited and this can cause pain in the joint.

[47]

In this project, particular attention was paid to providing the user with at least two degrees of freedom to allow flexion-extension in the sagittal plane, the most common movement in overhead work, and abduction-adduction in the transverse plane.

2.3.1 Shoulder center rotation

The GH joint connects the humerus to the shoulder girdle so that the variable amount of displacement of the center of the GH joint is equal to the overall translational movement of the shoulder girdle. It is possible to establish the coupling relationship between the variable amount of displacement of the joint centre relative to the thoracic coordinate system and the humeral elevation angle can produce the kinematic model of the shoulder complex for a given pointing position.

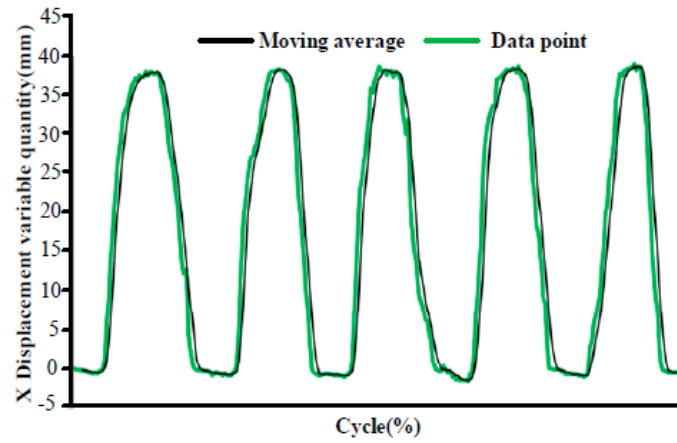
In order to evaluate the displacement of the joint center as a function of the humeral elevation, and possibly extrapolate the information on the motion, few experimental tests were carried out by few researchers[48, 49]. Prior to this, measurements of the GH joint movement information were taken with the subjects in an upright position, arms straight, right shoulder relaxed to hang naturally without bending the elbow.

At the start of the experiment, the subjects wore the recording mechanism and the wearer was adjusted so that the axes of three rotational joints intersected vertically at the centre of the GH joint. The detection mechanism includes a horizontal and a vertical tracking mechanism. This tracking system consists of two tracking mechanisms, one horizontal and one vertical. The first one places two DOFs, mounted on the support plate, and consists of two interconnected guide strip tracking mechanisms, equivalent to prismatic joints, and tracks the displacement variable of the GH joint in the horizontal plane. The second places a DOF, mounted on the horizontal mechanism and consists of a strip slide mechanism and a pulley mechanism. The strip slide mechanism tracks the displacement variable of the GH joint in the direction of the vertical axis, with sufficient range of motion to track the movement of the vertical axis of the GH joint. The pulley mechanism can balance the gravity of the vertical slide mechanism of the guide strip. The wear mechanism has three rotating DOFs with axes that intersect vertically at the centre of the GH joint and is mounted on the vertical mechanism. It consists of three interconnected rotating joints and follows the three-dimensional (3D) rotation of the GH joint. The function of the wearable mechanical system is to fully track the motion information of the GH joint in

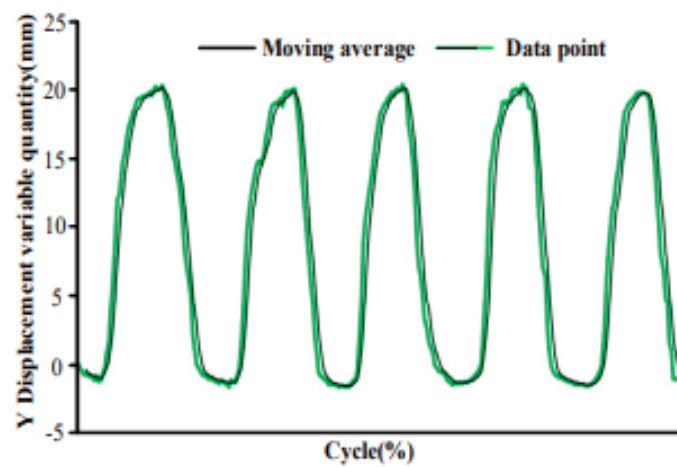
the upper limb accessible workspace.

Participants performed the elevation of their right arms in the sagittal and coronal planes, and the elevation angle varied from 0 to 120. During the natural lifting and lowering of the humerus, it was noted how it is impossible that the motion of the humerus is completely guaranteed in the single elevation plane. In fact, the angle of the elevation plane has a small variability (less than 5 degree). For small variations in the angle of the elevation plane, the variable amount of displacement of the centre of the GH joint is almost equal to zero. Thus, the plane of elevation of the single motion is assumed.

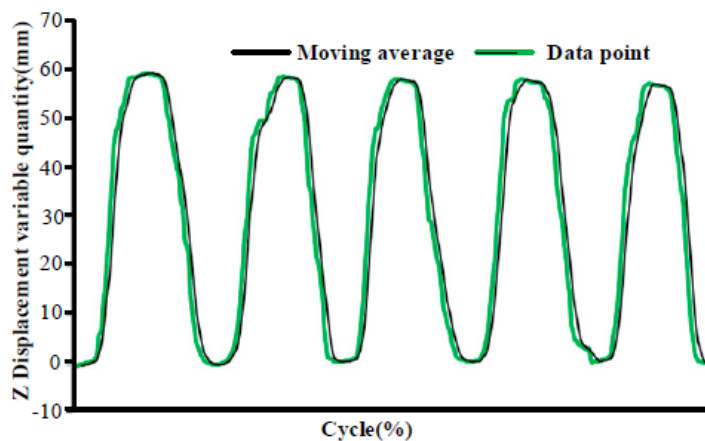
During the experiments, the movements of raising and lowering the humerus in the sagittal plane and the variable central displacement of the GH joint relative to the thoracic coordinate system were observed in the X, Y and Z directions, respectively, as shown in Figure 2.10, where the ascisse represent the degree of completion of the five cycles. the x-axis is equal to the frontal axis, and the direction is from the sternum to the GH joint center, the z-axis is equal to vertical axis and the direction is upward, y is the cross product of vector z and x, and the coordinate origin is the deepest point of the incisura jugularis. During the movement of raising and lowering the humerus, the variable displacement of the centre of the GH joint was large and smooth in the X, Y and Z directions, confirming the relationship of coupled movement between the variable amount of displacement of the centre of the GH joint and the humeral elevation angle in the sagittal plane. [47]



(a)

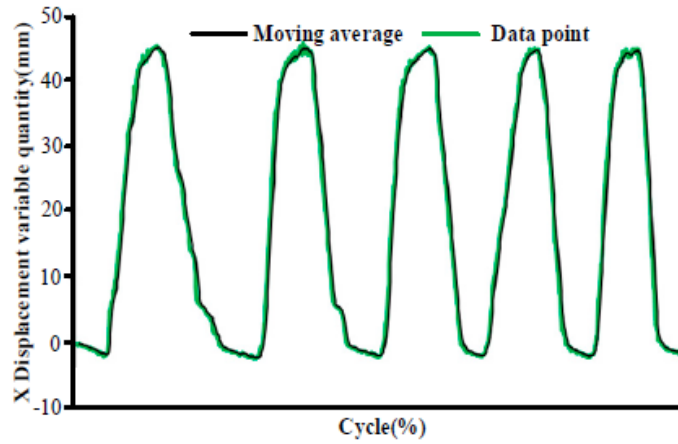


(b)

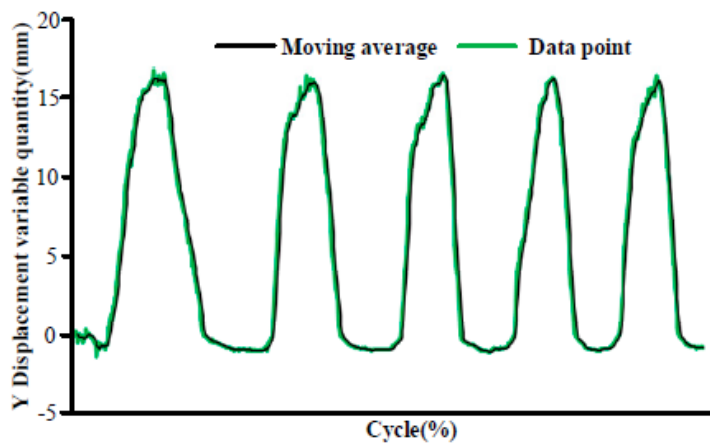


(c)

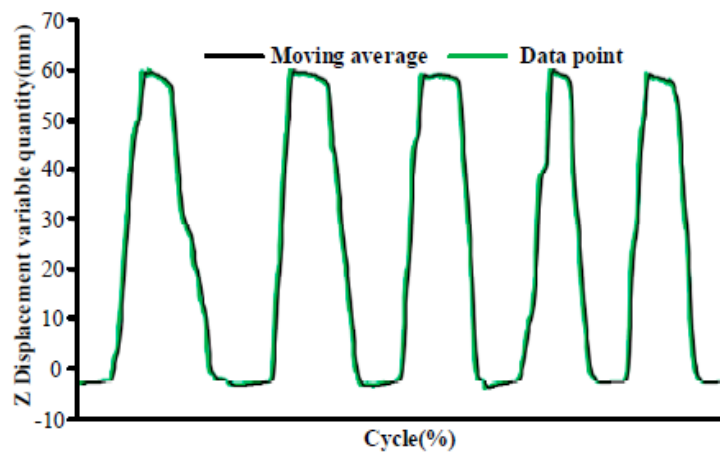
Figure 2.10: Diagrams of the glenohumeral (GH) joint motion information during humeral raising and lowering movements of five cycles in the sagittal plane: (a) X-direction of the GH joint displacement variable quantity, (b) Y-direction of the GH joint displacement variable quantity, and (c) Z-direction of the GH joint center displacement. [47]



(a)



(b)



(c)

Figure 2.11: Diagrams of the glenohumeral (GH) joint motion information during humeral raising and lowering movements of five cycles in the coronal plane: (a) X-direction of the GH joint displacement variable quantity, (b) Y-direction of the GH joint displacement variable quantity, and (c) Z-direction of the GH joint center displacement. [47]

By knowing the displacement of the CoR, it is possible to take this factor into account when designing wearable devices for the back and shoulders, although it is a problem to detect it visually on a person's body and design a device that follows the movement of the centre of the joint. Sometimes other solutions, such as adding rounded degrees of freedom, get around the obstacle.

2.4 Exoskeleton requirements

Design requirements of an upper arm exoskeleton device essentially include a proper choice of several DOF, correct dimension of the various parts, type of actuators, and the way of force transmission, in order to provide the desired functionality also accompanied by adequate ergonomics. Based on the knowledge of the state of the art in upper arm exoskeleton systems, the basic technical specifications could be inferred. [50]

The exoskeleton robot should generate natural movements of the upper limb without the wearer feeling any vibrations, jerks or sudden changes in movement. Small, high-torque actuators with a high power-to-weight ratio are essential to developing such an exoskeleton robot, which should not add undue weight to the wearer. These requirements can be focused on:

- **Comfort of wearing:**
the structures of exoskeletons should be flexible with high strength. These systems should be lightweight to avoid discomfort or fatigue for the user. Therefore, the materials of the exoskeleton structures should be specially considered so that the exoskeleton system becomes a second skin for the wearer [51];
- **Compatibility:** because upper limb exoskeletons need to operate in parallel with the human upper limb and are attached to the human arm in multiple locations, they need to adapt to different arm lengths of the wearer, requiring additional prismatic joints [50];
- **Power to weight ratio:** the amount of energy required to support each joint in the body is usually high. It is therefore essential to use actuators with a high power to weight ratio to create lightweight exoskeletons with sufficient force and speed to move the joints correctly. The weight must be reduced as much as possible to

avoid uncomfortable loads for the user; in fact, the lower the weight of the device, the lower the inertia in operation. The actuators are components that significantly increase the weight of the exoskeleton, so it is essential to reduce the number of actuators by incorporating passive and quasi-passive elements into the design. For example, it is important to include brakes or clutches to maintain a fixed position at certain times. In addition, shock absorbers reduce the impact of the system's own forces, and springs add some momentum to the initial phase of movement.[50]

- Range of motion: wearable exoskeletons are not able to provide a wide range of motion compared to the human upper limb. As the mechanisms supporting shoulder glenohumeral movements tend to reduce the actual upper limb workspace, several studies have attempted to address this limited workspace challenge in their design by considering shoulder girdle movements that accept complex and heavier mechanisms. To achieve the desired workspace, it is necessary to analyse the mutual ROM for the human arm and exoskeleton, which can be done by analysing the kinematic and dynamic model of both systems. However, the large ROM can only be achieved at the cost of a complex and heavier mechanism [51];
- Reduction load and discomfort: however, while exoskeletons can reduce stress on certain parts of the body, they can also have unintended consequences, such as increasing stress and/or discomfort in other areas of the wearer's body. Typically, discomfort occurs where the exoskeleton is in contact with the wearer's body. For example, in a simulation of overhead work, the use of a passive upper limb exoskeleton reduced the load on the upper arm and shoulder, but slightly increased the load on the lower back. Therefore, even if a mechanical advantage is confirmed, eliminating or minimising such discomfort is another design goal [50];
- Center of rotation of the shoulder complex: shoulder complex is one of the biomechanically complex area in the human body, in fact its center of rotation (CR) changes with its motions. So, design of a proper shoulder mechanism for an upper extremity robotic exoskeleton to change its CR with its motions is a very difficult task to be accomplished. Yet, it is necessary to cancel the ill effects caused by the position difference of the CR of the exoskeleton robot shoulder and that of the human shoulder. Redundant DOF is incorporated into the active exoskeleton struc-

ture to prevent misalignment, or at least to reduce the degree of misalignment. This is achieved by adding passive joints that perform these additional DOF, which are free to rotate or translate. [52]

The design of this exoskeleton attempted to meet the requirements as best as possible, and due to their specifications and characteristics, it was decided to use artificial muscles as pneumatic actuators, which will be discussed in more detail in the next chapter.

Chapter 3

Artificial Pneumatic Muscle

A pneumatic artificial muscle (PAM) is a pneumatic actuator capable of converting pneumatic power into pulling force. Besides to flexible actuators used in various applications, there are several types of conventional actuation mechanisms such as: electric motors, hydraulic actuators, pneumatic pistons, and shape memory alloys (SMAs). However, the use of artificial muscles is more advantageous than other actuation mechanisms due to their following benefits: [53]

- High force-to-weight ratio: PAMs are lightweight and produce a strong force;
- Flexible structure: PAMs provide flexibility and compliance for the applications in a pressurized or unpressurized condition;
- Variable installation options: PAMs deliver a safe and compatible interaction with the human environment only by controlling the volume flow rate of operating air into the muscle;
- No mechanical wear;
- Minimal compressed air consumption;
- Size availability;
- Low cost: Simple PAMs can be fabricated from inexpensive materials, which reduce the overall manufacturing cost;
- Strong reliability for human use: PAMs can be made to have a soft touch due to the intrinsic and adjustable compliance.

Flexible actuators are characterized by the presence of a thin-walled membrane, with high deformability, which delimits a chamber in which the pressurized fluid acts; it is lightweight and capable of collecting the force that results from the action of the pressurized fluid. On this deformable chamber, kinematic constraints are imposed selective and directional that allow it to expand along particular predefined directions, for example only radially or only axially, preventing the deformation in other directions.

An important feature of this type of actuators is the ability to operate with different fluids, generic, with no particular viscosity, homogeneity and compressibility characteristics. It can, therefore, use fluids that are safe, economical, explosion-proof and lightweight. These actuators can work with water, air, and oil. In addition, they can operate in hostile environments, with strong temperature gradients, vibrations, dust, electromagnetic disturbances.

Another important feature of these actuators is the possibility to operate easily in the presence of assemblies with significant misalignments, without introducing onerous stresses due to configurations that are hyperstatic.

In general, the PAM can generate large pulling forces with minimal compressed air consumption due to its high force-to-weight ratio and relatively small size. Infact, these actuators are statically sealed, free of friction losses and working fluid leakage. [54]

Their operating characteristic reports the actuation force generated at given pressure as a function of the fraction of stroke performed. The actuation force, in fact, depends not only on the level pressure of the working fluid p , but also by the fraction of stroke achieved k . Additionally, due to the inherent properties of the elastic-viscous material, to the geometric behaviors of the PAM shell, and to the compressibility of the air, PAMs have a nonlinear behavior, of the type of that of an active elastic element, for which the force generated is a function of the magnitude of the deformation achieved and the level of pressurization of the actuator. [55]

3.1 The story of the PAM

In the 1950s, the PAM was first invented by physician Joseph L. McKibben for the construction of artificial upper limbs for the disabled. At 1980s, a redesigned and more powerful PAM was introduced by the Bridgestone Company, and has been utilized for

paint applications in industry, for assistance to disabled people, and for service robotics. PAM has found application in various types of humanoid and advanced robot systems. It is primarily utilized as a robotic actuator in scenarios where compliance and a low power-to-weight ratio are crucial. This is particularly relevant for machines designed for walking, running, and humanoid robots. Shadow Group and FESTO for example, produce different models of PAMs for robotic and industrial applications. [55]

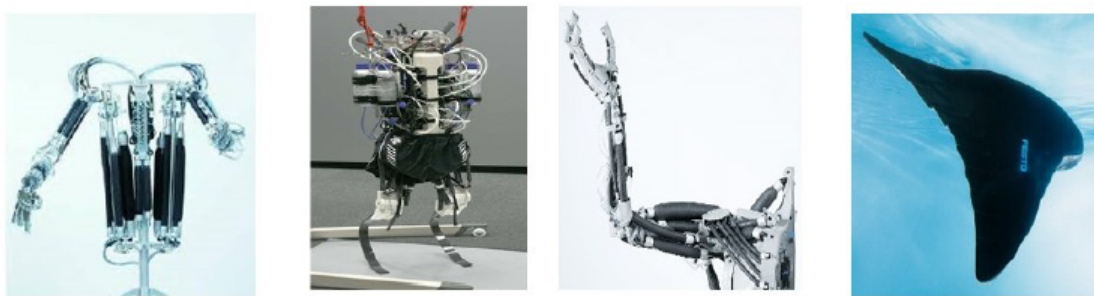


Figure 3.1: Biorobotic applications of PAMs. [53]

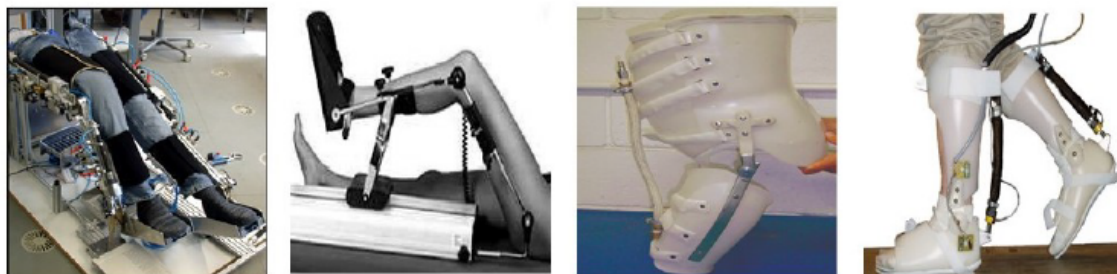


Figure 3.2: Medical applications of PAMs. [53]

Generally, PAMs are composed of a slender rubber tube, also known as a bladder, which is encased within a woven mesh shell. Both ends of the bladder are sealed, with one serving as the air inlet and the other connected to the load. When compressed air is supplied to the PAM through the inlet port, the inner bladder expands radially, exerting pressure against the braided mesh shell. However, since the braided mesh wires are not stretchable, this causes the actuator to contract axially and generate tensile forces when connected to the load. [56]

The physics underlying the fact that human muscles are similar in function to PAMs, which convert air power into traction force. Therefore, tensile force, length, air pressure, diameter, and material properties constitute the main parameters that influence the dynamic behavior of PAMs. The relationships between these parameters show significant variations among different PAM models.

Different types of conventional PAMs have been developed based on diverse operating principles, applications, and design concepts. In the figure 3.3 it is possible to see six various types of PAMs: braided muscles, pleated muscles, PAM reinforced by Kevlar Fiber, Yarlott Netted Muscle, Paynter Hyperboloid Muscle, ROMAC Muscle. [53]

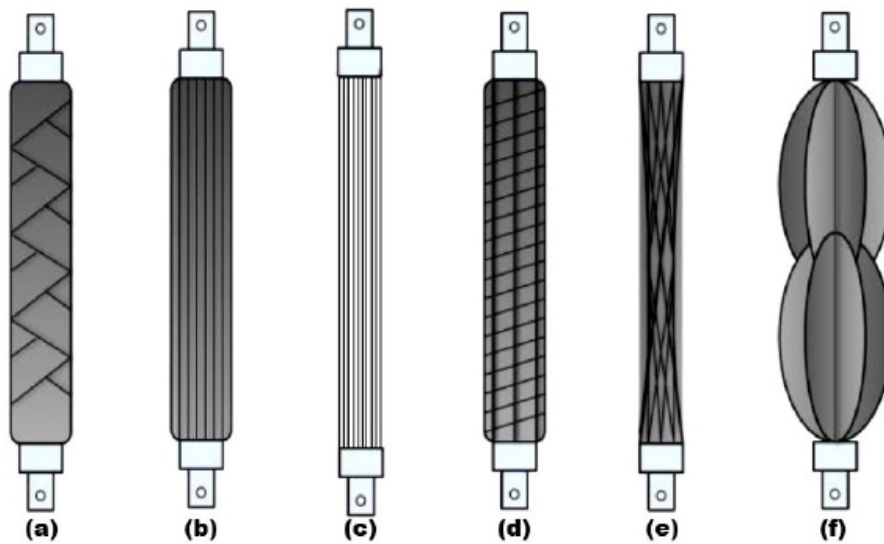


Figure 3.3: Types of conventional PAMs:(a) McKibben Muscle/Braided Muscle; (b) Pleated Muscle; (c) PAM reinforced by Kevlar Fiber; (d) Yarlott Netted Muscle; (e) Paynter Hyperboloid Muscle; (f) ROMAC Muscle. [53]

3.1.1 McKibben Muscle and its variants

Among the most common and widely used pneumatic muscles are the braided fiber muscles also known as the muscles of McKibben, patented by Gaylord in 1958 and applied in the biomechanical field by McKibben. His muscle consists of a deformable chamber of cylindrical shape, an outer mesh that forms the constraint to the chamber when it is pressurized, and two headers that allow connection to external constraints and load and feeding with the pressurized fluid.

The functionality of the McKibben muscle is based on the nonstretchability of the fibers wrapped helically around the inner inflatable chamber, which are firmly attached to the end caps.

This arrangement allows the actuator to be anchored and powered. When the inner chamber is pressurized, it expands, making contact with the non-stretchable fibers surrounding it. These fibers, attached to the end caps, bring the heads closer together as the pressurized fluid causes the chamber to assume a larger radial dimension. As a result, this mechanism accomplishes muscle contraction.

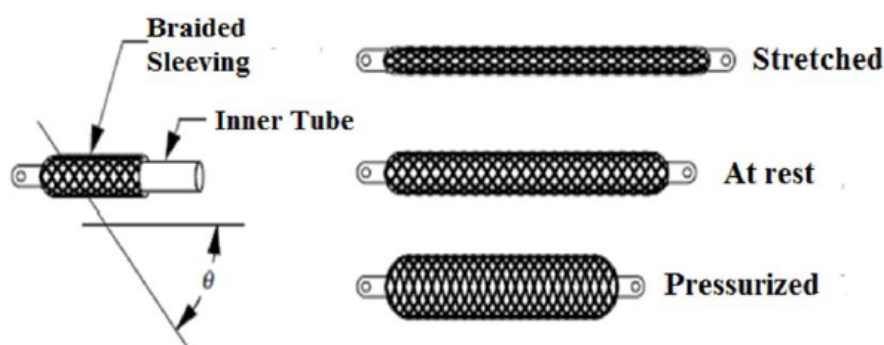


Figure 3.4: Diagram for structure of a McKibben muscle

PneumaticArtificialMuscles:actuatorsforroboticsandautomationFrankDaerden,
DirkLefebervrijeUniversiteitBrussel,
DepartmentofMechanicalEngineeringPleinlaan2,B-1050Brussels.

The structure of a variant of a braided McKibben muscle is shown in the Figure 3.5, the multifilament McKibben muscle. This one consists of developing a multifilament structure composed of several bundles of thin McKibben muscles to improve the contractile force and contraction ratio of thin McKibben muscles. The structure of a thin McKibben muscle is similar to that of the muscles of conventional McKibben muscles, the only thing that changes is the size of the diameter which is 2-4 mm, while the diameter of conventional McKibben muscles is more than 10 mm. [57]

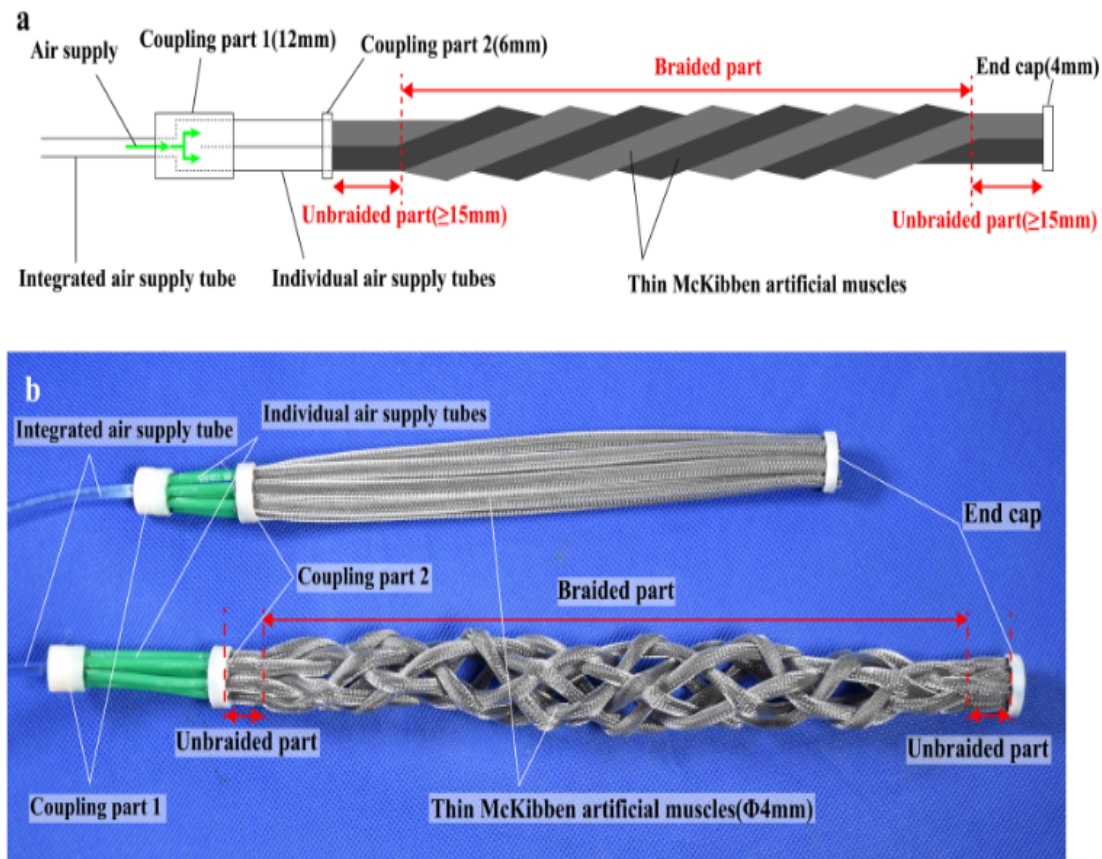


Figure 3.5: (a) Diagram for structure of a multifilament McKibben muscle; (b) with thin muscles arranged in parallel (top) and with thin muscles intertwined.(bottom) [57]

Another type of pneumatic muscle is the straight-fiber muscle, which is a McKibben muscle with the pitch of the fibers tending towards infinity. The fibers placed on the surface of the elastomer chamber are no longer arranged along a helix, as in the McKibben's muscle, but along the meridians of the pressure chamber. The straight-fiber muscle consists of carbon fibres and a latex-rubber tube. With this structure, the straight-fiber type muscle can only expand in the axial direction assuming a barrel shape compared to the McKibben muscle that has a radial expansion almost constant over the entire length. [58]

An interesting evolution of the straight is represented by the pleated muscle and the Yarlott muscle.

The pleated muscle has no material deformation and friction when inflated. This is due to the presence of numerous folds in the axial direction on the muscle membrane, and

at the time of inflating it unfolds the folds. In essence, no external energy is required to inflate the membrane, and due to the absence of friction, no hysteresis is observed. The characteristics of this type of muscle depend on the ratio of total length to minimum diameter, the deformation behavior of the membrane material, the speed of contraction, and the applied pressure applied pressure.

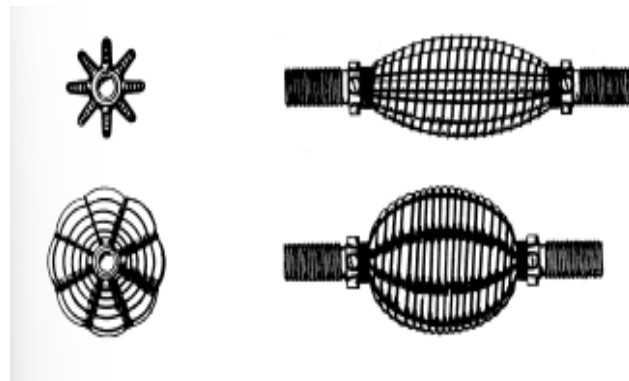
Instead, the Yarlotte muscle comprises a prolated elastomeric bladder of spheroidal shape, netted by a series of cords or wires. This actuator takes the shape of the spheroidal bladder when inflated, and when prolated, the axial wires straighten and push the bladder into a shape characterized by a series of ridges and valleys.

Another significant example of a muscle, which avoids energy losses in the deformation of the membrane, is the RoMaC muscle (Robotic Muscle Actuator). In the latter, the membrane is collapsible and, for the change of geometry of the chamber, there is no need for deformation of the material but the unfolding of the membrane. The RoMaC consists of an articulating polylobe bladder harnessed by a wire netting and closed at either end by fittings, where the bladder is made of a sheath that is characterized by its high tensile stiffness, flexibility, and fluid-tightness. The netting or harness is comprised of non-stretchable flexible tension links joining at nodes to form four-sided diamond-shaped apertures in the network.

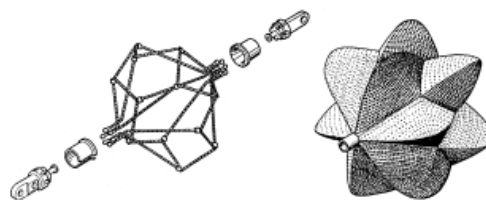
Figure 3.5 shows, respectively, a schematic of the pleated, Yarlott and RoMaC actuator, at rest and under load. [53]



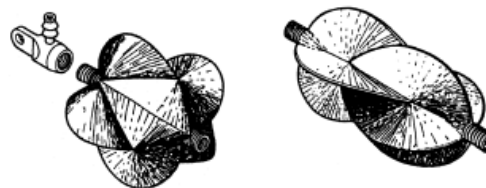
(a)



(b)



(a)



(b)

(c)

Figure 3.6: a) Actuator pleated b) Yarlott actuator c) RoMaC actuator c)a)standard version, c) b)miniature version. [53]

3.2 FESTO actuator

Another producer of different kind of PAMs is FESTO. The basic concept of FESTO muscle is to wrap a waterproof tube with non-elastic fibers arranged in a rhomboid pattern. This arrangement creates a three-dimensional grid structure, which deforms when compressed air is fed into the PAM generating a tensile force in the axial direction, resulting in muscle contraction.

The nominal length of the pneumatic muscle is determined at the time when it is unpressurized and free from any load, and this length corresponds to the visible part of the muscle between its connections.

When a fluid muscle is pretensioned by an external force, in a non-pressurised state, it expands lengthways. The ideal pretensioned length is 0.5% of nominal length.

On the other hand, when the muscle is pressurised, it contracts and its length decreases and develops maximum force with optimum dynamic characteristics and minimum air consumption. The most effective operating range is provided with contractions below 9%, but it can reach contraction values of up to 25%. The smaller the degree of contraction of the Fluidic Muscle, the more effectively it works.

When there is a change in external force, the muscle behaves like a spring and follows the application of force by aligning itself with the direction of the applied force.

With Fluidic Muscle, both the pretensioning force of this “pneumatic spring” and its spring stiffness can be varied. The Fluidic Muscle can be operated as a spring with constant pressure or constant volume. This produces different spring characteristics that enable the spring effect to be matched perfectly to the application. [59]

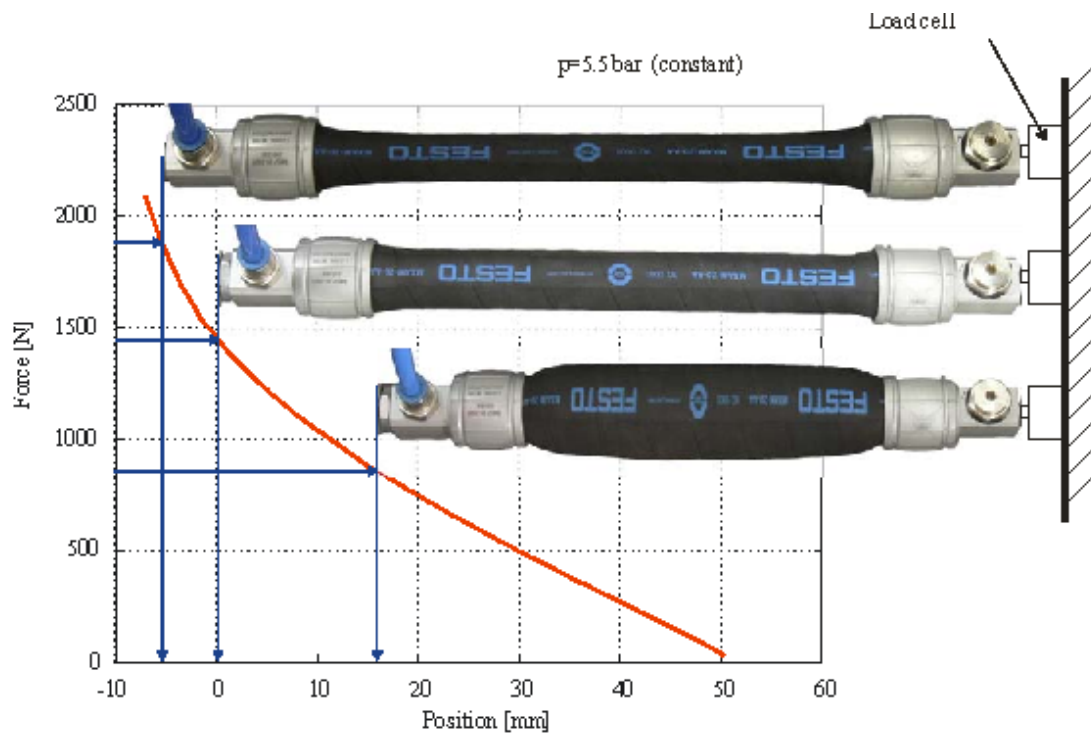


Figure 3.7: Example of a Fluidic Muscle DMSP elongated, at nominal length and contracted and its characteristic at the pressure of 5.5 bar. [60]

Chapter 4

Original idea of exoskeleton

The use of exoskeletons in the workplace is an innovative technical solution from both a functional and preventive point of view. When working at height, the contraction of the muscles of the human shoulder complex should compensate for the torque generated by the weight of the arm segments and possibly also by the weight of a tool.[61]

The idea behind this project is to develop a first prototype of an exoskeleton capable of reducing the work done by the shoulder muscles and compensating for it through the presence of FESTO artificial pneumatic muscles, presented in the previous paragraph, capable of developing large pulling forces.

The exoskeleton is designed to consist of an adjustable back structure that houses the muscles, and an arm, consisting of a strut and cuff that supports the wearer's arm while leaving the elbow and forearm free.

The exoskeleton is also characterised by the presence of two joints that allow two degrees of freedom:

- the elevation of the arm from 90 to 135 degrees on the sagittal plane, then a rotation around the medio-lateral axis;
- the abduction-adduction of the arm in the transverse plane by approximately 30 degrees in total.

An important role is played by the method considered for applying traction force, a strong wire connecting the free end of the rear frame muscles to the anterior cuff passing through a curved profile, located at a certain distance above the shoulder in the direction of the joint centre, which is called a cam. As the muscle contracts, it exerts a tensile force that

puts the wire under tension and allows the arm to be raised; then the wire under tension, passing through the cam profile at a certain distance from the joint centre, is able to exert a torque that reduces the effort required by the user. For the correct application of torque, it is essential that the wire passes through a cam profile at the ideal centre of rotation of the shoulder at a certain distance, in order to provide the appropriate torque. In this chapter, the design of the transmission system, based on a cam profile centered at the shoulder joint, will be outlined. In the next chapter, the whole exoskeleton architecture, along with all its component, will be discussed.

4.1 The cam profile

The cam profile consists of a rigid shoulder pad that must be fixed to the exoskeleton frame, while the wire runs along it, as the angle of elevation increases. It must then be centered in the shoulder joint of the exoskeleton, which must correspond to the ideal shoulder joint complex, to avoid misalignment between the axes of the exoskeleton and those of the user's body. Otherwise, it will cause pain and potential injury to the wearer, as well as inaccurate results. This profile is designed with an increasing radius:

- To increase the PAM pulling force arm as the angle of elevation of the arm increases, thus improving the compensation torque (M_{mu}), by balancing the reduction in PAM tensile force;
- Extend as far as possible the range of angles of elevation at which the compensation takes place, so that the force provided by the artificial muscle tyre is better distributed over this range;
- To ensure that the torque exerted by the PAM has a similar trend to the torque curve due to gravity. The more the values of the two moments are similar, the greater the action of the support; if the muscle moment curve is greater than the gravitational moment, the user must push downwards to achieve equilibrium; conversely, the user must push upwards.

4.2 Project features

One end of the wire is connected to the cuff, it slides without slipping on the shoulder pad always remaining tangent to it allowing the other end of the wire to be connected to the PAM.

In the Figure 4.1 it is shown a simplified diagram of the shoulder pad at both angles of elevation, 90 and 125 degrees:

- θ_1 is the elevation angle of the upper arm;
- C_0 is the distance between the bracelet and the shoulder joint (SJ);
- r is the lever arm of the tension force F_{mu} with respect to the SJ;
- b is the distance of the attachment point of the wire on the bracelet with respect to the final point of the shoulder pad (Z);
- T is the tangency point of the wire on the shoulder pad.

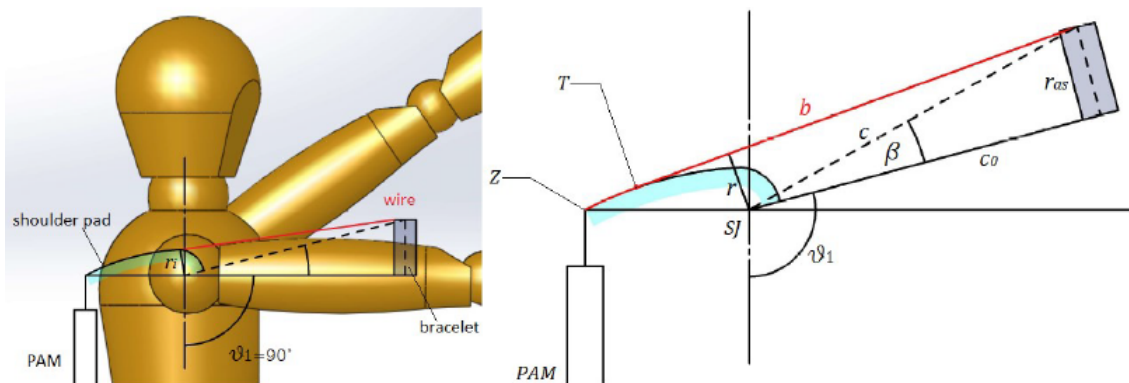


Figure 4.1: Simplified scheme of the shoulder pad, on the left with the upper arm at the elevation angle of 90 degree, on the right instead, 135 degrees.

A graphical method was used to design the shoulder pad. The initial lever arm, r_i , is equal to the initial cam radius (Figure 4.1 on left). As the elevation angle increases, the wire remains tangent to the cam profile (in Figure 4.1 right T is the point of tangency of the wire to the shoulder pad).

However, the lever arm of the tension force no longer matched the cam radius if θ_1 is not equal to 90 degree. For this reason, by considering that the wire must pass through the

fixed end point of the profile (Z in Figure 4.1 right), the lever arm r and b , the distance between the attachment point of the wire on the bracelet and the point Z on the shoulder pad, must be determined graphically from the CAD design, by ensuring the tangency condition of the wire on the profile, and from that the actual length of the PAM.

Bearing in mind that the shoulder pad must be designed to be fixed to the user's shoulder, a value greater than the acromion of 37 mm was chosen [62] as the value for the dimension r_i , where the acromion is the bone that forms the peak of the human shoulder complex. Therefore, the initial radius of the shoulder pad at $\theta_1=90^\circ$ is greater than this value, and was chosen to be equal to 45mm. The subsequent r_i values for angles of 105, 120 and 135 degrees, were derived graphically by knowing the length of the strut and the height of the cuff as shown in Figure 4.2.

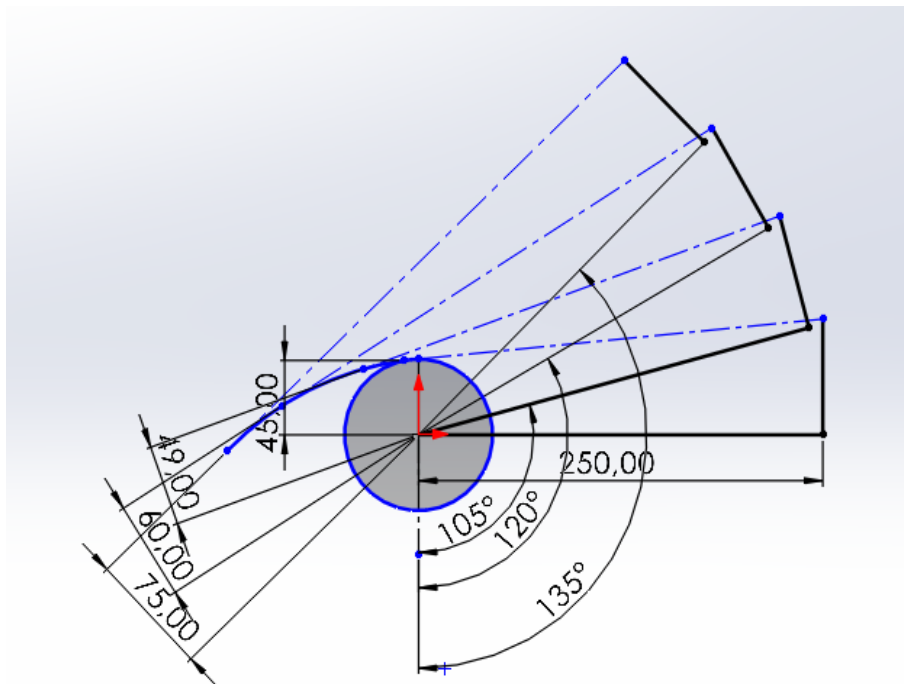


Figure 4.2: Shoulder pad CAD model

Thus, from the graphical discrete results, a 3-degree-polynomial function was applied to approximate the discrete profile of the shoulder pad, producing a continuous profile as shown in the Figure 4.3. The four points show the point of contact of the wire with the shoulder pad. The first on the right represent the camma radius of 45mm. In the Figure 4.4 it can be seen the increasing of the radius of the shoulder pad as the angle of elevation

increases.

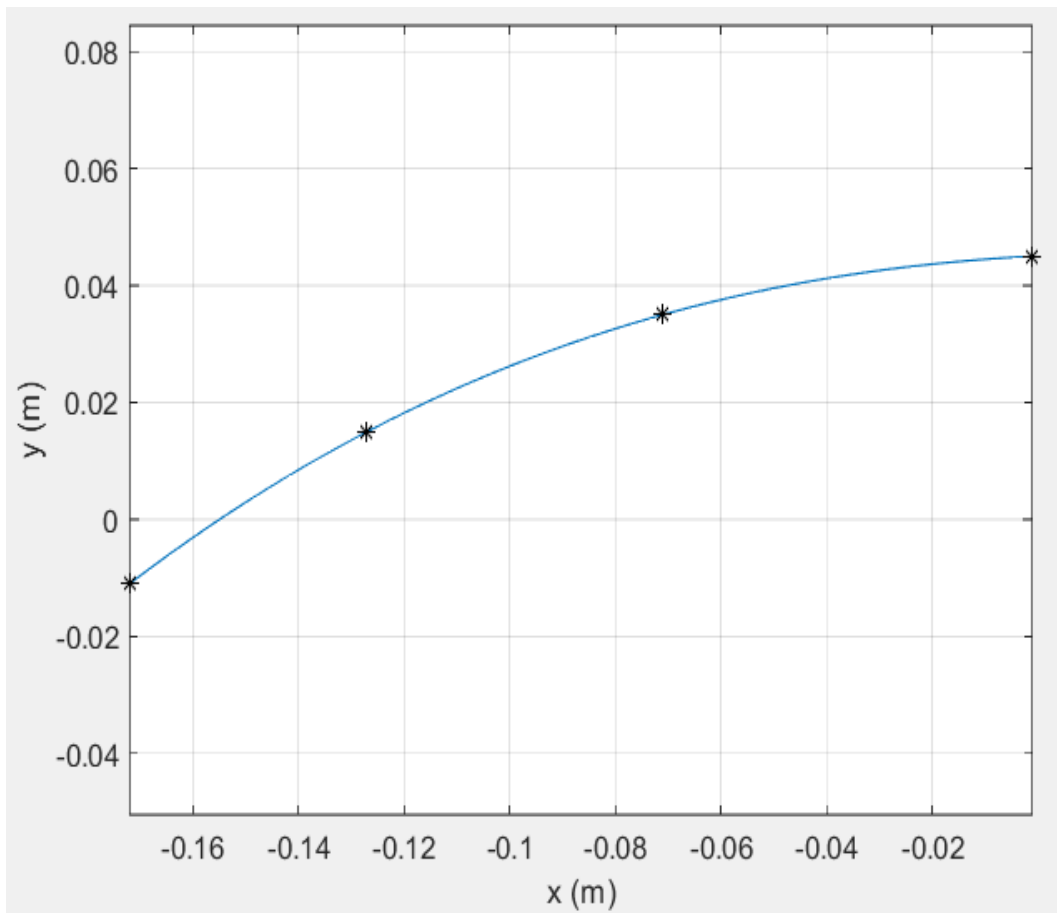


Figure 4.3: Continuous camma profile from graphic method.

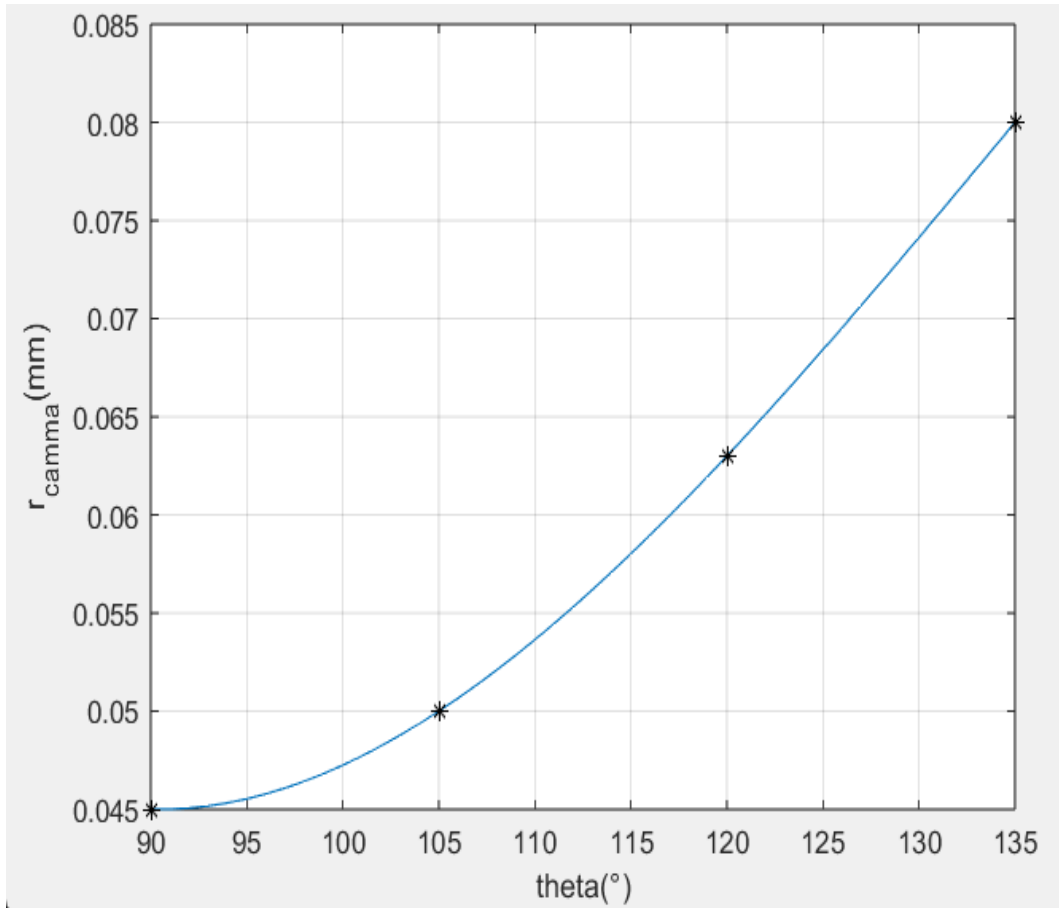


Figure 4.4: Development of radius as a function of elevation angle.

Knowing the nominal resting length of the PAM muscle L_0 , an initial contraction can be imposed by pretensioning the muscle and the shortening of the muscle can be calculated as the angle of arm elevation changes.

In this case two different nominal lengths of the muscle were tested and the best one was chosen for this project:

1. 30mm FESTO DMSP 10-100N;
2. 35mm FESTO DMSP 10-100N, that is the maximum length to take into account that allows it to be placed on the back of a user.

In the first case, an initial contraction of 0.5% was imposed, so the start length of the muscle correspond to 0.29mm. Then the shortening was calculated with the following formula:

$$k = \frac{L_0 - L}{L_0} \cdot 100 \quad (4.1)$$

Where L represents the muscle length for the different angle values shown in the Figure 4.5.

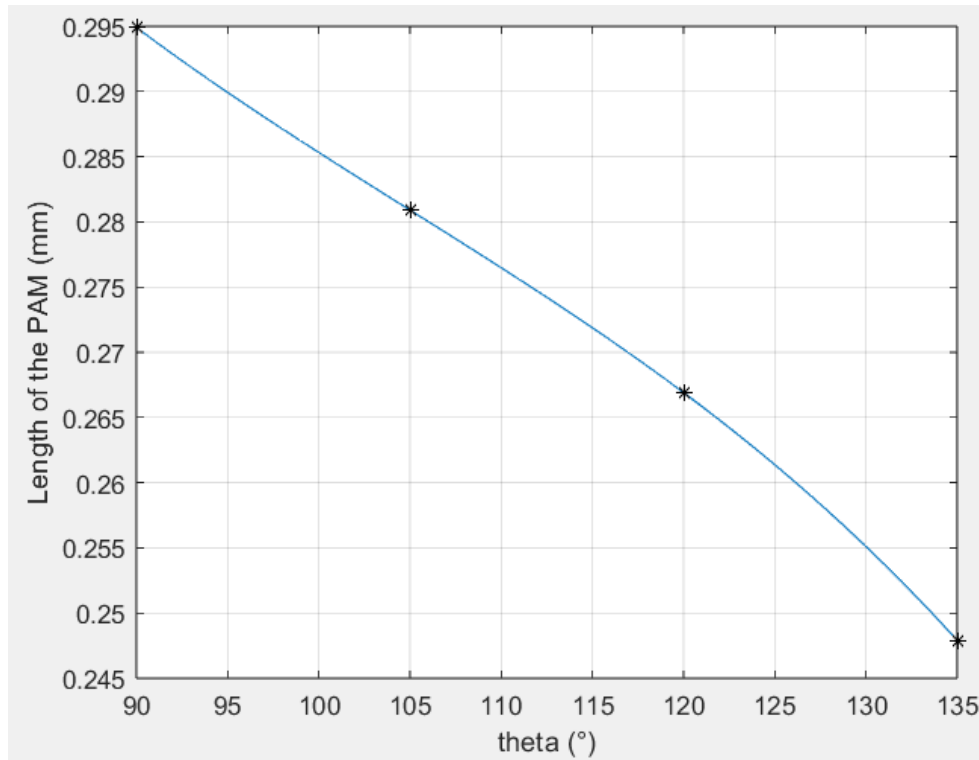


Figure 4.5: PAM shortening for increasing angle values for 30mm FESTO DMSP. The muscle contracts by 1.7%, 6.3%, 11% and 17.4% respectively for theta values of 90, 105, 120 and 135 degrees.

The same procedure was carried out for the second length of the muscle. It is pre-tensioned with the same percentage of the contraction and in this case the initial length of the muscle is 0.34mm.

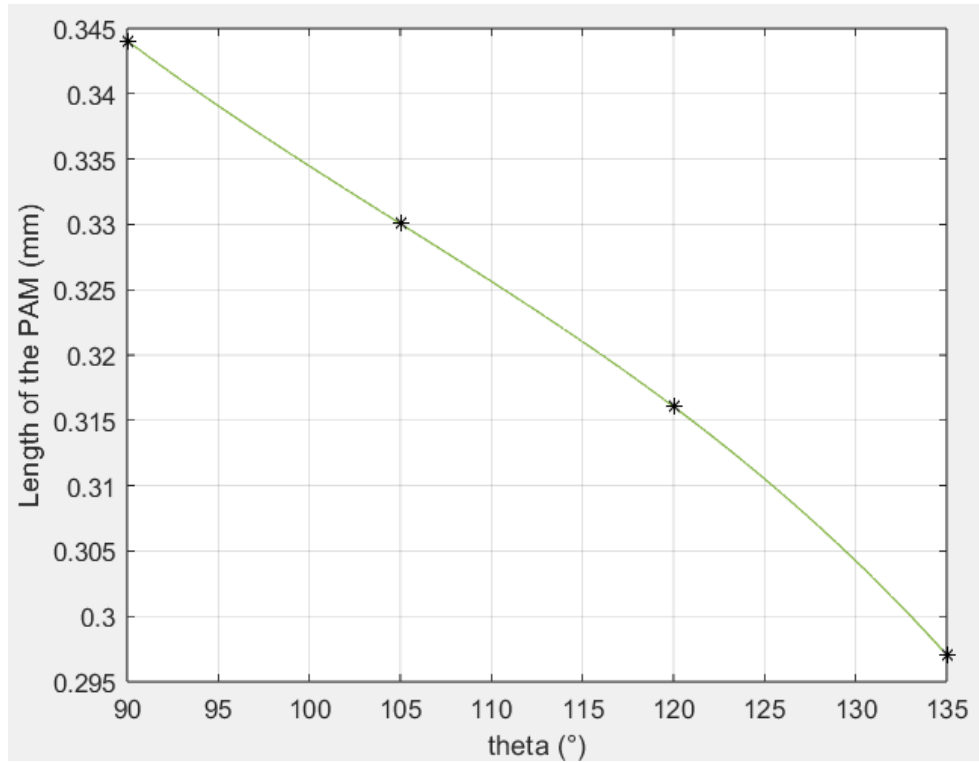


Figure 4.6: PAM shortening for increasing angle values for 35mm FESTO DMSP. The muscle contracts by 1.7%, 5.7%, 9.7% and 15.1% respectively for theta values of 90, 105, 120 and 135 degrees.

In order to select the optimal muscle for the exoskeleton, the moment of force of the PAM was calculated in relation to the gravitational torque of the joint. For the shoulder moment, it is necessary to know the mass and the length of the segments that make up the limb; the lever arm of the force and the angles that have to be performed during the lifting of the arm. This information has been taken from David A. Winter-Biomechanics and Motor Control of Human Movement-Wiley (2009). In the book, the length of the limb segments is referred to the height and are:

$$L_{uarm} = 0.186 * height; \quad (4.2)$$

$$L_{farm} = 0.146 * height; \quad (4.3)$$

$$L_{hand} = 0.108 * height; \quad (4.4)$$

The mass of the arm is the sum of the masses of the hand, forearm and upper arm:

$$m_{uarm} = 0.028 * weight; \quad (4.5)$$

$$m_{farm} = 0.016 * weight; \quad (4.6)$$

$$m_{hand} = 0.006 * weight; \quad (4.7)$$

$$m_{arm} = m_{hand} + m_{farm} + m_{uarm} \quad (4.8)$$

Then the arms of the weight forces of the upper limb elements and the arm of the resultant of the forces from their centre of mass to the centre of the shoulder joint (SJ in Figure 4.1) were calculated, considering the elbow extended, thus the arm and forearm aligned:

$$b_{uarm} = 0.436 * L_{uarm}; \quad (4.9)$$

$$b_{farm} = 0.430 * L_{farm} + L_{uarm}; \quad (4.10)$$

$$b_{hand} = 0.506 * L_{hand} + L_{farm} + L_{uarm}; \quad (4.11)$$

$$b_{tot} = \left(\frac{m_{uarm} \cdot b_{uarm} + m_{farm} \cdot b_{farm} + m_{hand} \cdot b_{hand}}{m_{arm}} \right) \quad (4.12)$$

The gravitational torque without load in the hand, considering only weight force is:

$$M_{shoulder} = m_{arm} \cdot g \cdot b_{tot} \cdot \sin(\theta); \quad (4.13)$$

Then, an external load in the hand of one, two and three kilos has been considered in the calculation of the shoulder moment:

$$m_{arm_{load}} = m_{hand} + m_{farm} + m_{uarm} + payload; \quad (4.14)$$

$$b_{load} = \left(\frac{m_{uarm} \cdot b_{uarm} + m_{farm} \cdot b_{farm} + (m_{hand} + payload) \cdot b_{hand}}{m_{arm_{load}}} \right) \quad (4.15)$$

$$M_{shoulder_{load}} = m_{arm_{load}} \cdot g \cdot b_{load} \cdot \sin(\theta); \quad (4.16)$$

In order to describe the actual behaviour of PAMs, several mathematical models have been developed to fit theoretical results to experimental ones and to work out the equation of the force produced by PAMs.

One of the oldest models considered for an engineering approach to muscle is the modified Hill's muscle model[63], which consists of a viscoelastic model with a variable damper and spring connected in parallel. Using this muscle model[64], several approximations of the static properties have been developed, including equations relating the output force to the

geometric parameters of the pneumatic muscle. For example, the dependence of muscle force F_{mu} can be approximated with good accuracy using an exponential function with six different unknown parameters $a_1, a_2, a_3, a_4, a_5, a_6$, as follows:

$$F_{mu} = (a_1 + a_2 \cdot p) \cdot e^{a_3 \cdot k} + a_4 \cdot k \cdot p + a_5 \cdot p + a_6 \quad (4.17)$$

Firstly, the coefficients of equation 4.17 were obtained by plotting in Matlab the force and contraction values for the different pressure values obtained from the theoretical curves given in the FESTO DMSP 10-100N manual. These values were interpolated through the *fitype* function to obtain the value of the six coefficients.

In equation 4.17, k was substituted for the value of muscle shortening obtained in equation 4.1 for both the 30mm and 35mm long muscles, and the force torque generated by the muscle was calculated by comparing it with the gravitational torque.

The equation for the PAM muscle torque is as follows:

$$M_{PAM} = F_{mu} \cdot r_{camma_{fit}}; \quad (4.18)$$

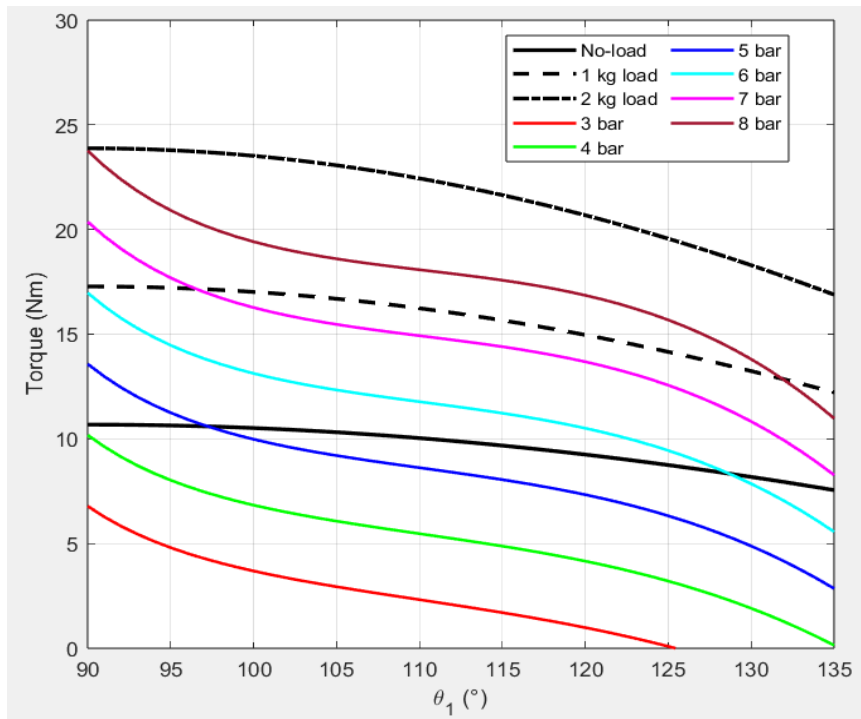


Figure 4.7: Comparison between gravitational torque and PAM torque for muscle length 30mm.

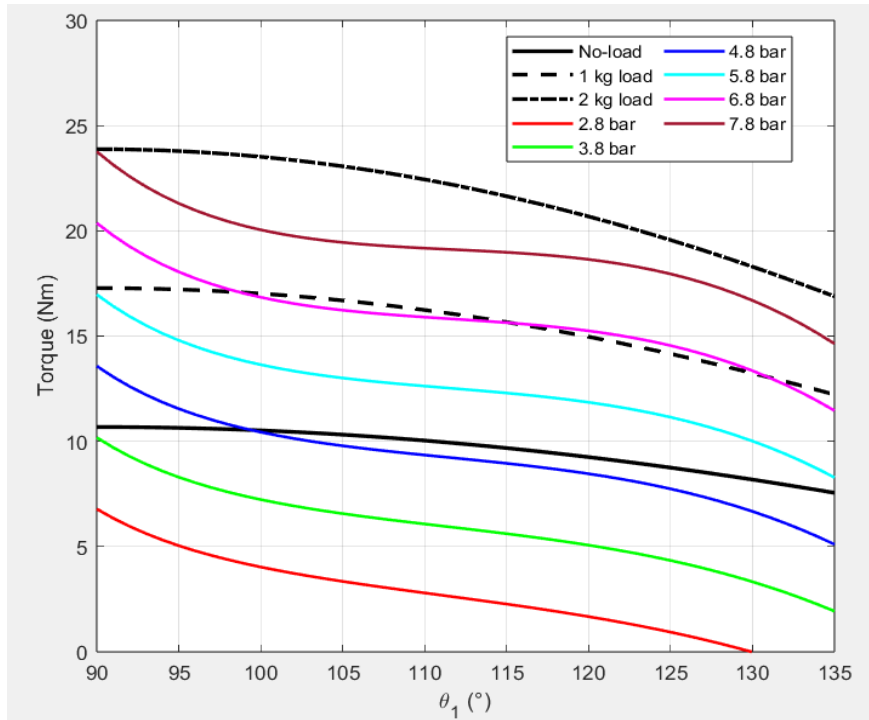


Figure 4.8: Comparison between gravitational torque and PAM torque for muscle length 35mm.

Table 4.1: Coefficients from theoretical curves of FESTO 10-100N 30mm length.

	coefficients	95% confidence bounds
a_1	0.01534	(0.005408,0.02526)
a_2	130.8	(123.3,138.2)
a_3	-0.3972	(-0.4116, -0.3827)
a_4	-0.02605	(-0.02669, -0.02541)
a_5	0.7911	(0.7775,0.8047)
a_6	-127.1	(-134.6, -119.6)

Comparing the two graphs, it can be seen that the gravitational torque curves for a subject holding 1kg on the hand follow the trend of the torque curves of the 35mm long PAM more closely when it is pressurised to 6.8 bar than 7 bar of 30mm long muscle. In order to best illustrate which PAM has the smallest difference, the average percentage errors between the gravitational torque and the torque generated by the muscle have been calculated for both, in order to see which follows the profile of the torque generated

by the PAM more closely and can therefore provide greater support during overhead tasks.

Table 4.2: Average percentage errors between gravitational and muscle torque

	0kg	1kg	2kg
<i>PAM30mm</i>	22.27%	8.4%	19.3%
<i>PAM35mm</i>	12%	3%	13%

The table 4.1 shows that the percentage errors for the 35mm muscle length are significantly lower than for the 30mm muscle length.

The minimum support torque over the entire flexion-extension range, expressed as a percentage of the required torque, was also calculated.:

- For 30mm FESTO, for a hand load of 0kg, 1kg and 2kg respectively, the torque support percentages are 37.7%, 67.7% and 65%;
- For 35mm FESTO, the percentages of torque support are 67.5%, 82.1% and 84.3% respectively.

In this way, it is possible to observe how the 35mm muscle offers greater support to the user and therefore better reflects the characteristics sought for the purposes of this project.

Secondly, we moved on to isometric and isotonic characterisation of the muscles in the laboratory, then experimentally calculating force and contraction values, interpolating them and finding new coefficients that best approximate the data thus obtained.

4.3 PAM characterization

The static characterisation of these actuators aims to know the trend of the force developed by the actuator for different values of the working fluid pressure and for different fractions of the stroke realised, in order to calculate the experimental coefficients to see any difference with the theoretical performance.

Isotonic characterisation tests can be carried out, thus at a constant load, using, for

example, calibrated weights, leaving one of the end caps free and suspending the actuator from the other; or isometric tests can be carried out, constraining both end caps and measuring the actuating force with a force transducer for different values of fluid pressure.

4.3.1 Isometric characterisation

Isometric testing was carried out on 300mm long FESTO DMSP 10-100N muscle.

The first step was to prepare the test bench on which the above tests were carried out. This consisted of a load cell, model Dacell series UMM-K100, calibrated and connected to the test bench at the top, to which one end of the muscle was attached, which in turn was connected to a pneumatic bench as a constant pressure source via a small tube running the distance between the pressure source and the muscle. To check the exact value of the pressure and avoid leakage, the pressure gauge was placed close to the muscle, at the same height as the pressure inlet. The other end of the muscle was fixed to a moving crosshead, clamping it at a certain height by pressurising the locking cylinders, to respect the nominal length of the muscle. To check that the length of the muscle remained constant, the metre has been used as a measuring instrument. Figure 4.9 shows how the components of the test bench are positioned for testing.

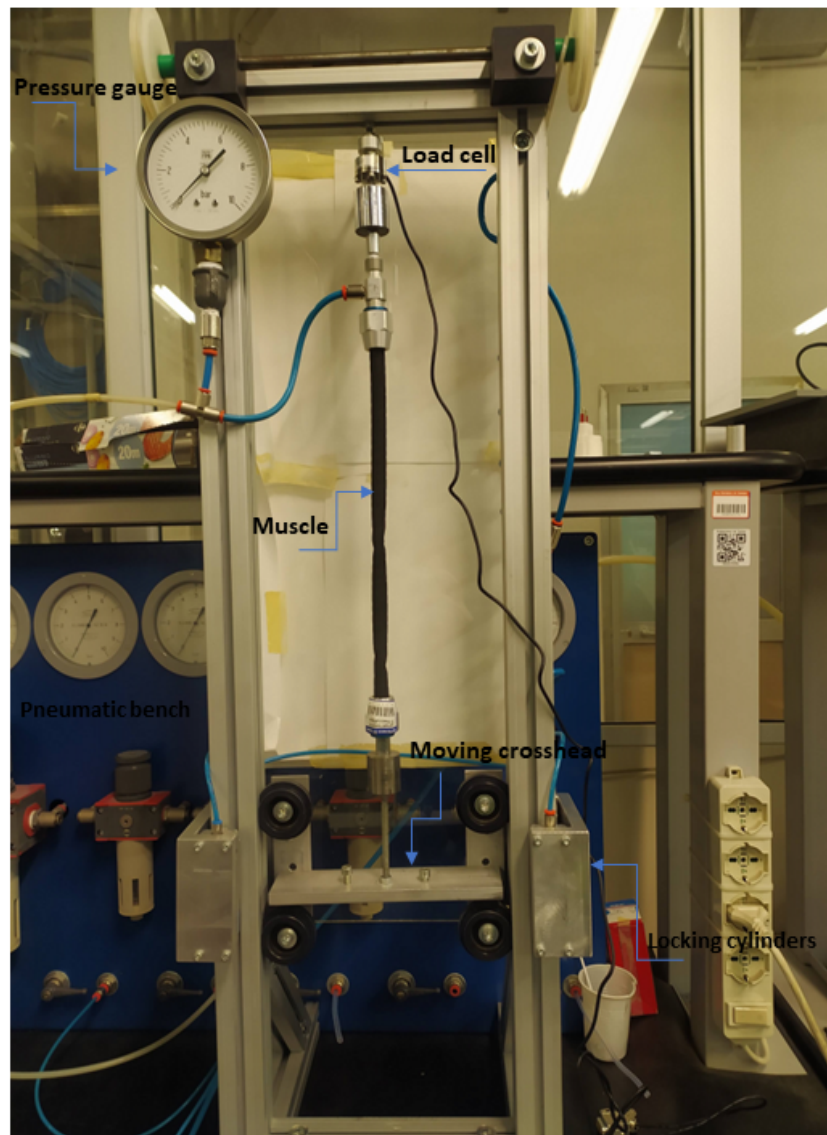


Figure 4.9: Test bench: configuration of isometric test.

The isometric tests were performed by pressurising the muscle with a supply pressure of 0 to 8 bar at 1 bar intervals, representing the working pressure range, while keeping the length of the muscle constant. An upward cycle of increasing pressure values was performed first, followed by a downward cycle of decreasing pressure values to test hysteresis.

This test was carried out on different lengths of muscle, corresponding to the length reached by the muscle each time it was subjected to different levels of pressure, without any load and with only the upper end fixed.

In this way, the load cell can measure the force generated by the muscle as a function of pressure for different values of muscle length.

Figure 4.10 shows the force characteristics for the 300-mm-long muscle. It can be seen that the maximum contraction of the muscle is 22% of its nominal length than the maximum allowable contraction of 25%.

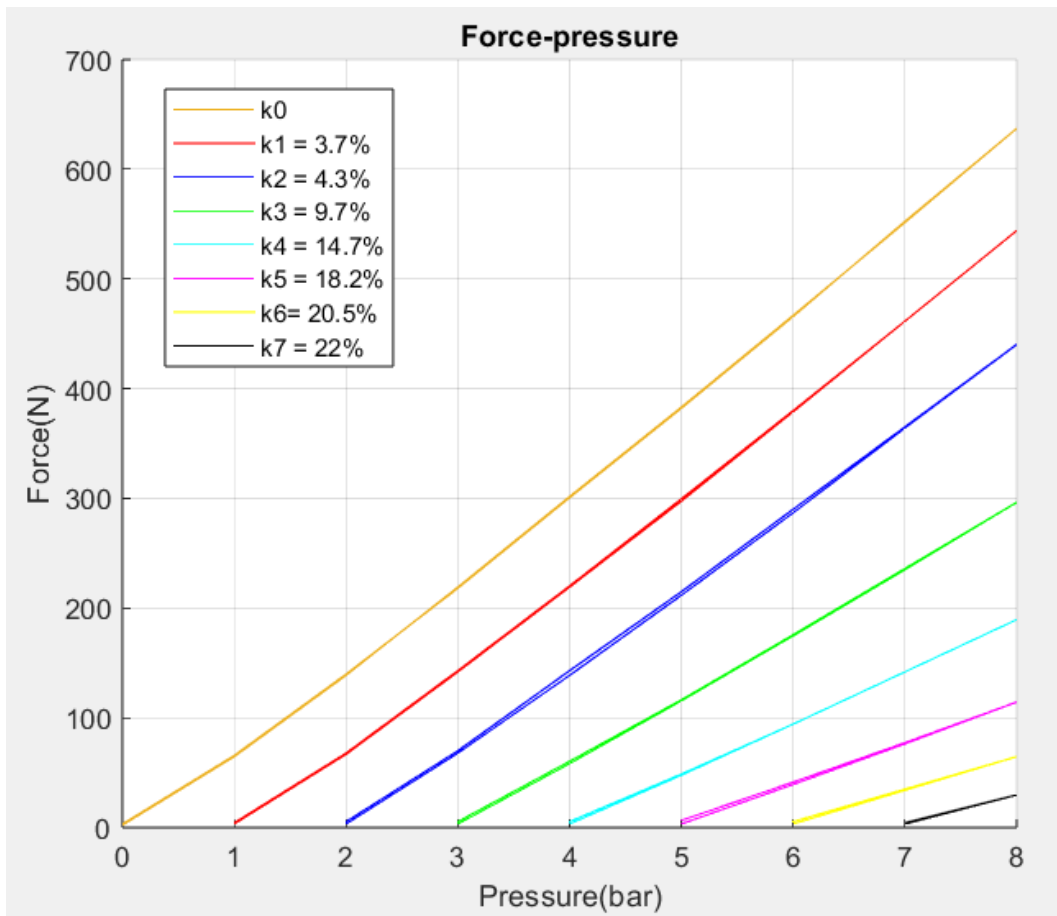


Figure 4.10: Force evolution as a function of pressure for different contraction values.

4.3.2 Isotonic characteristic

For the constant load test, calibrated weights of 0, 5, 10, 20, 30, 40, 50 and 60 kg are suspended to one of the headers while the other is fixed to the frame. In this way, by applying different values of supply pressure, it is possible to determine the stroke variation of the free header by measuring their displacement. Figure 4.11 shows several curves of the actuator contraction as a function of the supply pressure; these curves are parametrized with respect to the external load, which was controlled, so that the force generated is known.

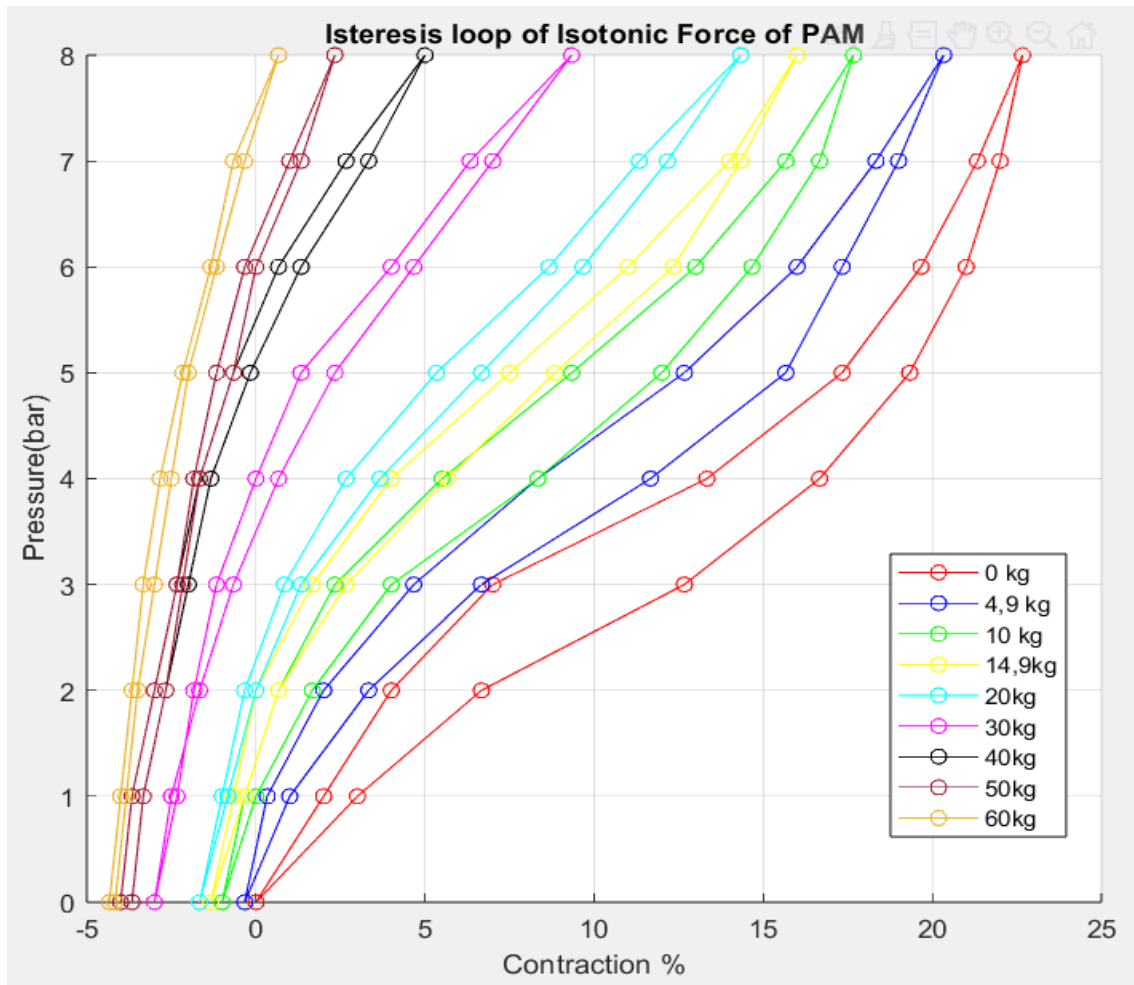


Figure 4.11: Trend of the pressure as a function of the contraction for different force values with an obvious hysteresis for a low load.

Based on equation 4.17, a graph of the values of the force generated by the muscle as a function of the percentage of contraction for the allowed pressure values was obtained, knowing the force and pressure, and replacing k with the experimental shortening values. The experimental values were then interpolated using *fitype* Matlab function to obtain the six coefficients of the equation that best approximated the force evolution.

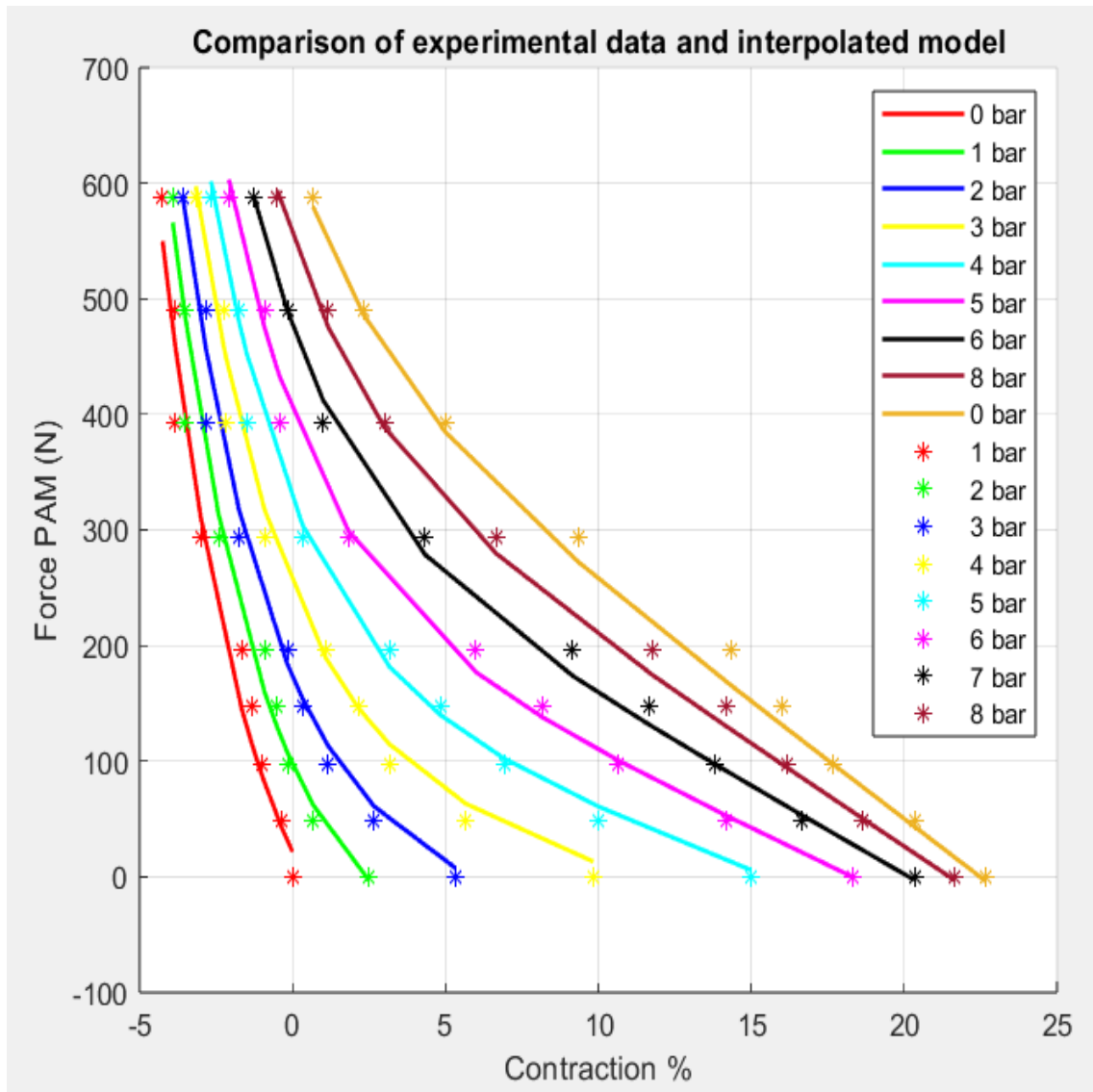


Figure 4.12: Trend of force as a function of contraction for different pressure values.

In the figure 4.12 the asterisks represent experimental data while continuous lines represent the approximation of experimental data by mathematical formula. It can be seen how well the found model approximates the experimental data.

In the table 4.3, there are reported the value of the six coefficients and their range of belonged, which represents the 95% of confidence bounds.

Table 4.3: Coefficients from eq. (4.17) for Festo DMSF-10-100N static characteristics

	coefficients	95% confidence bounds
a_1	0.01521	(-6.272e+13, 6.272e+13)
a_2	163	(140.3, 185.7)
a_3	-0.34	(-0.371, -0.3089)
a_4	-0.02522	(-0.02745, -0.02298)
a_5	0.7438	(-6.272e+13, 6.272e+13)
a_6	-141.5	(-164.3, -118.7)

Using the coefficients just found, the torque generated by the muscles was calculated and compared with the gravitational torque.

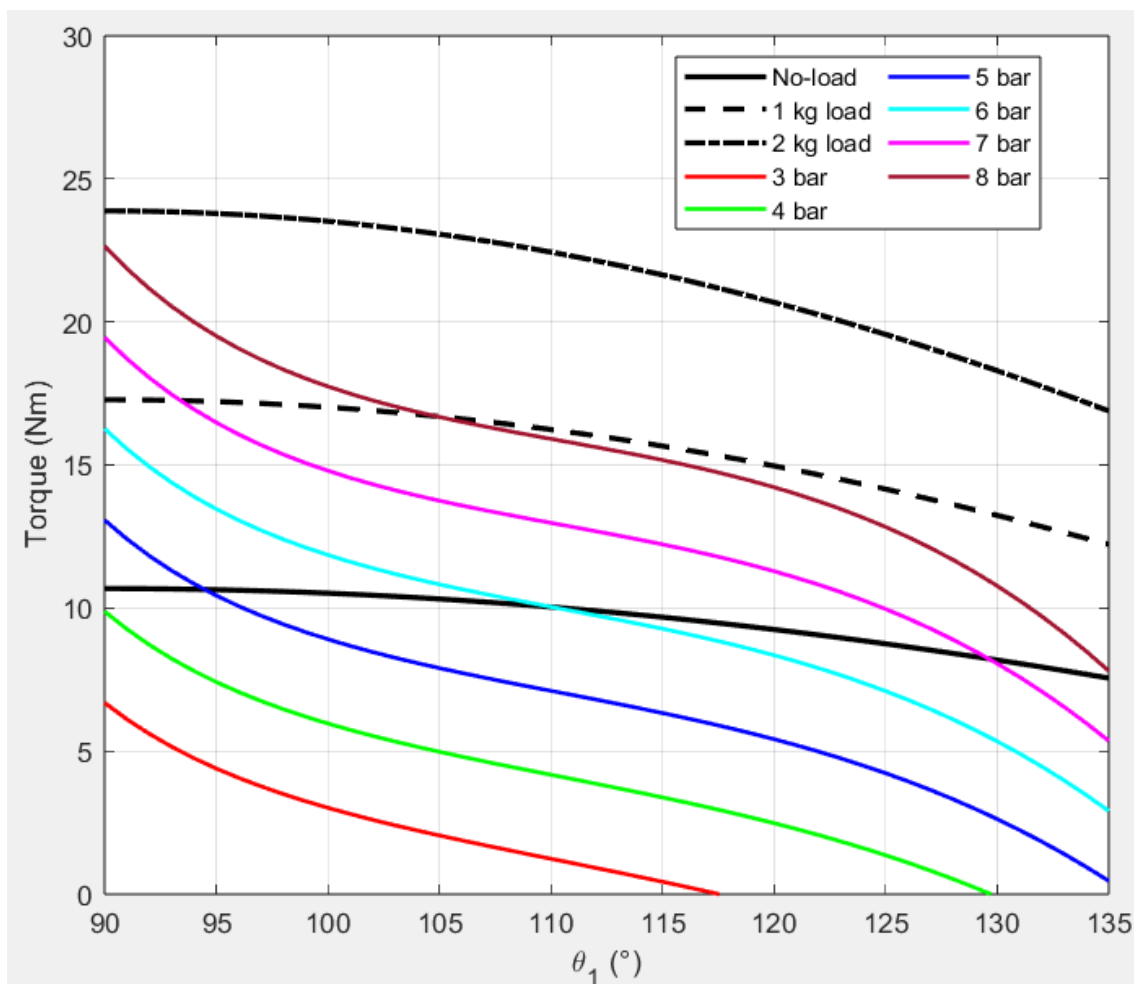


Figure 4.13: Comparison between gravitational torque and PAM torque experimentally obtained for muscle length 30mm.

The figure 4.13 shows that the gravitational torque generated by holding a 1 kg weight has a tendency more similar to the curve of the muscle pressurised at 8 bar, and that with a 2 kg weight, on the other hand, no torque of the muscle can follow the tendency of the gravitational torque. In this case, the experimental approximation of the force results in poorer support for the gravitational torque.

4.3.3 FESTO DMSP-10 -100N of 350 mm

The same procedure was performed to characterize the muscle of length equal to 350mm. Here below it is possible to see the curve of isotonic characterization of the muscle and the comparison between sperimental datas and fitting model.

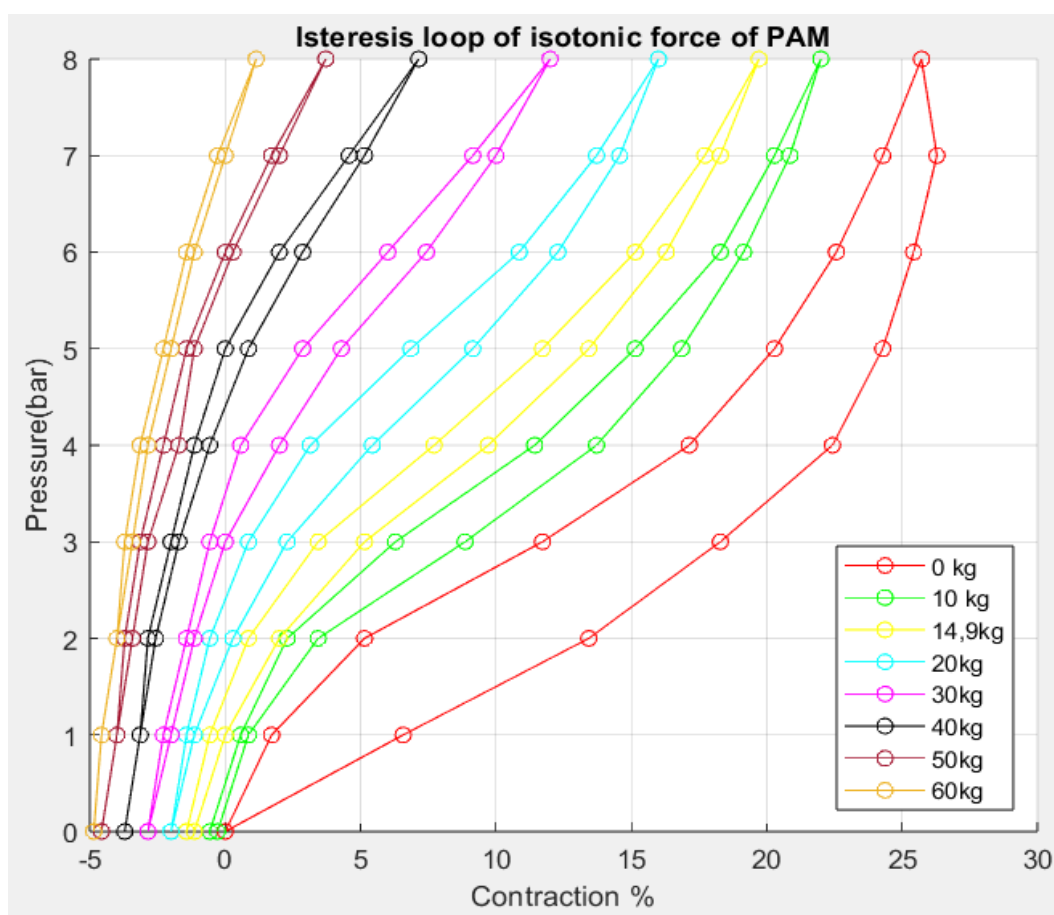


Figure 4.14: Isotonic characteristic of the muscle.

In the Figure 4.14, there is a small overshoot of the guaranteed contraction for the value of the fluid pressure above 6 bar, for the load of zero kg.

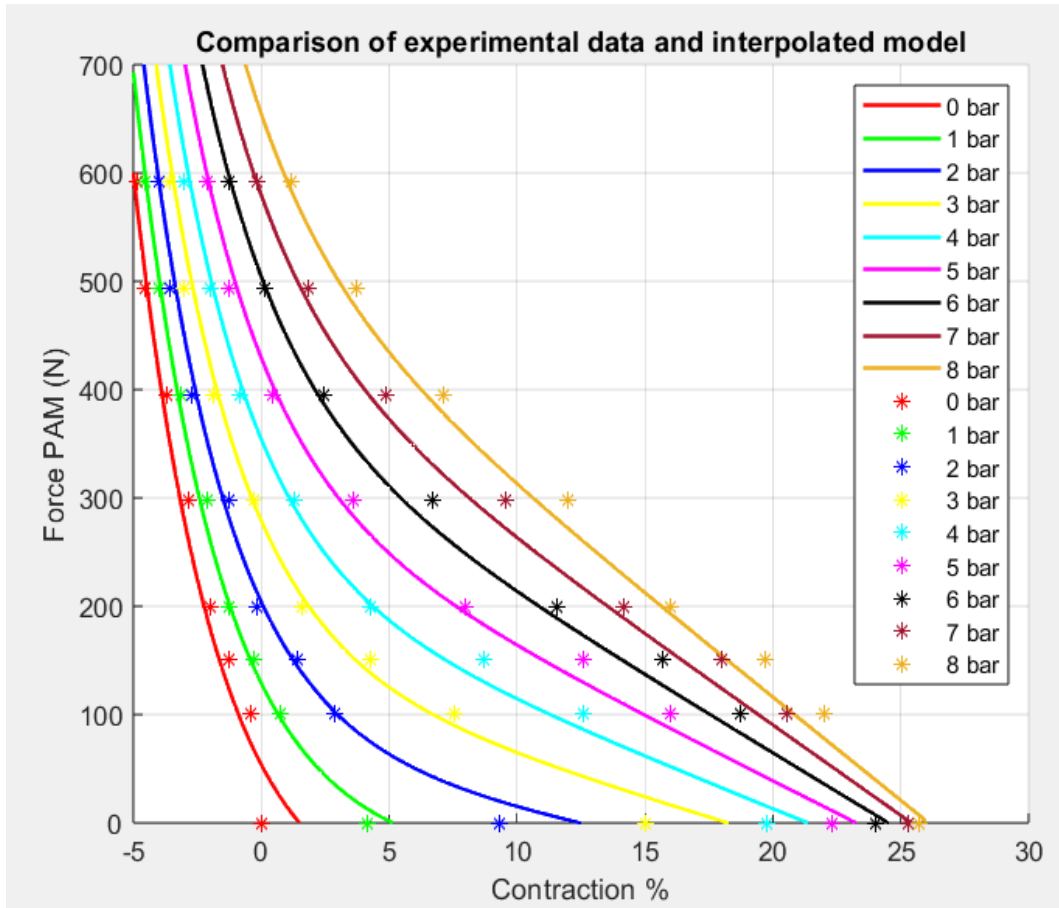


Figure 4.15: Trend of force as a function of contraction for different pressure values.

Table 4.4: Coefficients from eq. (4.17) for Festo DMSP-10-100N of length 350mm static characteristics

	coefficients	textbf95% confidence bounds
a_1	0.01733	(-2.254e+14, 2.254e+14)
a_2	144	(128.7, 159.3)
a_3	-0.3133	(-0.3343, -0.2922)
a_4	-0.02379	(-0.02518, -0.02241)
a_5	0.7336	(-2.254e+14, 2.254e+14)
a_6	-90.41	(-106.4, -74.45)

As before, the coefficients obtained were used to produce the trend of the force torque generated by the 350 mm long muscle and to compare it with the gravitational torque.

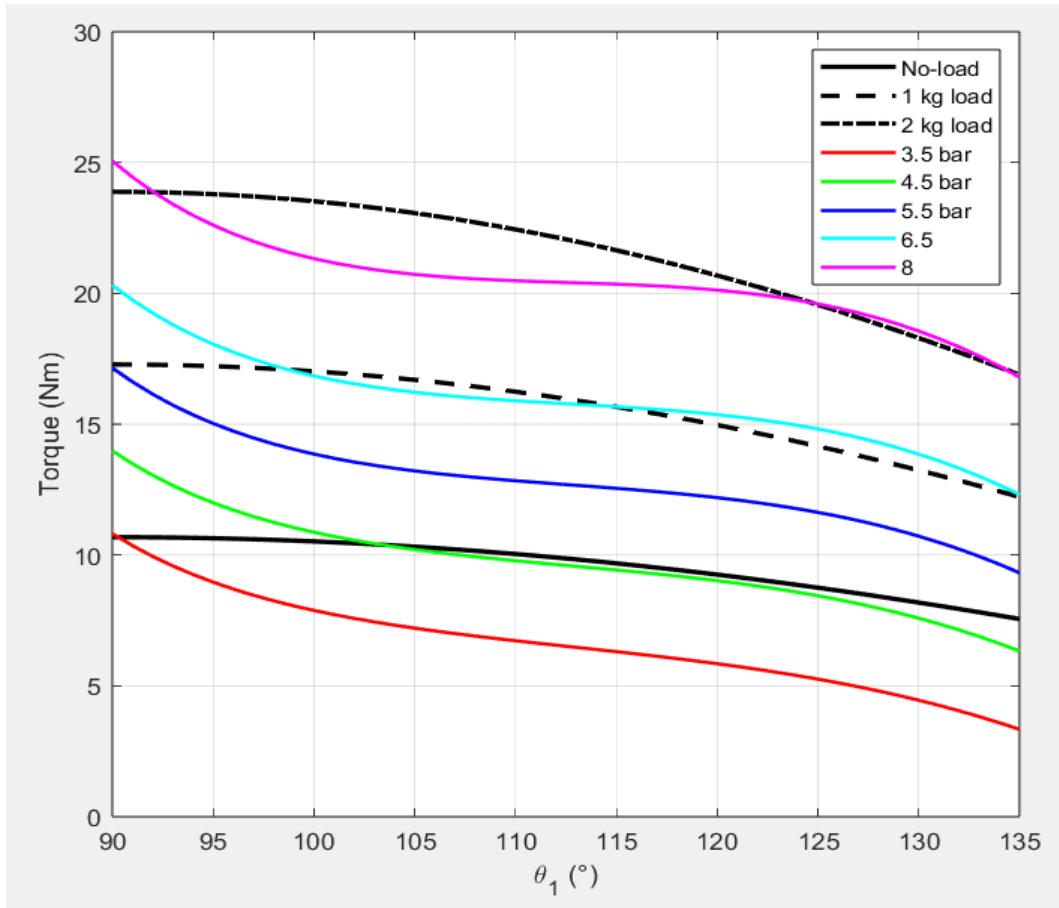


Figure 4.16: Trend of force as a function of contraction for different pressure values.

The Figure 4.16 shows that the muscle torque curves follow the gravitational torque very well in all three cases:

- With no load, it can be seen for angles greater than 105 degrees, the muscles exerts a torque that completely compensates for the user's muscular work;
- With a weight of 1 kg, the two curves are very close, the difference is very small, so that the PAM muscles also compensate for the gravitational torque in this case;
- For a weight of 2 kg, it is difficult in all cases to completely compensate for the subject's muscular action, but this is the best case presented so far, as for angles greater than 125 degrees the two curves are very close and there is compensation.

For the muscle torque, the pressures were chosen whose curves' trends were closest to those of the gravitational torques. Initially, all the curves corresponding to the pressure values ranging from 3 to 8 bar were plotted at a step of 0.5, in order to accurately choose

those with the most similar trend to the gravitational torques, which turned out to be 4.5 bar, 6.5 bar and 8 bar respectively.

Expressing the support torque as a percentage of the required torque, it has 69.1%, 82.4% and 89.8% respectively, which are higher than the support given by theoretical coefficients.

The FESTO 10-100N, 35mm long, was chosen for this project because it has shown the best characteristics so far, giving the user the greatest and best contribution and support.

Chapter 5

Exo design

The exoskeleton aims to help all workers who spend hours a day working above their heads, which can cause serious health problems in the long term.

For this project, the exoskeleton has been designed to be worn by a user of medium height and to be connected to the PORTWEST 2 POINT-COMFORT HARNESS, which is characterised by the presence of three D-rings, one on the back and two at the side of the hips, where it is attached to the exoskeleton by means of Velcro. It is equipped with a breathable molded back, easy-to-adjust buckles for excellent fit and comfort, and polyester straps for maximum durability.

The exoskeleton consists of two main parts, the back frame and the arm. The frame has the function of unloading the forces generated by the muscles that allow the arm to be elevated on the hips. Both the width of the shoulders and the length of the back can be adjusted for a user who is between 1.70 and 1.80 metres tall, to be as comfortable as possible and to fit the user's body as best as possible, using two square bars that slide into a square tube at shoulder height and two telescopic bars that slide down the back. The length of the back is between 48.96 and 51.84 centimetres, while the width of the shoulders ranges from 44.03 to 46.62 centimetres. The exo arm must allow the two degrees of freedom described in the previous chapter, namely flexion of the arm in the sagittal plane between 90 and 135 degrees and abduction-adduction in the transverse plane of 30 degrees, which is possible thanks to the presence of two joints.

CAD design was performed in Solidworks 2022. In this chapter, we will examine in detail all the components of the exoskeleton.



Figure 5.1: PORTWEST 2 POINT-COMFORT HARNESS a)Frontal view b)Back view

[https://www.safety-harness.com/all-harnesses/
portwest-2-point-comfort-harness--pack-of-5-/fp14rer](https://www.safety-harness.com/all-harnesses/portwest-2-point-comfort-harness--pack-of-5-/fp14rer)

An overview of the exoskeleton is shown in the figure 5.2.

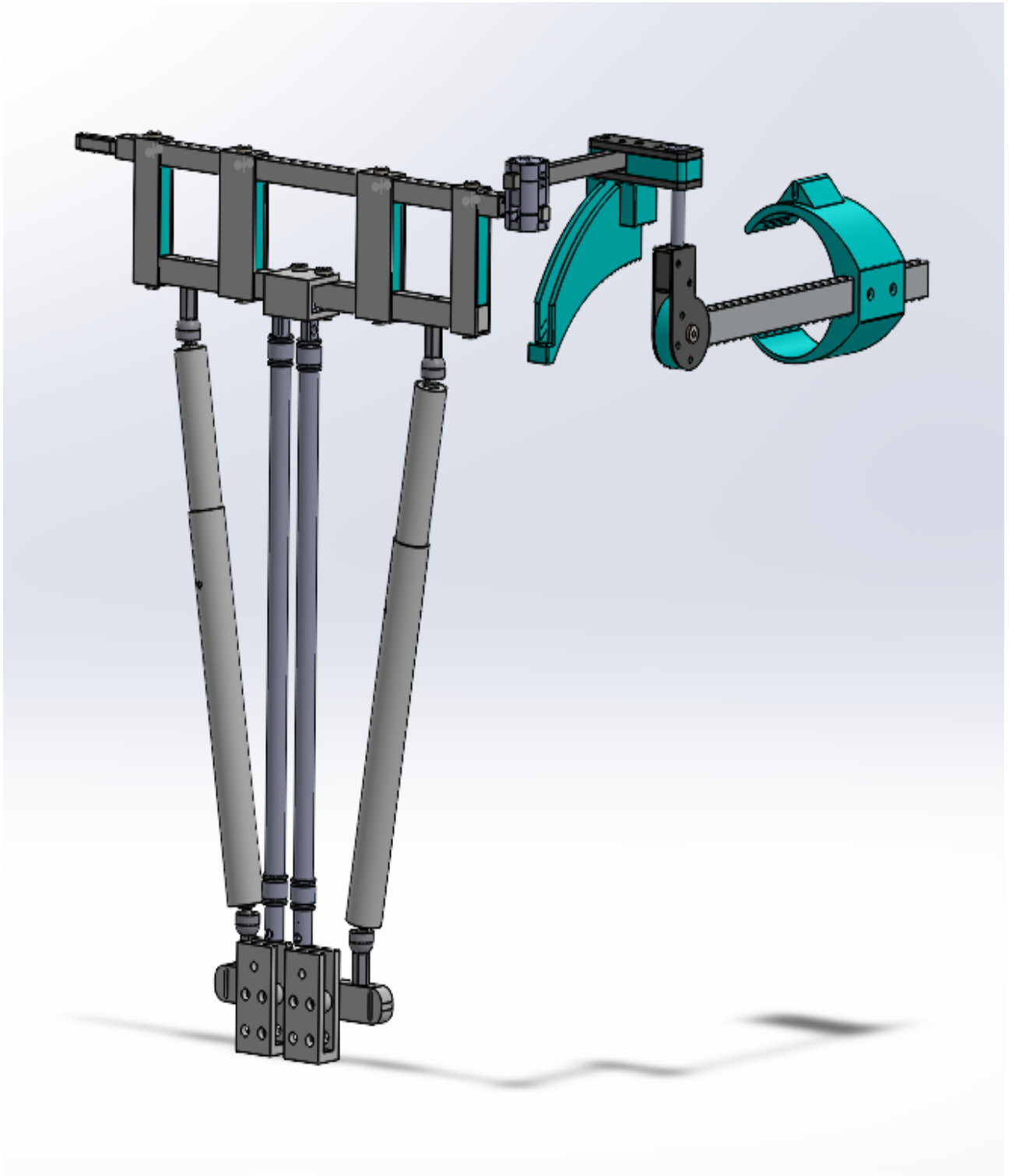


Figure 5.2: The exoskeleton composed of arm and back frame.

5.1 Exoskeleton arm

In detail, the arm is made up of a series of parts connected by hinges, pins and screws that allow movement. In the figure 5.3 it can see a frontal view of the exoskeleton arm.

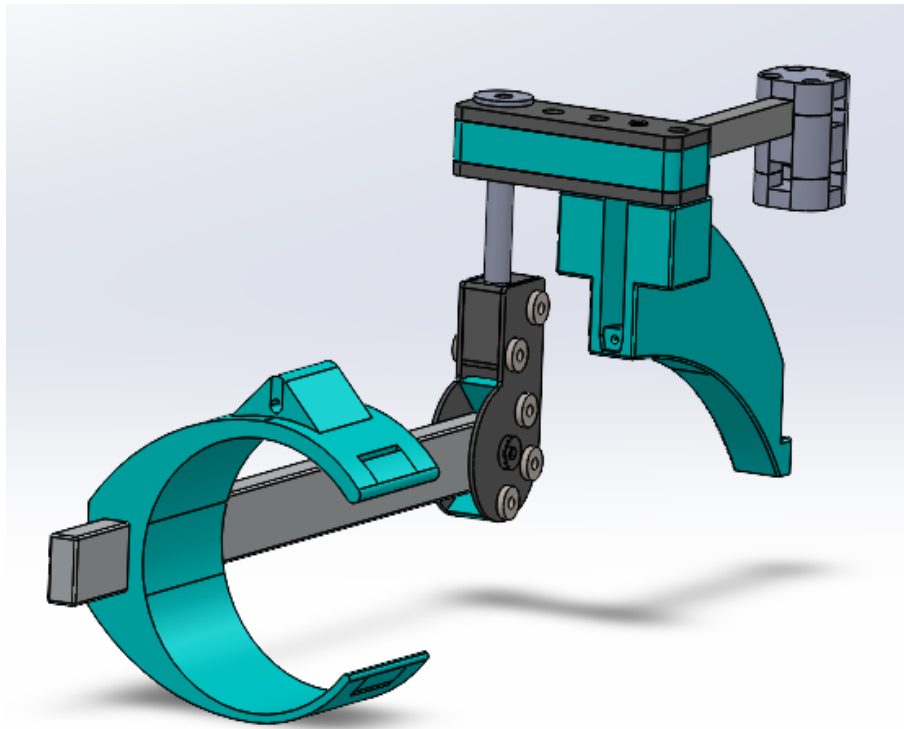


Figure 5.3: A frontal view of exoskeleton arm.

In the sagittal plane, from front to back, the arm consists of a rigid strut that runs along the outside of the arm, from the elbow (excluded) to the user's shoulder, where the median lateral axis of the center of the GH joint passes. The strut must necessarily be rigid given the amount of horizontal forces developed by the wire, otherwise the bracelet would end up flowing along the arm.

The bracelet has the shape of a C and is placed at the beginning of the strut, to which it is attached through two M4 countersunk screws that allow its position to be adjusted than the six holes on the strut. The bracelet is designed to wrap around the user's arm and is tightened with Velcro, in fact, it has openings to allow the passage. The inside of the bracelet is later covered with a sponge to ensure maximum comfort while the bracelet is made of PLA and the strut is made of alluminium. In the upper part of the bracelet, there is a space that allows the passage and hooking of the wire that connects the end of

the muscle that is in the back frame, to the bracelet, as described in Chapter 4.

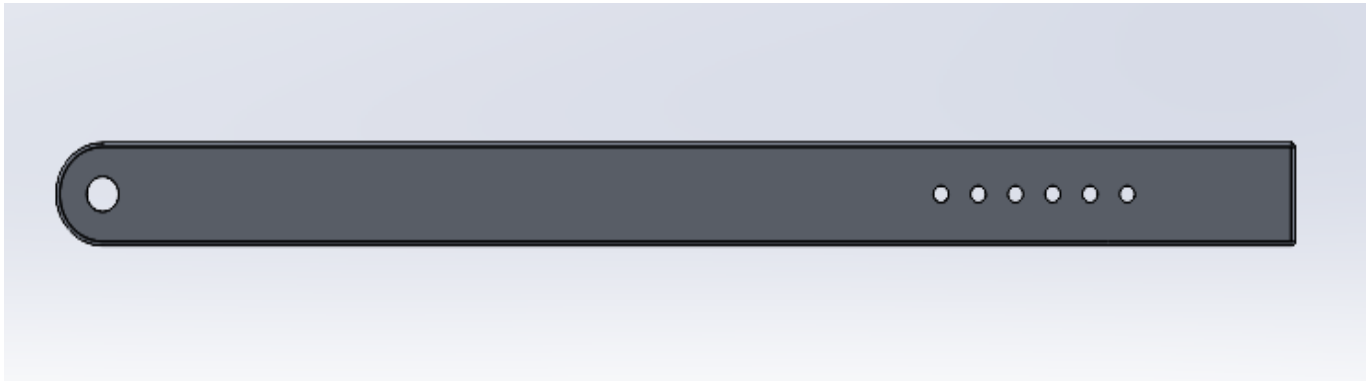


Figure 5.4: Rigid strut that runs along the outside of the arm, from the elbow (excluded) to the user's shoulder.

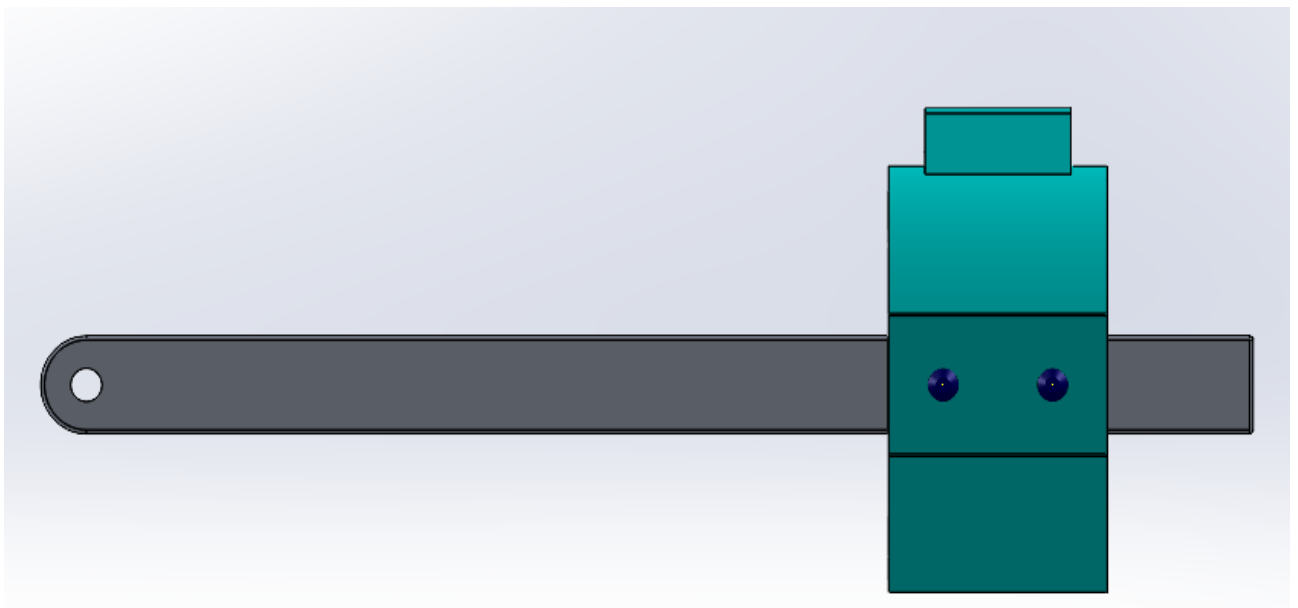


Figure 5.5: The C bracelet placed at the beginning of the strut through two M4 counter-sunk screws.

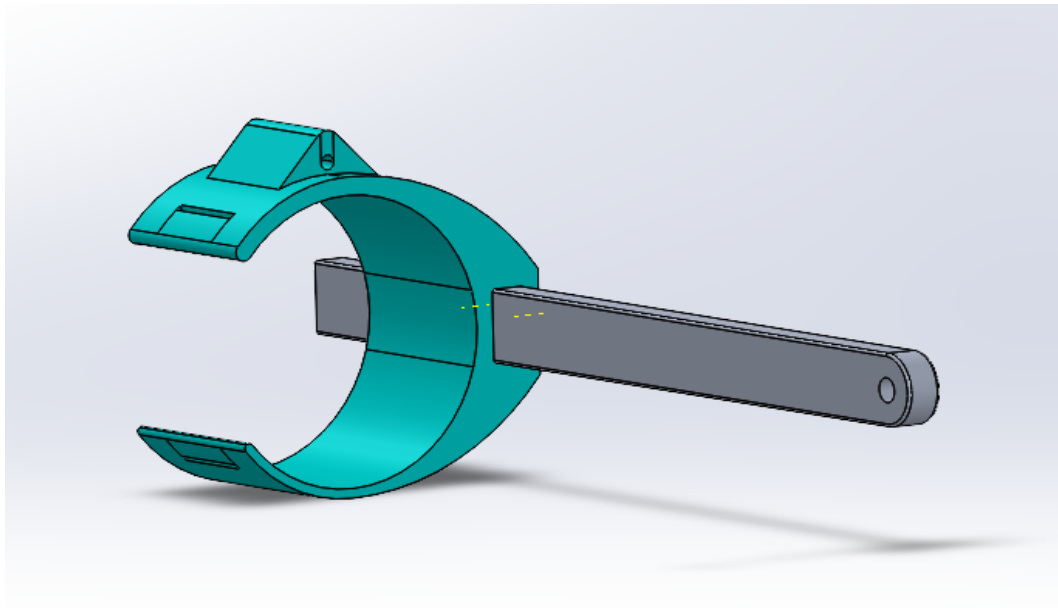


Figure 5.6: Interior view of strut and bracelet.

The end of the strut is not rectangular but circular with a hole in the centre and inside this hole a bushing is inserted to allow the rotation of the strut around the lateral medial axis, which must correspond to the same axis as the GH shoulder joint.

The end of the strut is located between two rounded L-shaped plates held together by five M4 screws, three passing through a PLA filling and two passing through an aluminium filling.

As Figure 5.5 shows, the PLA fill surrounds the end of the strut and defines the range of movement of the arm elevation, 45 degrees upwards and 30 degrees downwards in relation to the horizontal axis. The first degree of freedom is therefore given by the hinge formed by the M5 hole and the bushing, which allow the arm elevation.

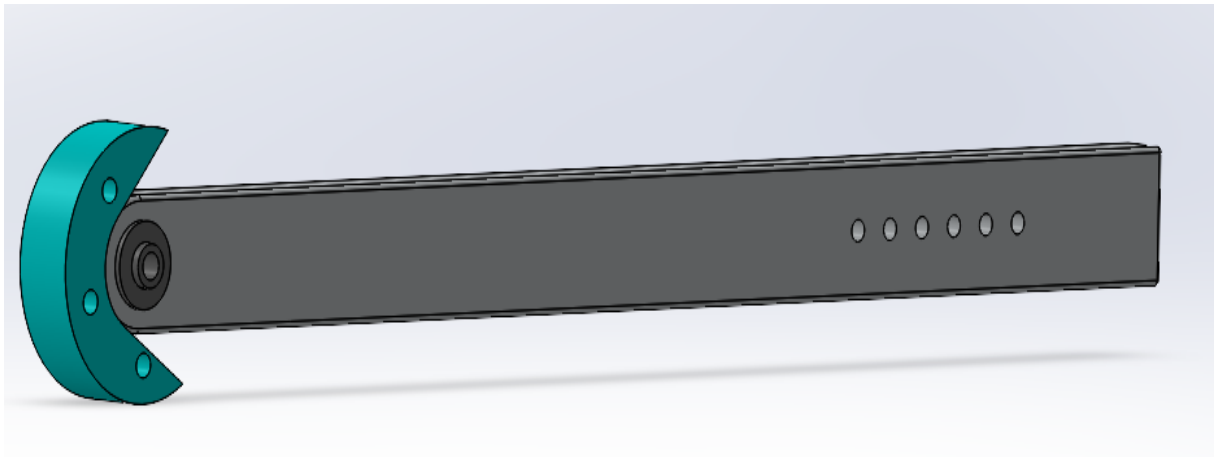


Figure 5.7: PLA filling that defines the arm range of movement at the end of the struct.

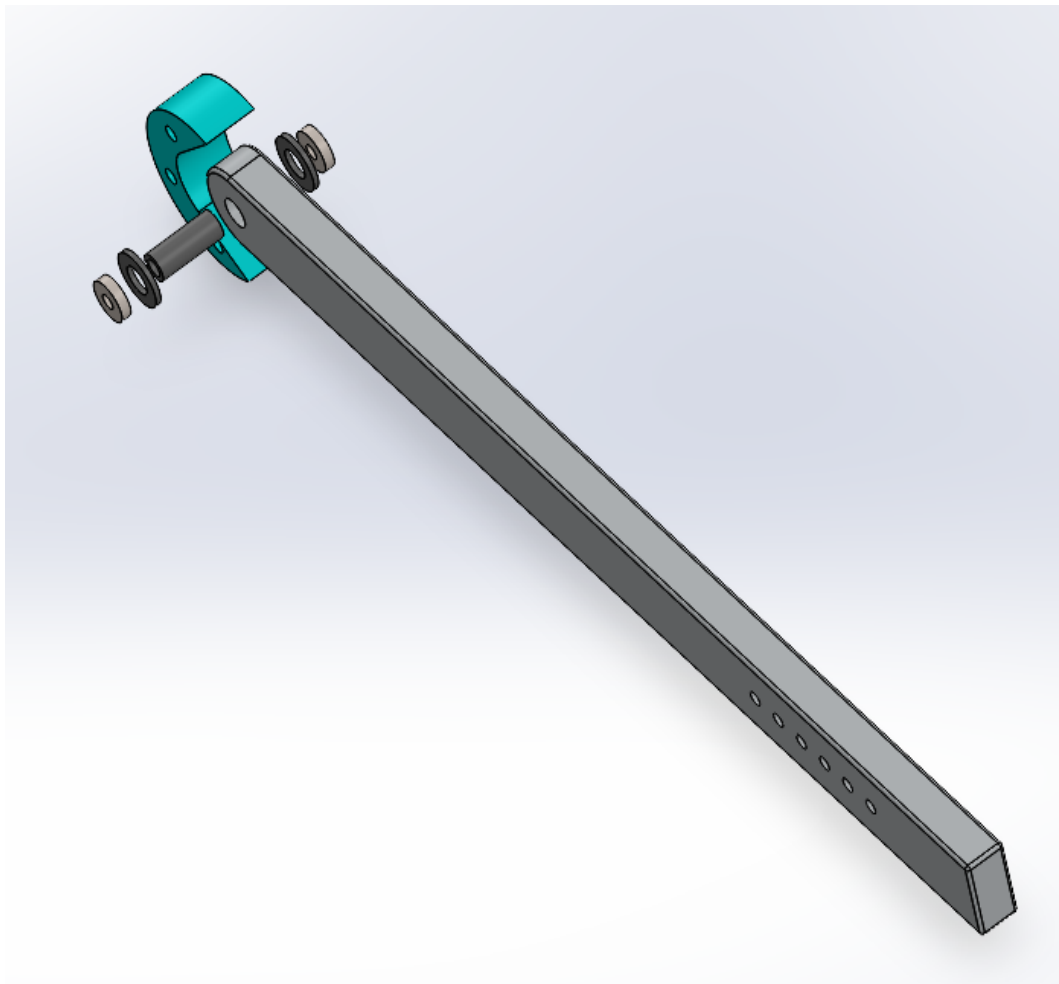


Figure 5.8: Exploded view of the joint that represents the first degree of freedom.

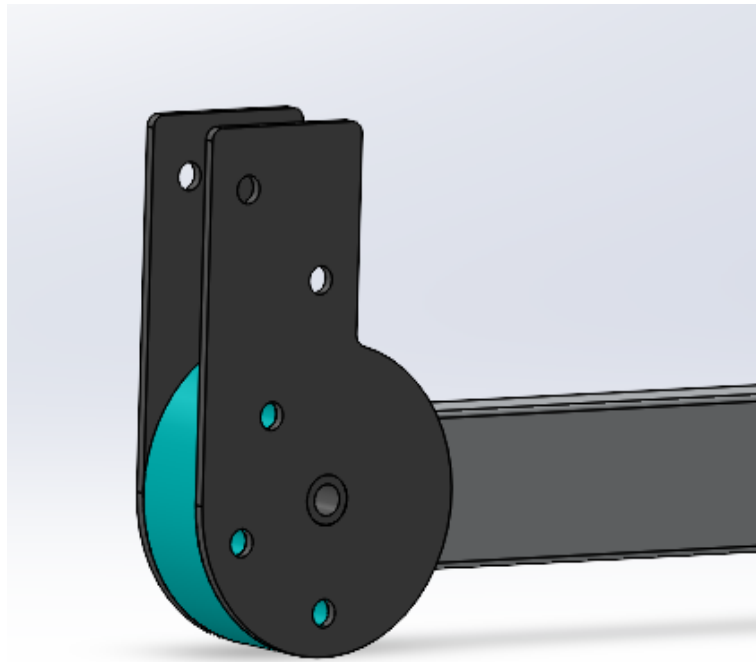


Figure 5.9: Rounded L-shaped plates with the hinge that allows the first arm degree of freedom.

The aluminium filler, on the other hand, has a rectangular shape and is positioned to coincide with the upper part of the L-shaped plates. On the upper surface it has an M10 hole that houses a pin that connects the part just described with the second joint, which allows the arm to be abducted and adducted in the transverse plane, to which the cam is also attached. Both the pin and the hole are threaded, which makes it possible to adjust the length of the pin and consequently the distance from the cam to the subject's shoulder, since if the pin is screwed all the way into the hole, the minimum distance between the shoulder and the cam is 8 mm because the distance between the acromion and the joint centre for an average-sized man is 37mm and that of the cam is 45mm; this, however, can be adjusted depending on the subject.

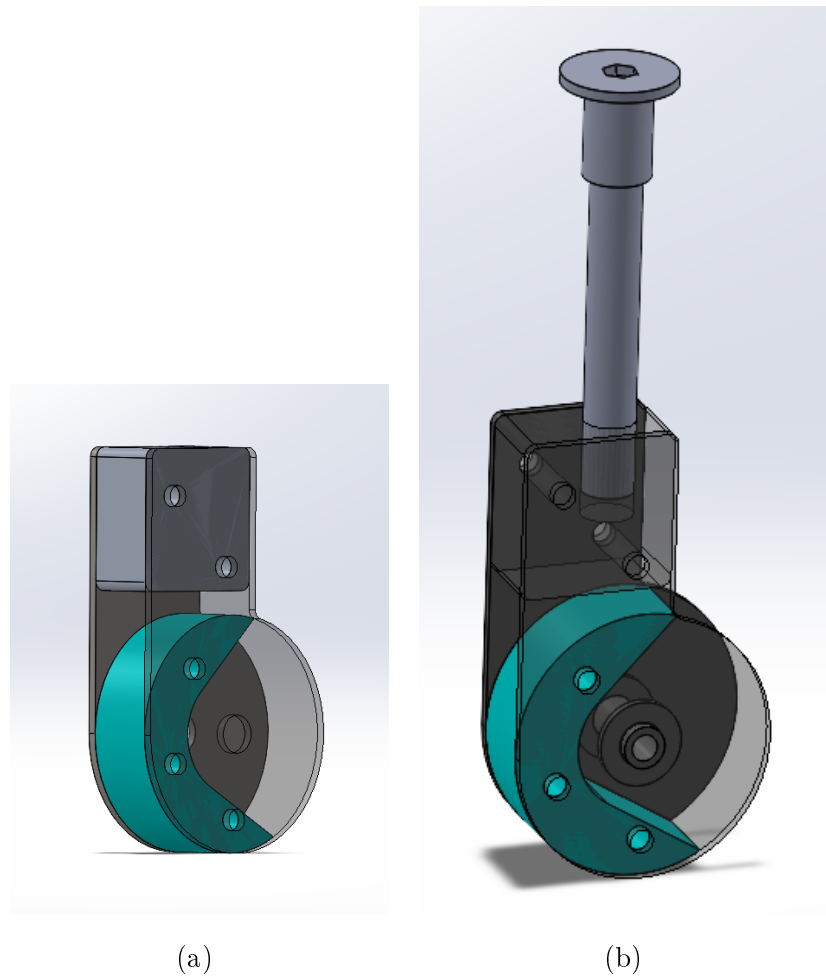


Figure 5.10: Alluminium filler a) frontal view b) with the M10 pin.

In the figure 5.11 it can see how the second joint is designed:

- The pin is attached to two plates (1)(2) placed at a certain distance by another PLA (3) filler;
- The PLA filler has a space where a bushing (4) is inserted to allow a steel rod (5) to rotate 30 degrees around the longitudinal axis passing through the bushing. A fundamental requirement is that the longitudinal axis crosses the lateral mid-axis around which the first joint rotates in the subject's shoulder joint centre, in this way the movements permitted by the exoskeleton arm are carried out in a natural manner and avoid the risk of injury or pain.

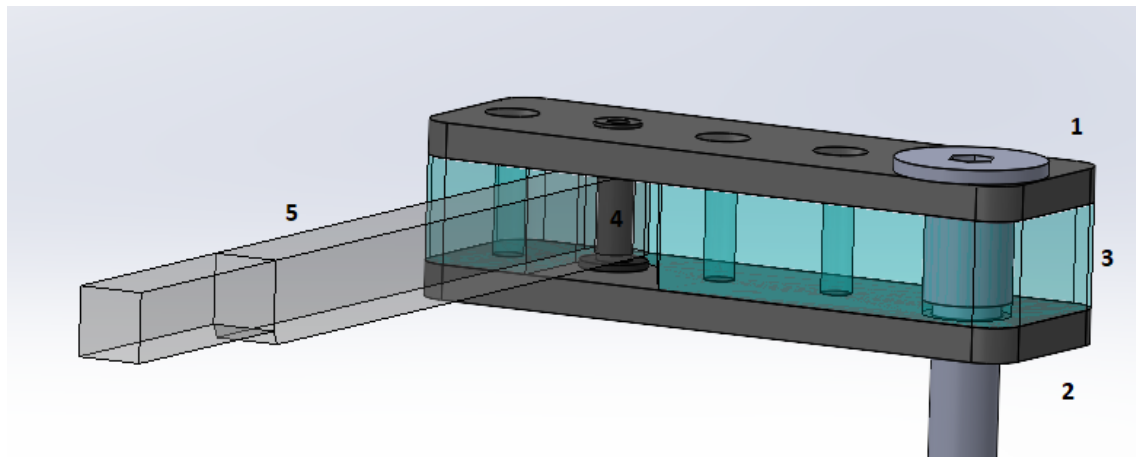


Figure 5.11: Description of the second joint

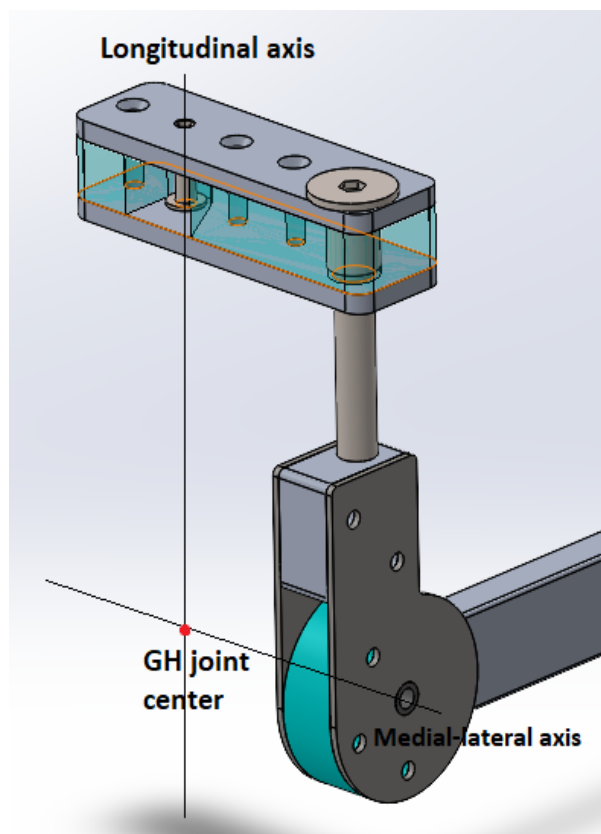


Figure 5.12: Mechanism that allows the two degrees of freedom.

The cam is connected to the lower plate via two through bolts. The cam is designed so that the wire follows its profile and remains tangential, with the presence of two sheath stops, one at the entrance of the wire and one at the exit. The cam is integral with the joint and moves with it during arm movements, so that the wire is always taut and follows the

same trajectory at all times. It is also important that the cam does not touch the user's shoulder but that the distance between the two bodies is always maintained otherwise the forces would risk to discharge on the user's shoulder and therefore the function of the frame would be null.

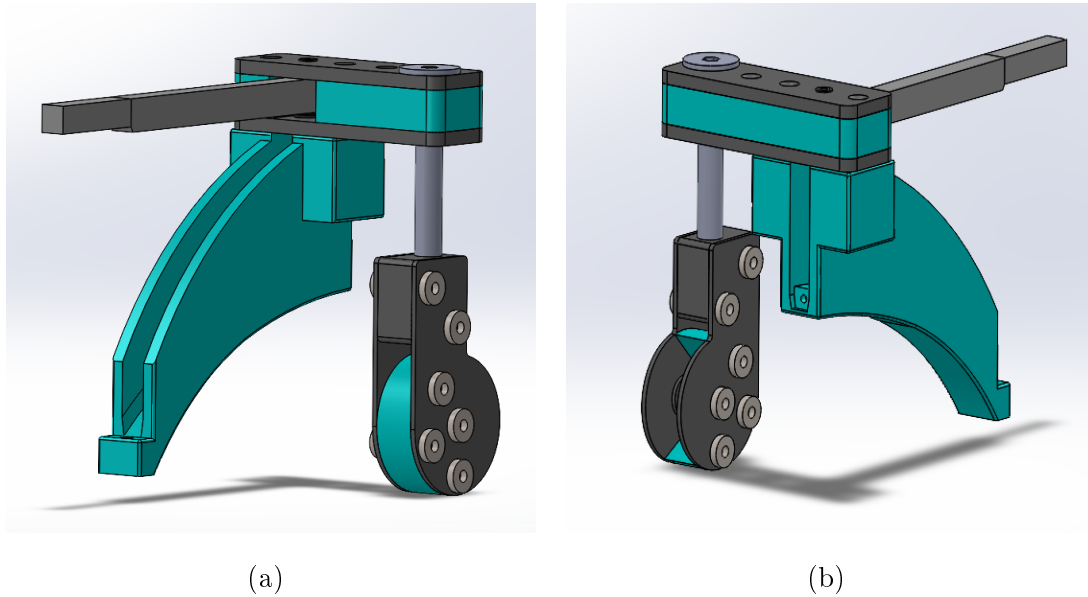


Figure 5.13: a) Back view and b) frontal view of the cam.

The steel bar is attached to the rear frame by means of an angle joint, to which the frame's square bar is also attached, which slides into the square tube at shoulder height and allows the width of the shoulders to be adjusted.

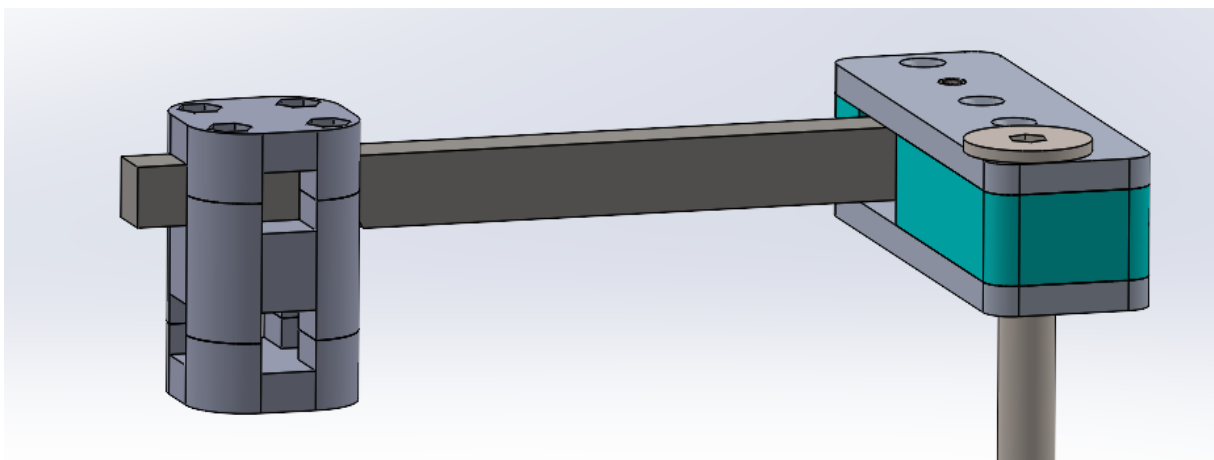


Figure 5.14: Angular joint that connects the arm to the back frame .

The arm of the exoskeleton has a weight of 1.2kg, considering both arms, it has a total weight of 2.4kg for the user's arms.

5.2 The back frame

The rear frame has two adjustment mechanisms: the first allows the user to adjust the shoulder width, the second the distance between the shoulders and the hips.

The first mechanism consists of two square bars that slide inside a square tube and are locked in position by two pin in one of the three holes in the square tube, as shown in the figure 5.15 and 5.16.

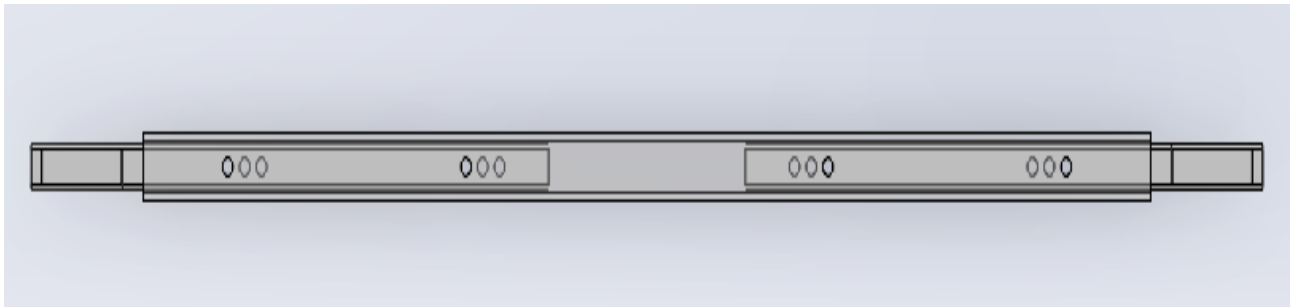


Figure 5.15: Square tubo with square bars, top view

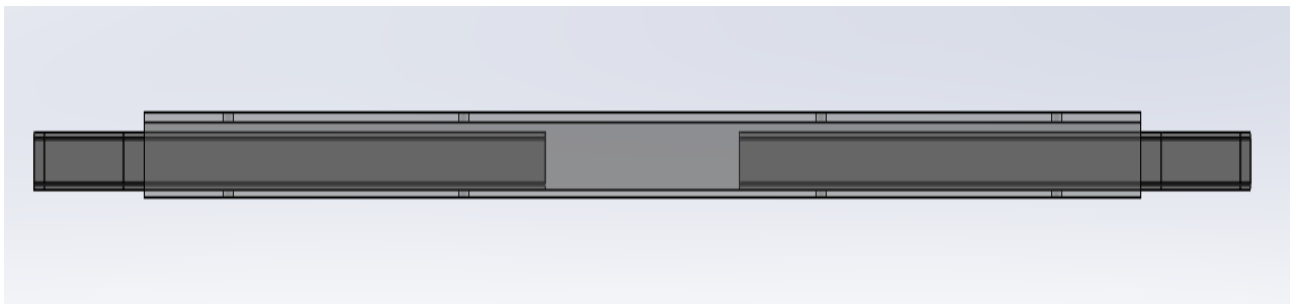


Figure 5.16: Square tubo with square bars, frotral view

In the previous figure, the square tube is transparent to show the square bars that can adjust the shoulder opening for a medium-sized subject. According to[62], for a subject between 170 and 180 cm tall, shoulder width is between 44 and 47cm, which is why there are three holes so that by locking them in one of the three positions it is possible to cover

this range. At the visible ends of the square rods, the angle joint is attached to allow connection to the exoskeleton arm.

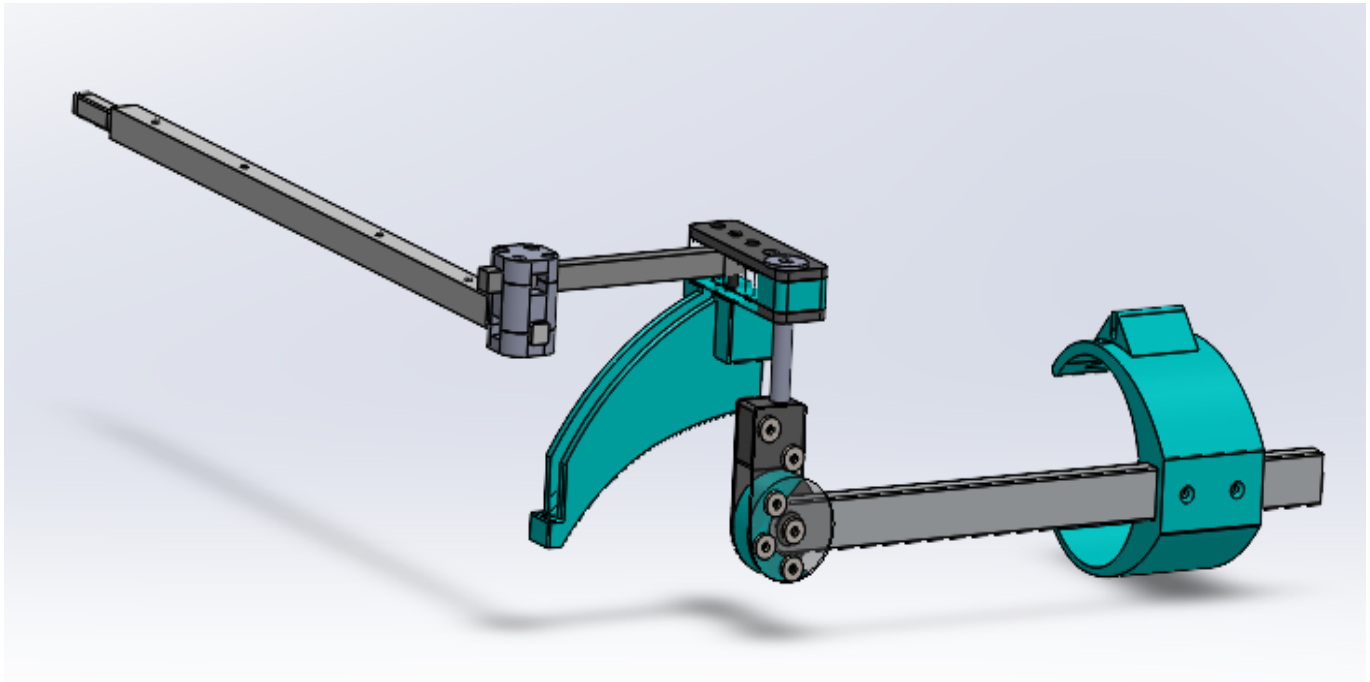


Figure 5.17: Connection between the back frame and the arm of exo.

In figure 5.18 it can see how the exoskeleton frame is composed:

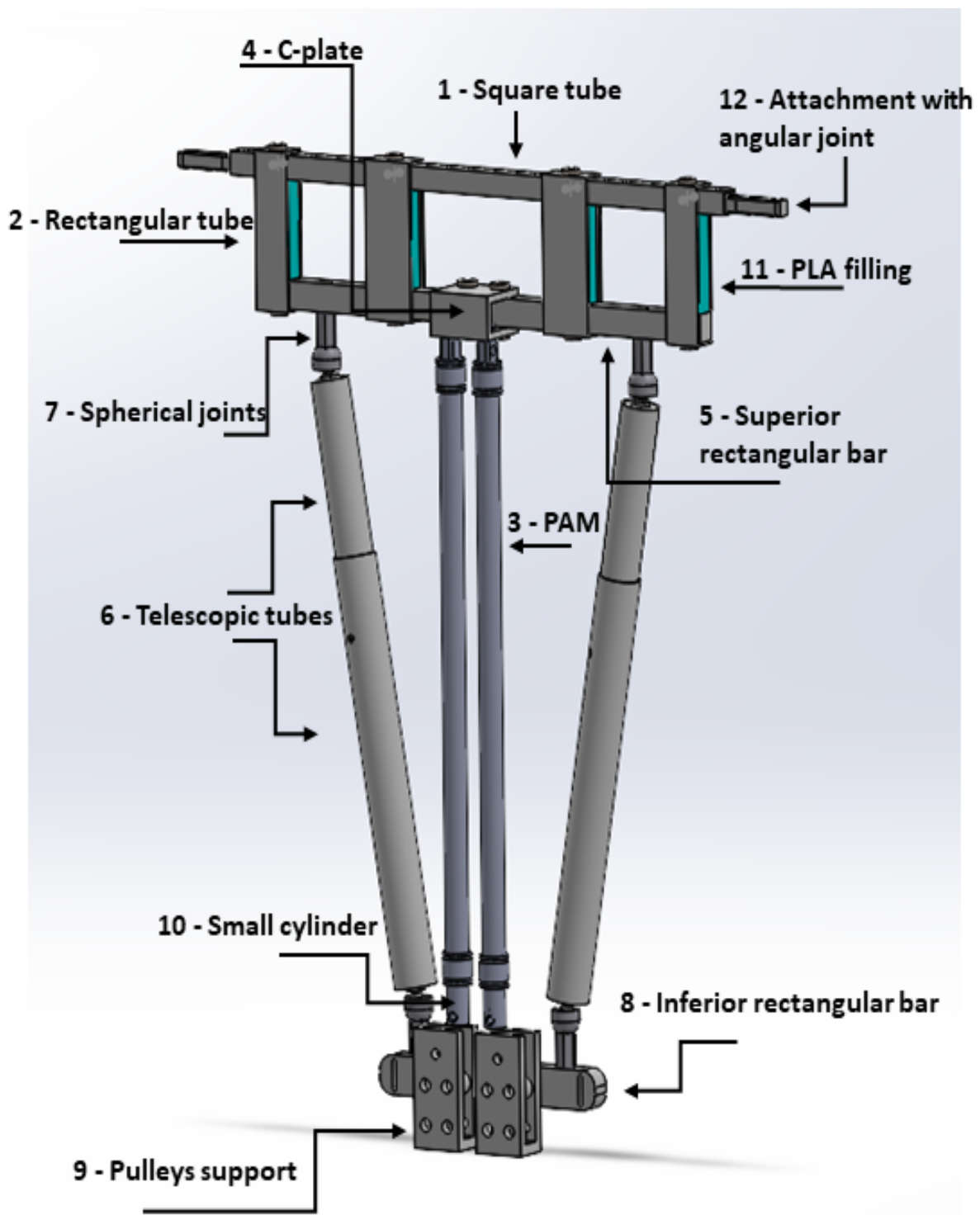


Figure 5.18: Components of the exoskeleton back frame.

1. The square tube (1) is connected to another rectangular bar (5) through four rectangular tubes (2) that enclose the tube and the bar;

2. The two muscles (3) are connected to the rectangular bar by a C-plate (4) and the two telescopic rods (6) through two spherical joints (7). The latter are connected to telescopic tubes via a threaded terminal inside the corresponding end of the rods. It is possible to regulate the length of the tubes and blocking the position using a self-locking pin in one of the holes on the tubes;
3. At the bottom the telescopic tubes and muscles are connected to another rectangular bar (8), to which two supports for the return pulleys (9) are connected in the central part of the bar, so that the wire attached to the free end of the muscle through a small cylinder (10) with a hole, passes through the pulley and connects to the arm through the cam profile;
4. For convenience, the supports for the pulleys are placed at this distance to ensure that the wire attached to the free end of the muscles falls perpendicular to contact with the pulley. In addition, two positions of the pulleys are possible to adjust the position in combination with the adjustment of the telescopic rods for different users to adjust wire length so that it is always taut;
5. In this model of the frame, the muscles are positioned internally and the telescopic rods externally; to make this possible the muscles do not have to lie on the same plane of the rods but must be positioned out of phase, in the direction of the pulleys, that is why the C-plate to which the muscles are attached protrudes in the back of the frame, thus making the wire, to connect to the front of the exoskeleton, does not intersect the telescopic rods but has the free path;
6. The rectangular bar is placed above the chest height so that it is anchored to the upper D-ring of the sling and provides the first attachment point between the exoskeleton and the sling. Anchorage between the exoskeleton and the sling is provided by the use of Velcro straps that are designed to be attached to the upper horizontal bar on the pins that hold the muscle support. The fact that the rectangular bar is not exactly at the height of the ring and therefore of the chest, does not cause a problem thanks to the use of velcro;
7. The exoskeleton in the lower part is hooked to the side rings of the harness at the level of the hips always via Velcro passing through special slits that are located on

the lower rectangular bar, but it could also be connected in the same way as the top ring, considering the pins holding the support for the pulley;

8. The rectangular tubes are not empty, but inside was inserted the PLA (11) that acts as a spacer between the two parts, and to give greater support to the top square tube without weighing the structure too heavy;
9. The spherical joints were chosen for their mechanical resistance, and because they allow a greater range of motion, making the exoskeleton more comfortable to use. For the same reason, the bars are positioned at a slight angle to the longitudinal axis.

The back frame now weighs 1.9 kg.

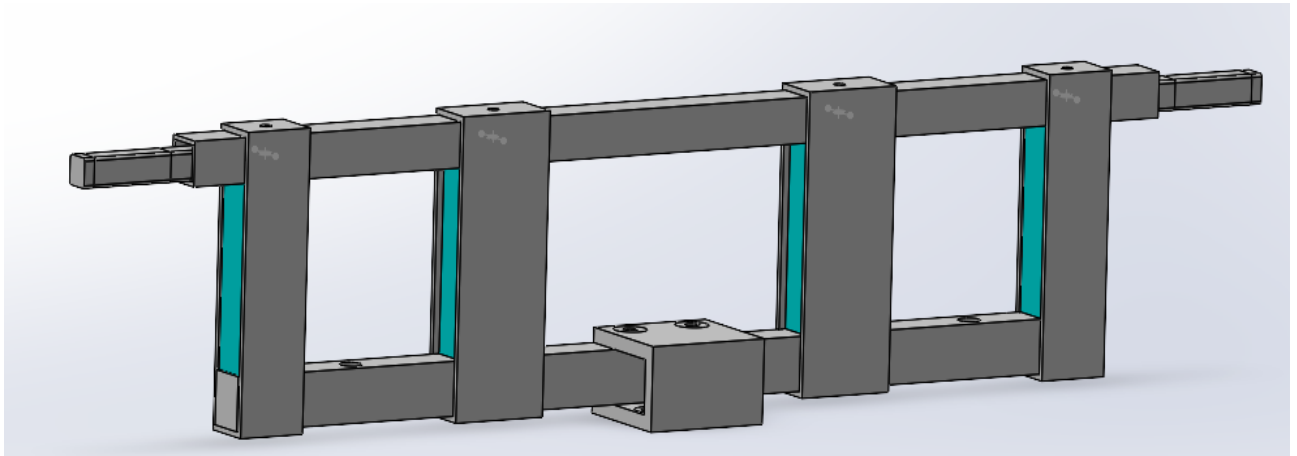


Figure 5.19: Connection between the square tube and the rectangular bar and the C plate for supporting PAMs.

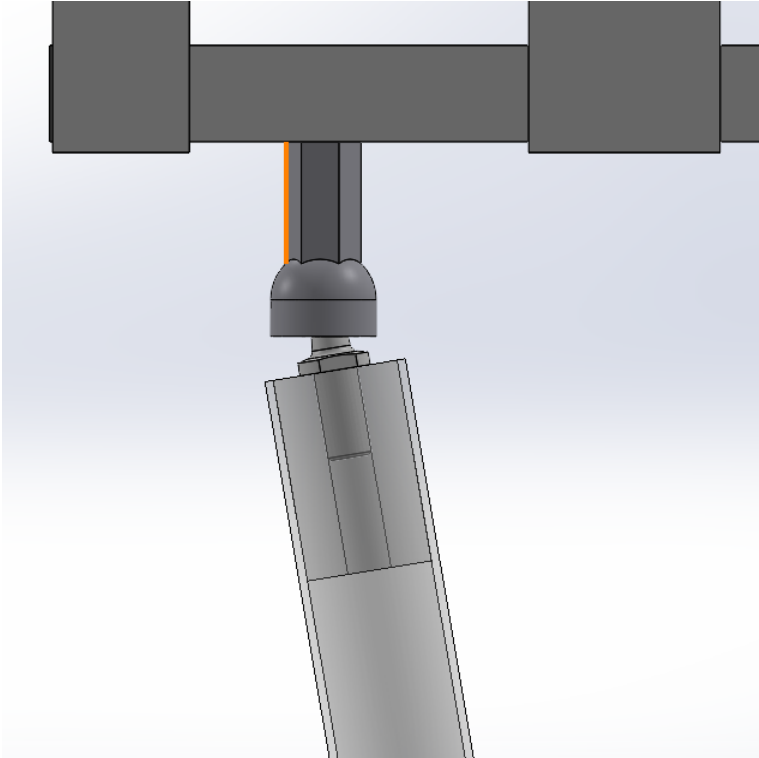


Figure 5.20: Spherical joint attached to the orizzontal rectangular bar.



Figure 5.21: Threaded terminal inside telescopic rods.

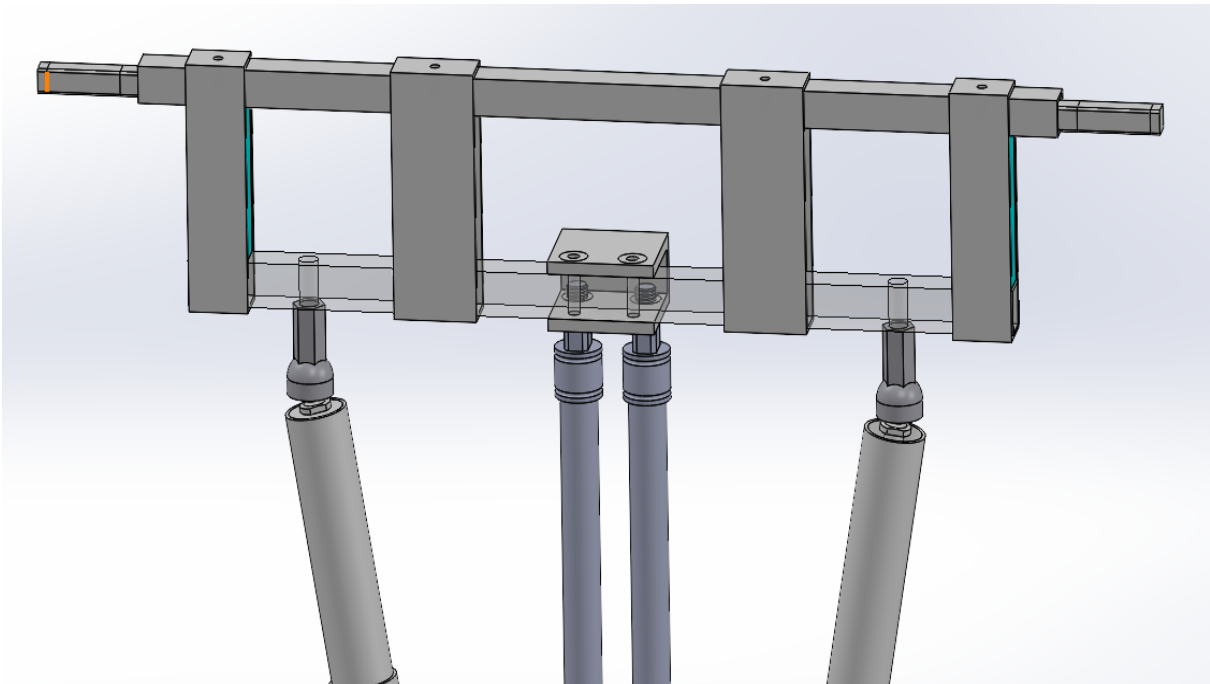


Figure 5.22: C-shaped plate where PAM are fixed.



Figure 5.23: Self-locking pin to block the position of telescopic rods.

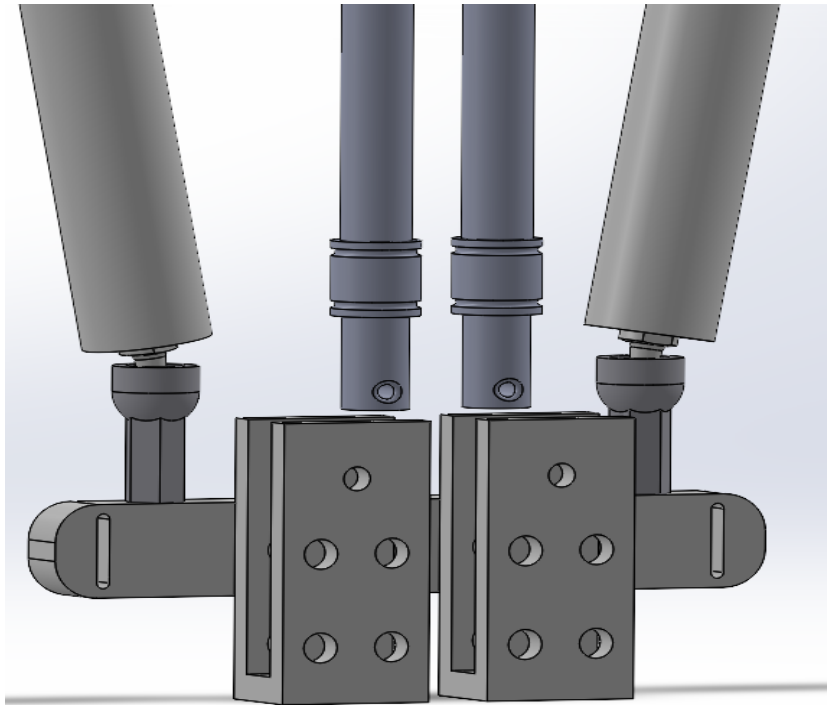


Figure 5.24: U-shaped supports fixed to the inferior rectangular bar where pulleys are attached, with two slots for velcro.

Later it was reconsidered the way in which the square tube is connected to the upper rectangular bar as it was realised that the configuration with the outer rectangular tube containing tube, bar and pla filler inside was not sufficient to not ensure residual play between the three parts, and thus the stability of the upper part of the exoskeleton. By replacing two rectangular tubes and the PLA fillings with a single larger rectangular tube, as shown in Figure 5.24, the tubes provide a certain distance and stability between the square bar and the tube. In doing so, the weight of the rear frame becomes 1.7 kg.



Figure 5.25: Completed new version of exo with one arm.

Table 5.1: Components with square or rectangular section.

Components	Section(mm)	Length(mm)	Thikness(mm)	Material
Square tube(1)	12x12	390	1.5	Al6082 T6
Square bar(11)	10x10	200		Al6082 T6
Superior rectangular bar(5)	15x18	350		Al6082 T6
Rectangular tube(2)	63x118	15	3	Al6082 T6
Inferior rectangular bar(8)	15x25	170		Al6082 T6
C-plate(4)	18x36	45	5	Al6082 T6
U-plate(9)	13x68	35	7	Al6082 T6
Strut	12x25	320		Al6082 T6
Steel rod (5)	12x10	150		AHSS alloy steel
Alluminium filling	30x18	30		Al6082 T6
plates (1)(2)	30x98	30	5	Al6082 T6
L-shaped plates	84.15x50		2	AISI304
PLA filling	15x30	98		PLA

The strut and the L-shaped plates are made by Bicchi companies [65]. The others components of the exoskeleton have been realised by us from aluminium profiles. During the realisation of the prototype, some component dimensions varied slightly for ease of construction.

Table 5.2: Components with circular section.

Components	Inside radius(mm)	Thikness(mm)	Length(mm)	Material
Smaller telescopic tube(6)	23	3	270	Al6082 T6
Bigger telescopic tube(6)	26	3	270	Al6082 T6
Small Cylinder(10)	8	7	25	Al6082 T6
PLA filling	12.5	12.5	16	PLA

Table 5.3: Information about commercial components.

Commercial components	Productor	Model
Sherical joint	IGUS otion plastics	Igubal® rod ends - AGLM08
Angolar joint	RK ROSE + KRIEGER	KPVV - Block form
Self-locking pin	ELESA	GN 113.3
Threaded terminal	ELESA	NDL.T
Pulley	MISUMI	MBRF20-1.5-H6.35

Chapter 6

Simulations and discussion

Finite Element Analysis (FEA) was used to carry out static structural analyses to study the stresses in the CAD model and thus verify the static failure of components. Solidworks software was again used for this purpose. As well as being an excellent programme for CAD modelling, it also allows FEM analyses to be carried out and the results analysed.

The model was simulated assuming that the subject was in the worst condition for one arm namely holding a 2 kg weight with one hand, with the arm at 90 degrees and the elbow extended, pressurising the muscle at maximum pressure (8 bar) to develop maximum strength; instead, the other arm, always at 90 degrees with the elbow extended, but not supporting any weight, was pressurised to 4.4 bar that allows the PAM to lift it. The simulations were carried out separately for back frame and arm. It's important to define the right constraints, loads and connections in order to get the most likely result.

Assuming that the frame is attached to the harness, three constraints are imposed, one for each attachment in order to best simulate the situation where a person is wearing the harness and therefore the exoskeleton, while avoiding stiffening the structure too much. For the dorsal ring, mid-lateral and antero-posterior movements are restricted, while cranio-caudal movement is permitted. For the two hip rings, cranio-caudal and antero-posterior movements are restricted and medio-lateral movement is permitted.

A diagram of the forces applied on the back frame can be seen in the figure 6.1.

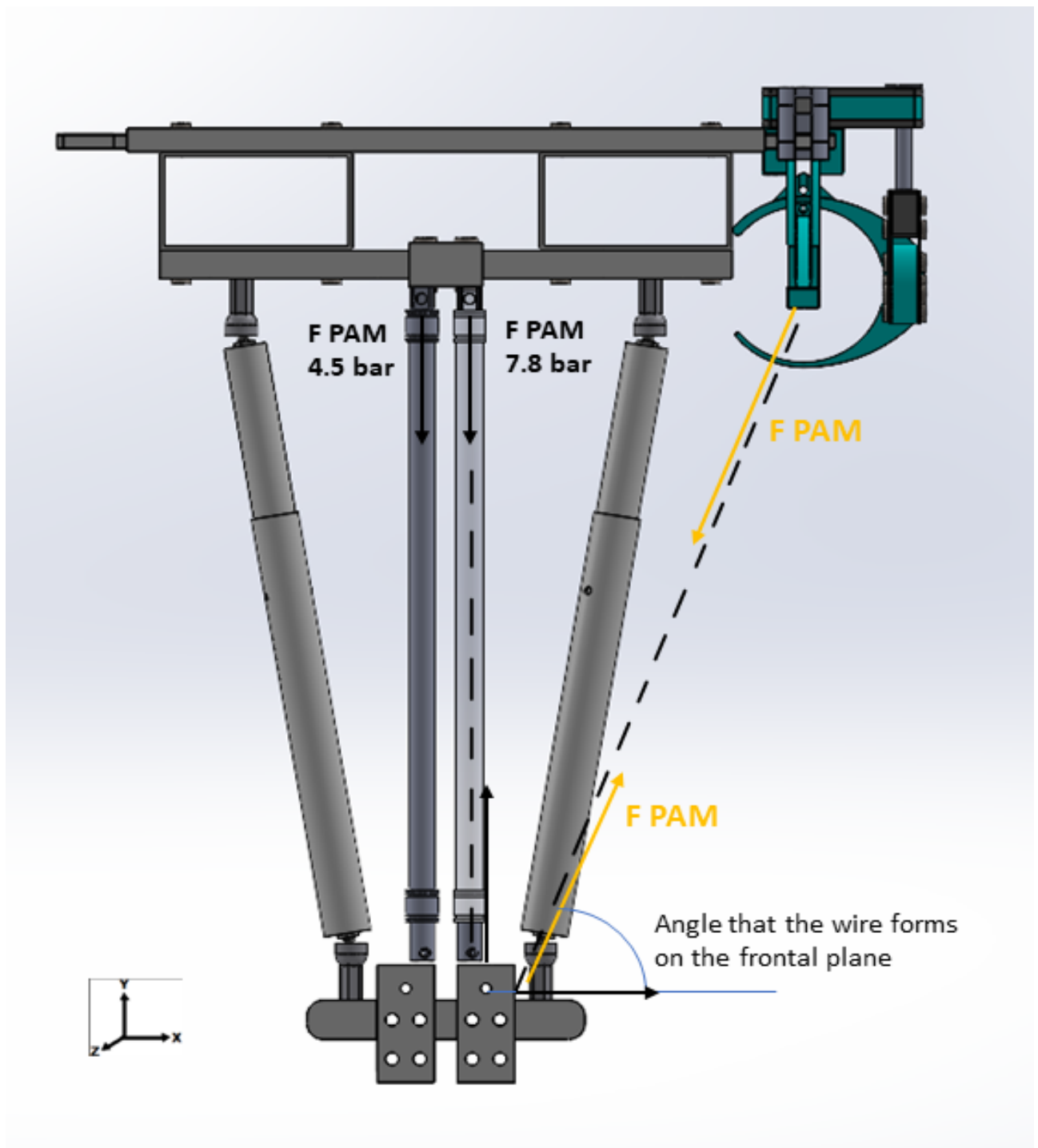


Figure 6.1: Diagram of the forces applied on the back frame reported on the right side.

The loads applied are the following:

1. On the surface of plate C to which the muscles are attached, two downward forces are applied, one of 543 N corresponding to the arm lifting the load of 2kg, while 317 N for the unloaded arm, these values correspond to an arm position of 90 degrees,

which represents the worst case;

2. The resultant forces applied on the pulleys are two and are due to the two directions the wire has when entering and leaving the pulley. The wire enters the pulley in a vertical direction so the force only has a component along y, while the force of the wire exiting the pulley has three components, a vertical one that is added to the previous vertical force, the component in the z direction depends on the inclination of the wire in the frontal plane when it exits the pulley and heads towards the cam, and the last component along x depends on the inclination of the wire in the lateral plane. For the load arm the components are $F_x = 212\text{N}$, $F_y = 1043$ and $F_z = 52\text{N}$, while for the load arm they are $F_x = 124\text{N}$, $F_y = 609$ and $F_z = 30$;
3. There are reaction forces on the bars that connect the frame to the arm, because the simulations were carried out separately for the bracelet and the frame. These reactions derive from the balance of forces applied on the arm and compensate for the force exerted by the thread entering the lower part of the cam. The components are always three because the wire is inclined on two planes and, considering the angles of inclination, the components for the arm under load are $F_x = 212\text{N}$, $F_y = 497\text{N}$ and $F_z = 52\text{N}$, while for the left arm are: $F_x = 123\text{N}$, $F_y = 290\text{N}$ and $F_z = 30\text{N}$.

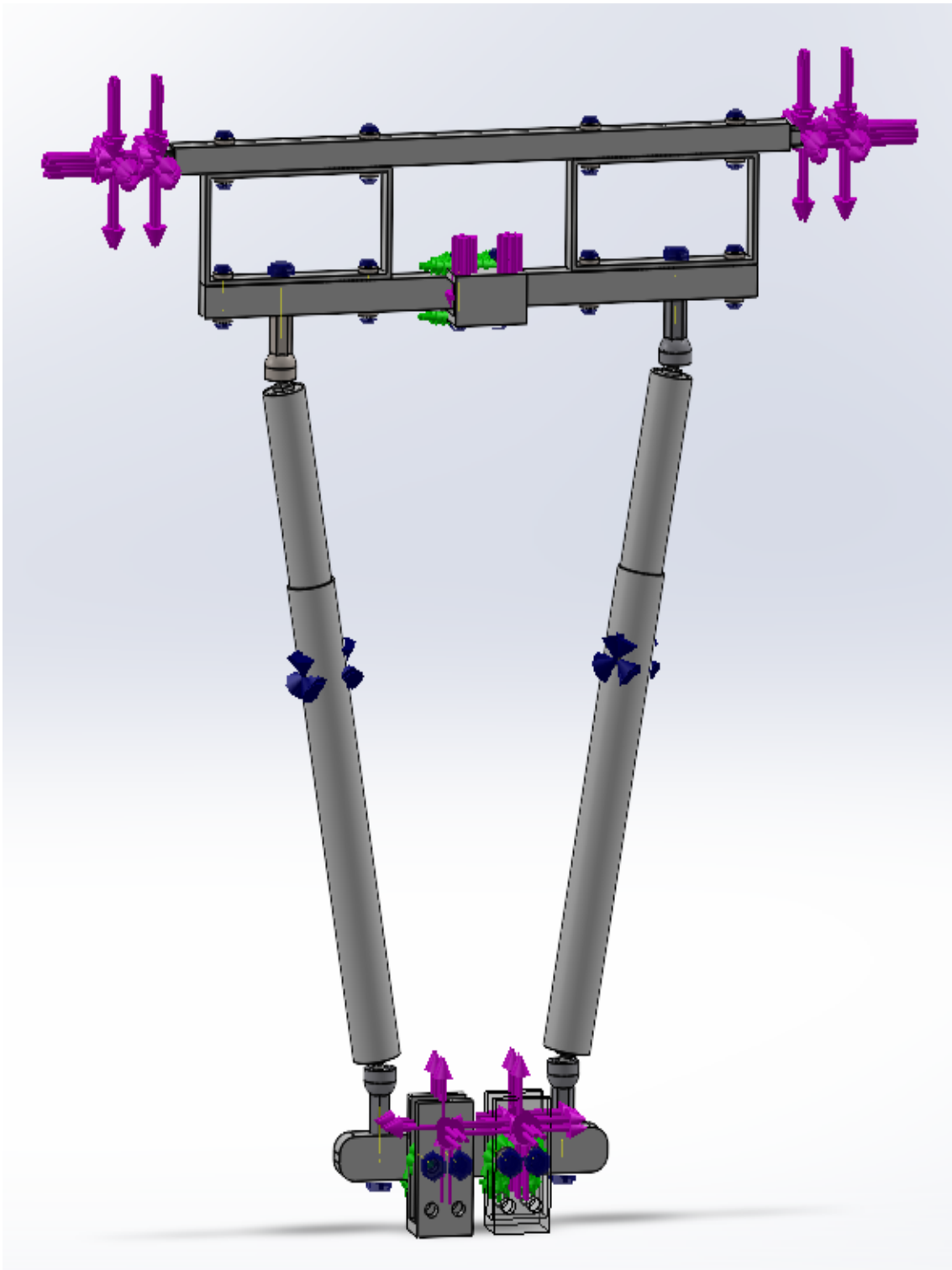


Figure 6.2: Exoskeleton back frame with loads and constraints applied.

Constraints are also applied for the arm: the rotation around its own axis has been constrained in the point of attachment of the steel rod to the frame and the M10 pin; the vertical movement is also constrained to the point of attachment of the wire to the cuff and the mid-lateral movement of the inner surface of the cuff is constrained to simulate the presence of the arm.

A diagram of the forces applied on the exo arm are shown in the figure 6.3.

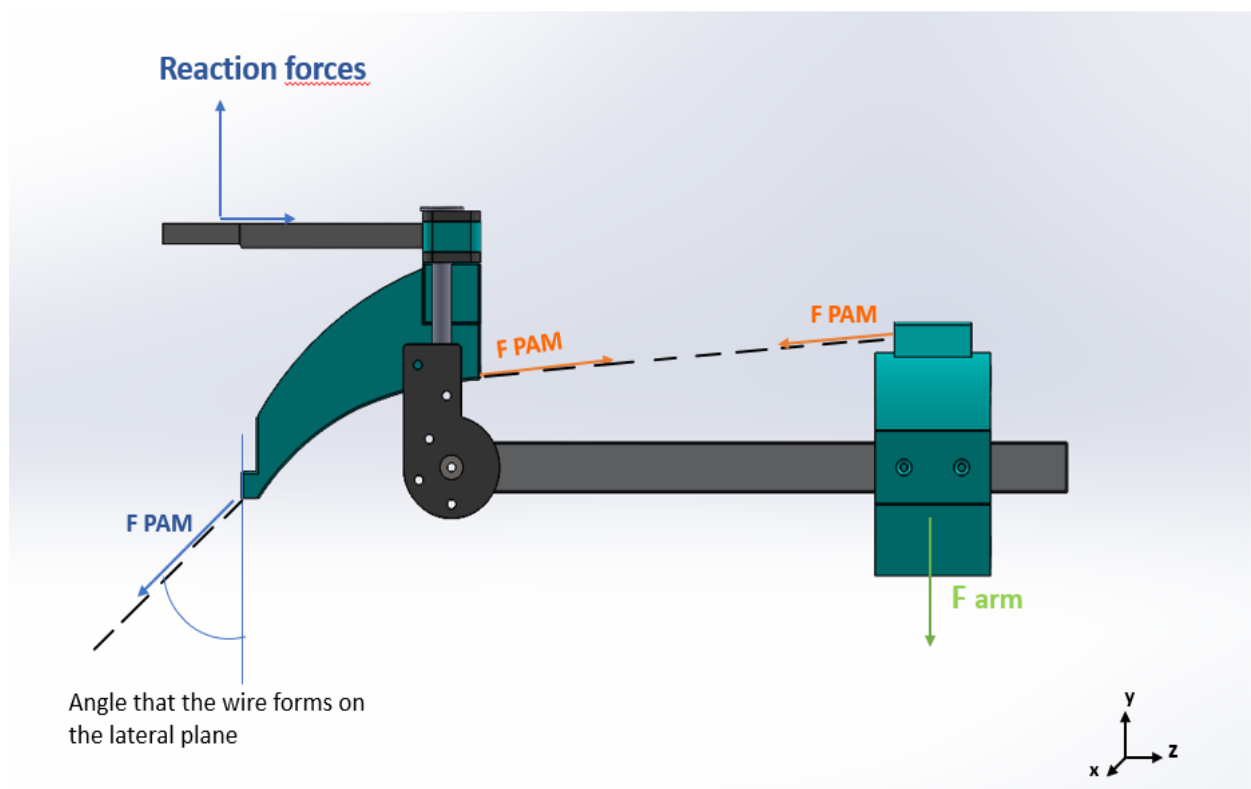


Figure 6.3: Diagram of the forces applied on the exo arm.

For the arm, on the other hand, the forces applied are shown in the Figure 6.3: the forces applied are due to the tension exerted by the wire on the cam and cuff, allowing the arm to be lifted. The forces exerted on the lower part of the cam are equal and opposite to the reactions forces on the frame bars; the components on the upper part of the cam depend on the inclination with which the wire is directed on the cuff and are equal and opposite to the tensions of the wire on the cuff, $F_y = 32\text{N}$ and $F_x = 542\text{N}$. There is also a vertical force directed downwards on the cuff, which indicates the presence of the arm and it is equal to 95N considering a weight of 2kg in the hand. Finally, the force ex-

erted by the Velcro fastener to close the cuff is also taken into account and is equal to 40N.

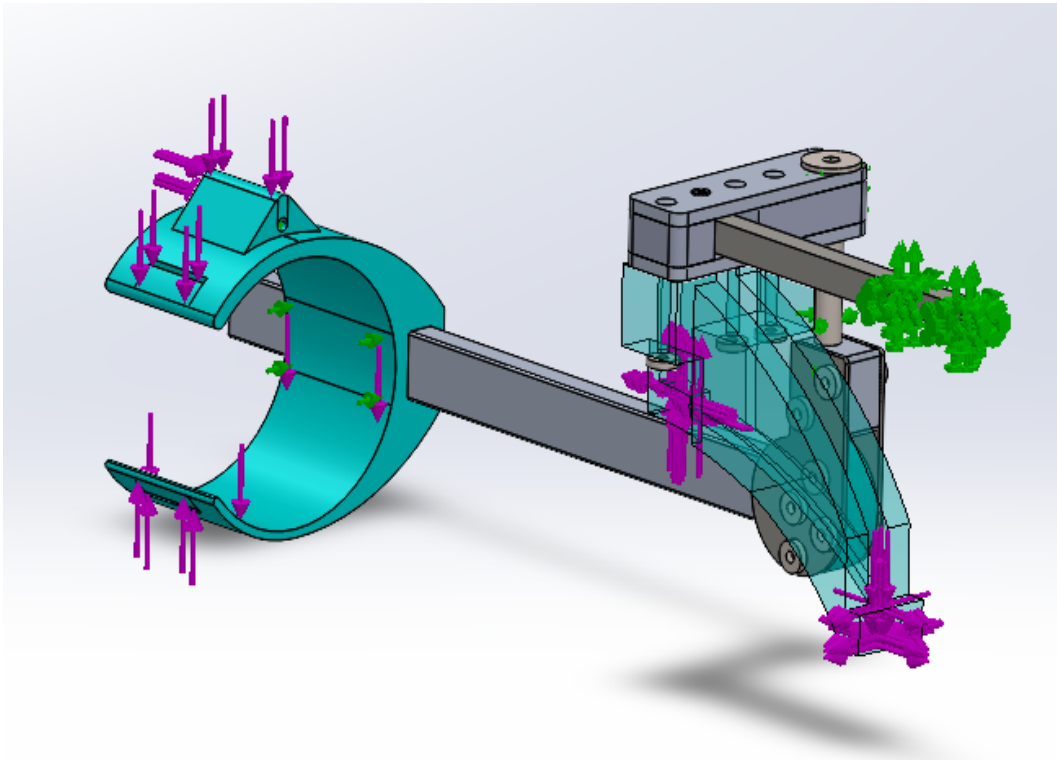


Figure 6.4: Exoskeleton arm with loads and costraints applied.

6.1 Results

After assigning the materials, applying the loads and constraining the model, the static finite element analysis was started creating the tetrahedral curvature-based mesh of the model, with minimum dimension of the element for the back frame equal to 1.13 mm and maximum 5.6 mm; for the arm the minimum size is 4.24 mm and maximum size is 21.2mm, by applying a control mesh with element dimension 1.4 mm, and the following results were obtained:

- As far as the arm is concerned, the maximum stress is found at the hinge that allows the abduction and the adduction of the arm in the transverse plane; in this joint the maximum Von Mises stress is equal to 578 MPa and occurs on the washer interposed between the steel bar and the upper plate;

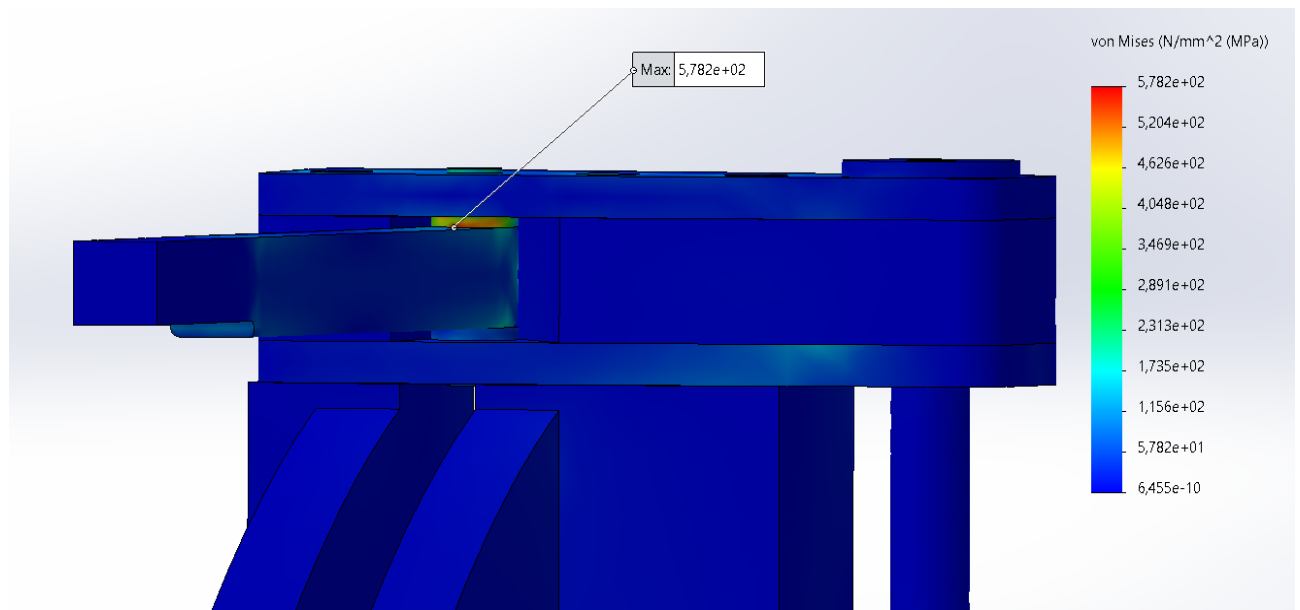


Figure 6.5: Von Mises stresses distribution on the washer.

- A stress of about 480 MPa is on the lower part of the steel rod always corresponding to the joint, which if it consider a steel with a high yield strength as the AHSS alloy steel, with added niobium, titanium, vanadium and zirconium to refine the grains, making the material stronger. They have high yield strength (up to 550 MPa) and at the same time high ductility.

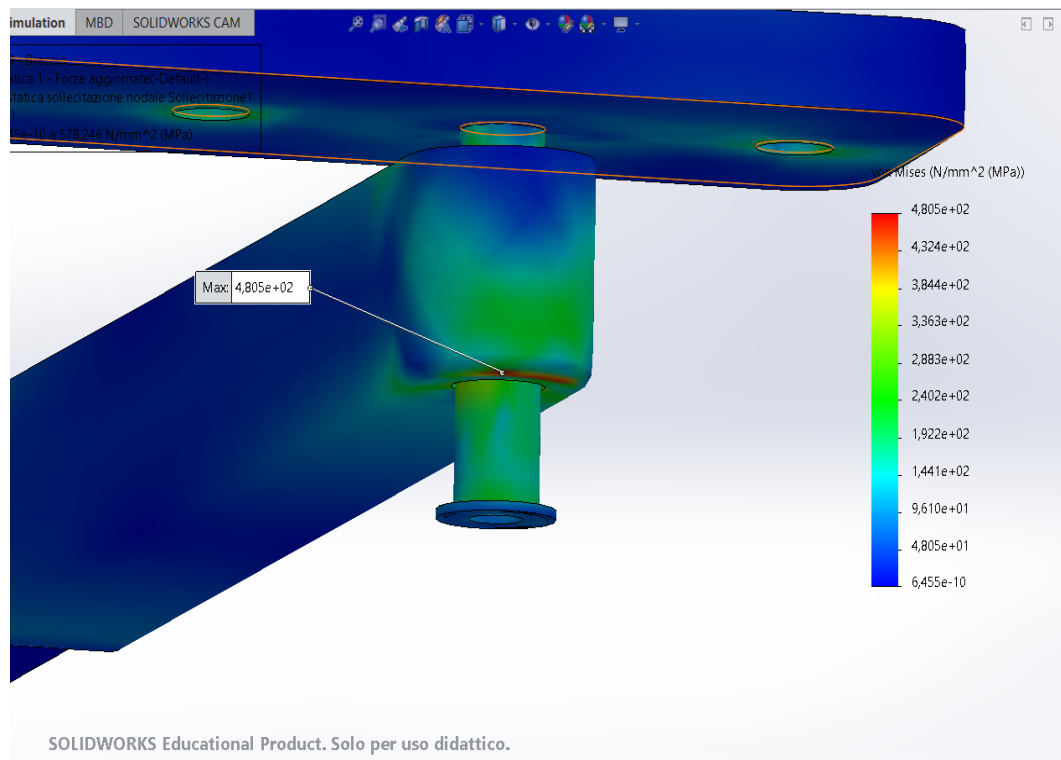


Figure 6.6: Von Mises stresses distribution on the steel rod.

- In addition, there is a maximum displacement in the negative direction of about 2 mm corresponding to the lower part of the cam, predictable result due to the force with which the wire pulls during the contraction of the muscles.

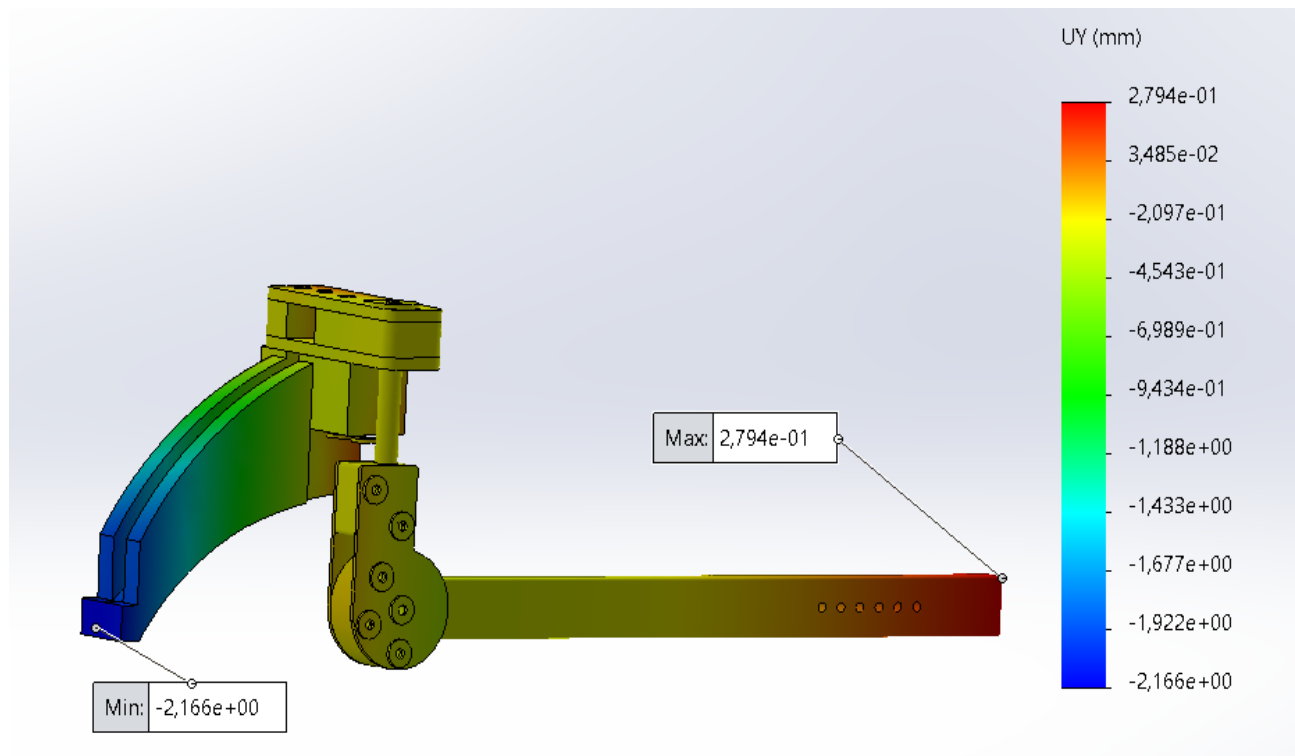


Figure 6.7: Visualizzazione di maximum and minimum displacement of the exo arm.

In the frame, the maximum forces are on the washers of the M4 bolts that connect the square tube to the upper rectangular bar. Because the bolts are preloaded, the maximum stress is right there, and by using washers you can reduce the direct stress on the aluminium tube and dissipate it on the steel washer, which is much more durable. The same happens for the washers placed on the support that sustains the muscles. The highest stresses are found in these points, for the rest on the chassis do not act excessive forces, and in no component the stress exceeds the point of yield.

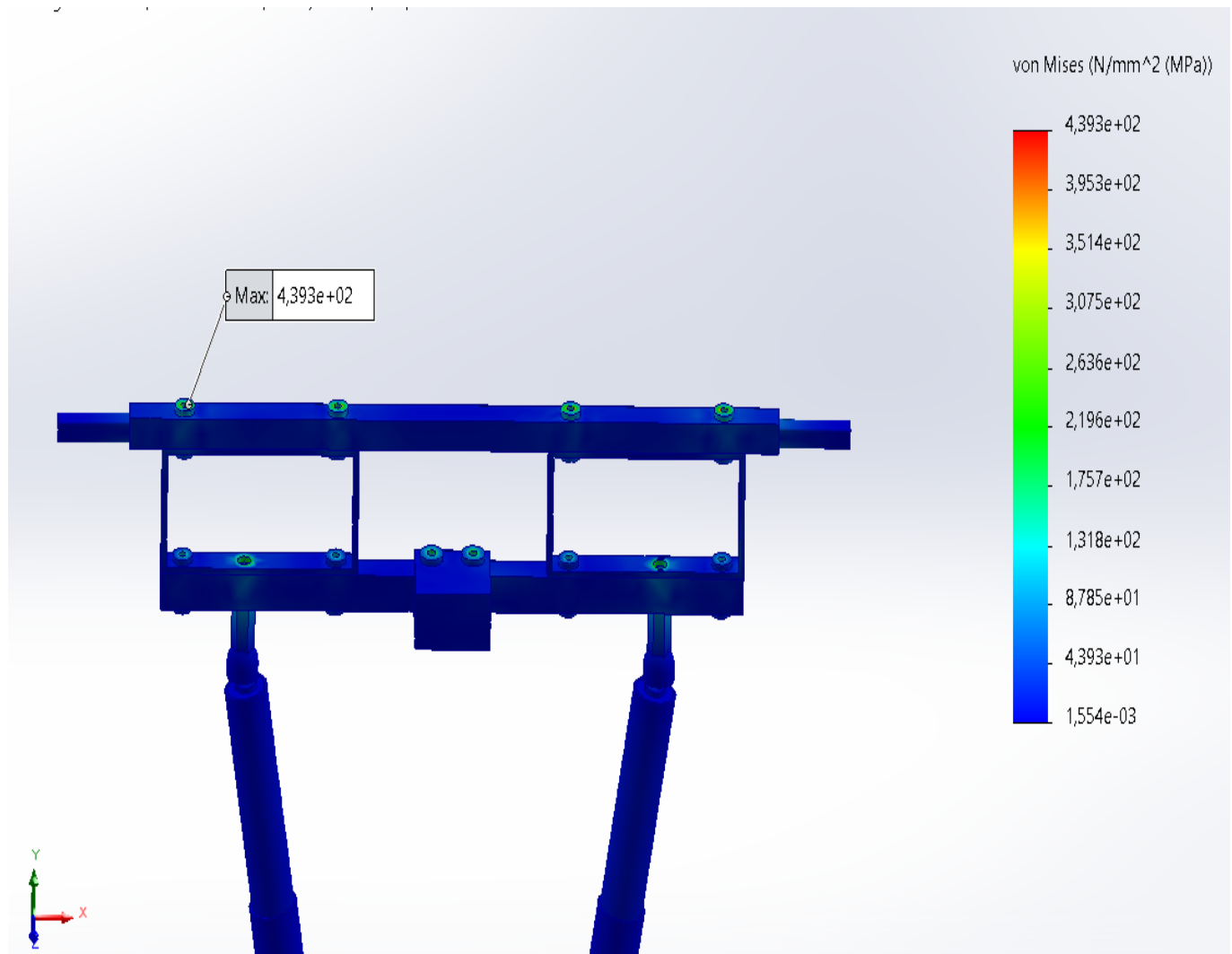


Figure 6.8: Maximum frame tension at washers M4.

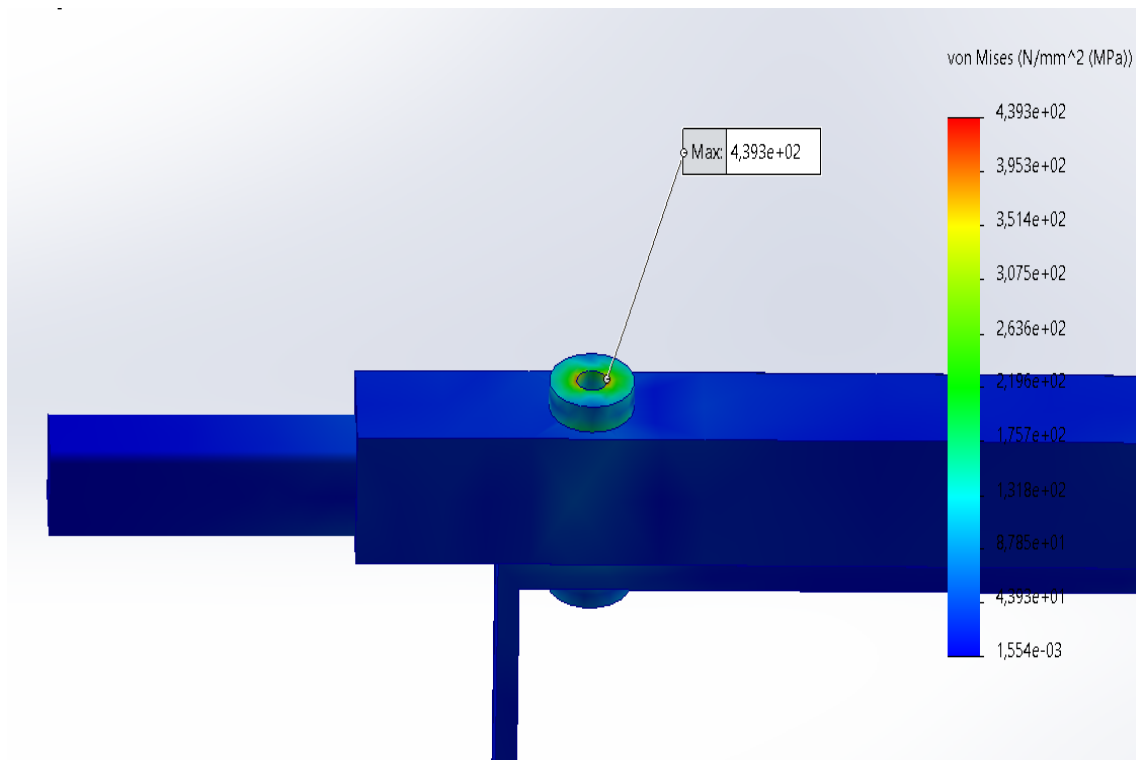


Figure 6.9: Zoom of the previous picture on the critical region.

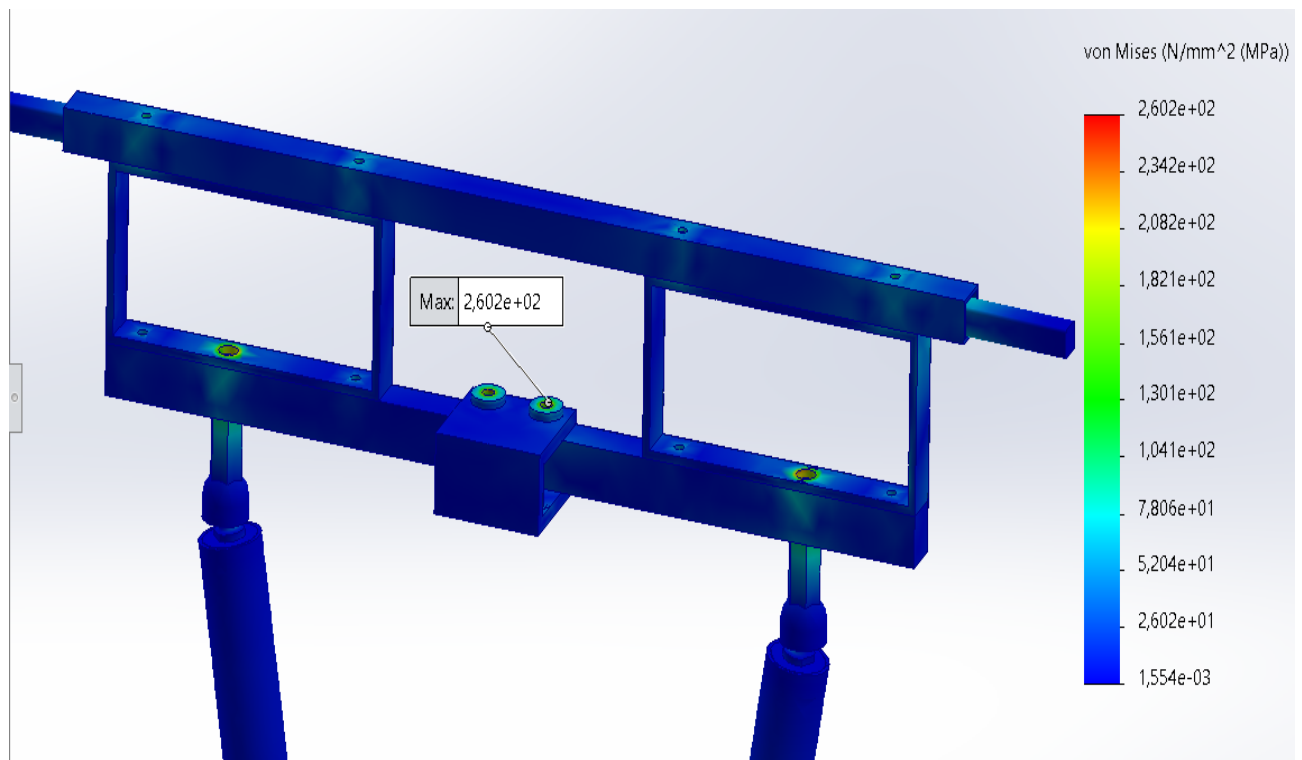


Figure 6.10: Maximum force at the washers M5

As for the displacement, it is maximum in the negative direction of the y-axis, at the end of the square rod that runs inside the square tube, where the angle joint that connects to the arm frame is connected. This is a predictable result, since it is the part that connects to the arm that carries the thread that transmits the force exerted by the muscles, and is therefore subject to a maximum force of 500N. The displacement is 1 mm, an acceptable value in any case. In total, the lowering of the rod plus the lowering of the cam gives 3 mm, which is acceptable to avoid contact between the cam and the shoulder.

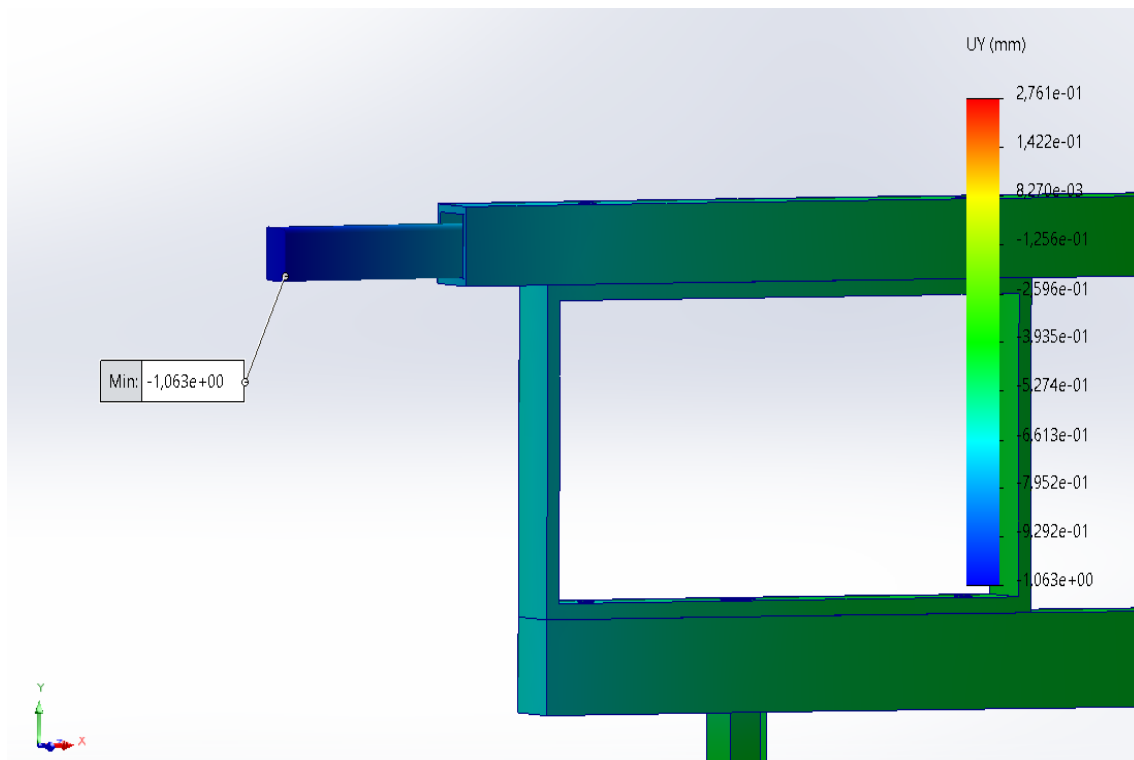


Figure 6.11: Maximum negative displacement on the extremity of the square rod.

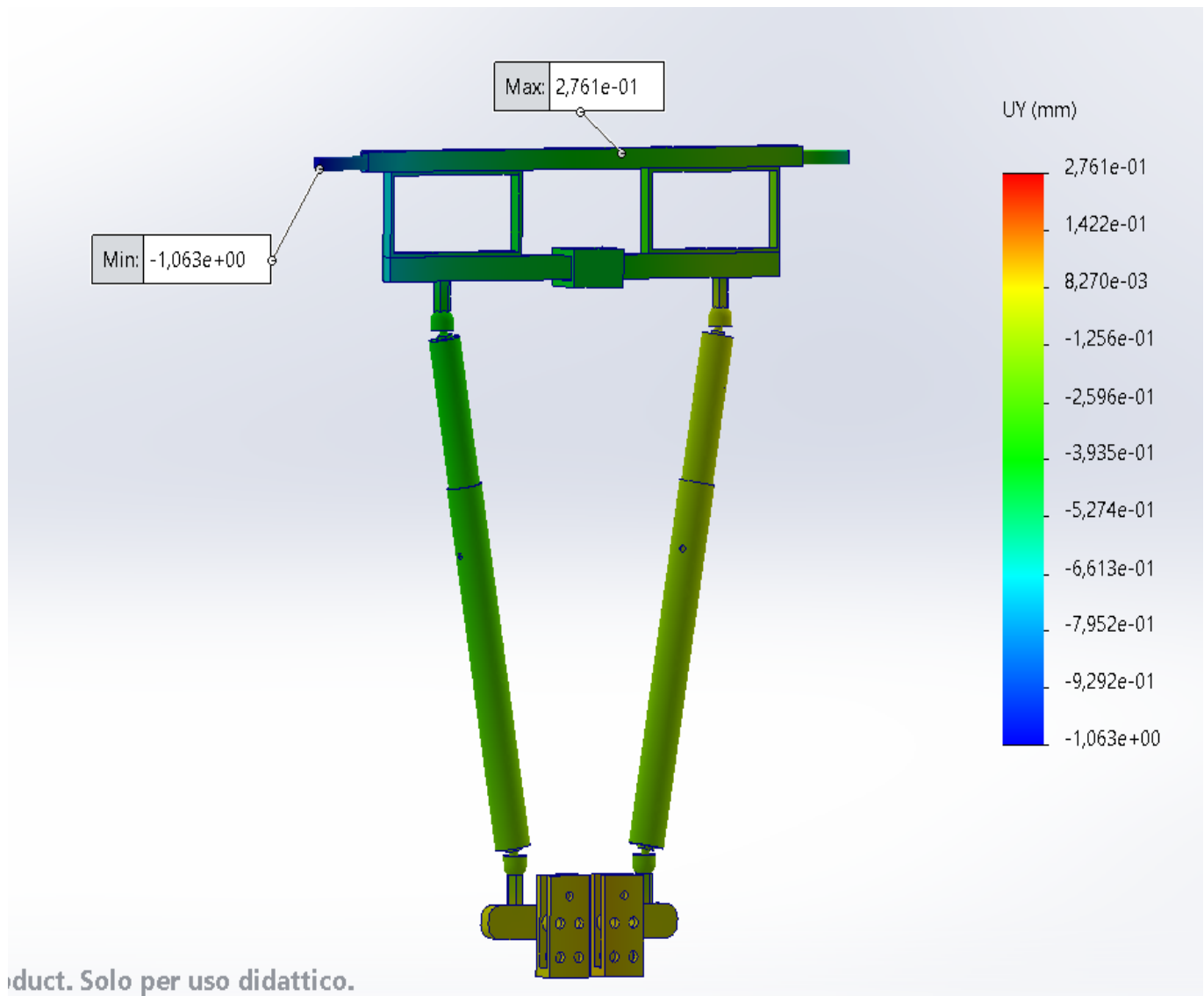


Figure 6.12: Total view of back frame displacement.

If the lower part of the cam is shifted downwards by 2 mm, this means that the distance from the point where the wire exits the cam and reaches the pulley is reduced and therefore the muscles will have to contract 2 mm more than they already do at different pressure levels to keep the wire taut. To this must be added the downward displacement of the steel bar of about 1 mm and thus take into account an additional muscle contraction of 3 mm. For this reason, the moment of the muscle pair was calculated taking into account a shortening of the muscle by 1 to 5 mm more than the initial contraction value.

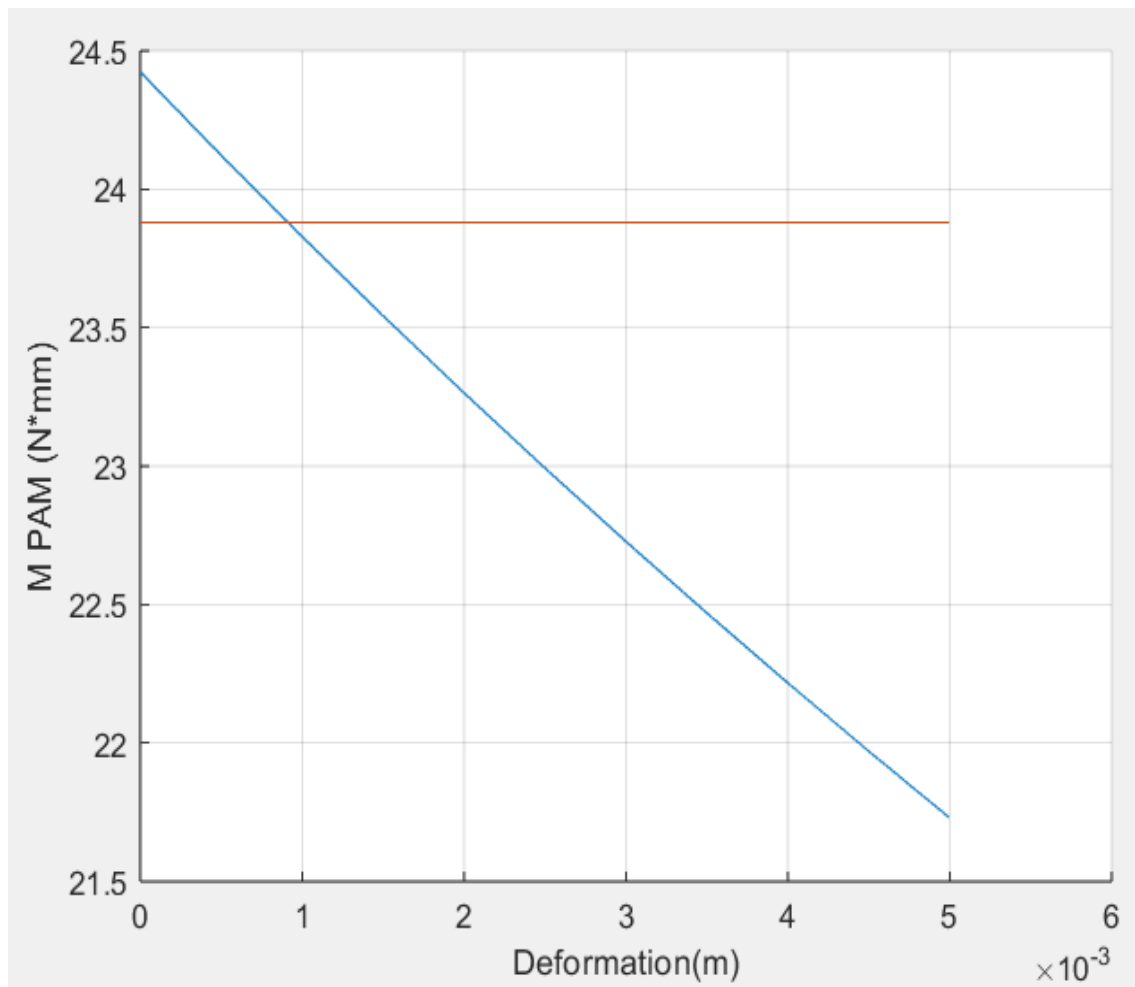


Figure 6.13: Comparison with muscular torque considering the additional shortening.

As can be seen in Figure 6.13 the gravitational moment is highlighted in red with a weight of 2 kg, which the pair of muscles must follow, while the blue curve represents the muscular moment when the muscles are pressurised to 8 bar as a function of the additional shortening, from 1 to 5 mm. It can be seen that up to about 2 mm, the torque exerted by the muscles is still able to balance the gravitational torque by providing the user with support equal to the percentage values calculated in Chapter 4, since the moment at 2 mm is equal to the initial moment; beyond 2.5 mm, the value of this percentage begins to decrease because the moment provided begins to deviate more from the gravitational torque, but still remains greater than 50%.

Chapter 7

Conclusions and future development

Solutions to perform difficult, long and repetitive tasks while maintaining quality and precision are needed in industrial applications. However, many tasks still require the experience, cognitive skills, dexterity and flexibility of humans, even though programmed robotic systems are a valuable response. For this reason, several wearable exoskeleton systems have been developed to support human tasks in industrial environments. They are designed to support and relieve human muscles from heavy loads, or simply to support human limbs and reduce muscular activity when moving, while maintaining the quality of working.

This is the example of the passive upper limb exoskeleton design proposed in this paper, which is intended to provide a torque at the shoulder joint to (at least partially) counterbalance the torque due to gravity of the upper limb, thus reducing the effort required of the shoulder complex muscles when performing overhead tasks. The output torque is generated by a McKibben pneumatic artificial muscle which, when pressurised, exerts a traction force by contraction according to the position of the arm, acting as a passive device.

The artificial pneumatic muscle chosen was the 35 cm long FESTO DMSP muscle, as it is the muscle that develops the force-moment profile closest to that developed by the gravitational torque. To confirm this, the muscle was characterised through isometric and isotonic tests, the experimental coefficients that best approximated the curve were found and the result was positive, as the two moment profiles follow a very similar profile.

Once the basic requirements of the exoskeleton were established, the CAD model was designed and static finite element analysis was carried out to estimate the von Mises stresses

and maximum displacements that occur in the model when the torque due to the arm's gravity is at its maximum, in order to obtain the best combination of materials to prevent static failure and to obtain the lightest possible structure.

From the results obtained, the maximum stresses developed do not exceed the yield stress of the chosen materials, so it has to pay attention to the steel you choose to make the rod of the joint of the arm of the exoskeleton, which must have a high yield value, An alloy steel, for example, would be fine. As far as displacement is concerned, there is a maximum overall negative displacement in the y-direction of about three millimetres, a predictable and entirely acceptable result both to ensure that the cam does not touch the user's shoulder and to ensure that the moment generated by the muscles provides support and compensates for the gravitational torque at least 50%.

However, it is possible to make some improvements to the design of the exoskeleton, which may be the subject of future developments:

- Add an additional degree of freedom that allows the abduction adduction on the frontal plane;
- Design a mechanism that considers the displacement of the shoulder joint center;
- Make the adjustment of the exoskeleton faster and more autonomous because the way the exoskeleton is designed now requires the presence of a second person to help the user adjust the exoskeleton.

Bibliography

- [1] VALACHI, B., & VALACHI, K. (2003). Mechanisms leading to musculoskeletal disorders in dentistry. *The Journal of the American Dental Association*, 134(10), 1344–1350. doi:10.14219/jada.archive.2003.0048
- [2] <https://simshospitals.com/musculoskeletal-disorders/>
- [3] Bernard BP, editor. U.S. Department of Health and Human Services, Centers for Disease control and Prevention, National Institute of Occupational Safety and Health. *Musculoskeletal disorders and workplace factors: a critical review of epidemiologic evidence for work-related musculoskeletal disorders of the neck, upper extremity, and lower back*. July 1997. DHHS (NIOSH) Publication No. 97-141.
- [4] *Musculoskeletal Disorders Among Healthcare Workers: Prevalence and Risk Factors in the Arab World* Sameer Shaikh, Ammar Ahmed Siddiqui, Freaah Alshammary, Junaid Amin, and Muhammad Atif Saleem Agwan.
- [5] NIOSH workers health chartbook 2004. NIOSH Publication No. 2004-146. Washington, D.C.
- [6] National Research Council and the Institute of Medicine (2001). *Musculoskeletal disorders and the workplace: low back and upper extremities*. Panel on Musculoskeletal Disorders and the Workplace. Commission on Behavioral and Social Sciences and Education. Washington, DC: National Academy Press.
- [7] <https://osha.europa.eu/en/themes/musculoskeletal-disorders>
- [8] Ergonomics and musculoskeletal disorders: overview. *Occupational Medicine* 2005;55:164–167 doi:10.1093/occmed/kqi081
- [9] *Overhead Work – Reduce the Injury Risk* Kayla M. Fewster & Clark R. Dickerson

- [10] B.P. Bernard, *Musculoskeletal Disorders and Workplace Factors*, A Crit. Rev. Epidemiol. Evid. Work. Musculoskelet. Disord. Neck, Up. Extrem. Low Back. (1997).
- [11] R.M. Van Rijn, B.M. Huisstede, B.W. Koes, A. Burdorf, Associations between work-related factors and specific disorders of the shoulder - A systematic review of the literature, *Scand. J. Work. Environ. Heal.* (2010). <https://doi.org/10.5271/sjweh.2895>
- [12] S.W. Svendsen, J.P. Bonde, S.E. Mathiassen, K. Stengaard-Pedersen, L.H. Frich, Work related shoulder disorders: Quantitative exposure-response relations with reference to arm posture, *Occup. Environ. Med.* (2004). <https://doi.org/10.1136/oem.2003.010637>
- [13] D. Anton, L.D. Shibley, N.B. Fethke, J. Hess, T.M. Cook, J. Rosecrance, The effect of overhead drilling position on shoulder moment and electromyography, *Ergonomics.* (2001). <https://doi.org/10.1080/00140130120079>.
- [14] J.N. Chopp, S.L. Fischer, C.R. Dickerson, The impact of work configuration, target angle and hand force direction on upper extremity muscle activity during sub-maximal overhead work, *Ergonomics.* (2010). <https://doi.org/10.1080/00140130903323232>.
- [15] Y. Blache, L. Desmoulins, P. Allard, A. Plamondon, M. Begon, Effects of height and load weight on shoulder muscle work during overhead lifting task, *Ergonomics.* (2015). <https://doi.org/10.1080/00140139.2014.980336>.
- [16] C.R. Dickerson, D.B. Chaffin, R.E. Hughes, A mathematical musculoskeletal shoulder model for proactive ergonomic analysis., *Comput. Methods Biomech. Biomed. Engin.* 10 (2007) 389–400. <https://doi.org/10.1080/10255840701592727>.
- [17] D. Sood, M.A. Nussbaum, K. Hager, H.C. Nogueira, Predicted endurance times during overhead work: influences of duty cycle and tool mass estimated using perceived discomfort, *Ergonomics.* (2017). <https://doi.org/10.1080/00140139.2017.1293850>.
- [18] E.L. Flatow, L.J. Soslowky, J.B. Ticker, R.J. Pawluk, M. Hepler, J. Ark, V.C. Mow, L.U. Bigliani, Excursion of the Rotator Cuff Under the Acromion: Patterns of Subacromial Contact, *Am. J. Sports Med.* (1994). <https://doi.org/10.1177/036354659402200609>

- [19] E.G. McFarland, C.Y. Hsu, C. Neira, O. O’Neil, Internal impingement of the shoulder: A clinical and arthroscopic analysis, *J. Shoulder Elb. Surg.*(1999). [https://doi.org/10.1016/S1058-2746\(99\)90076-9](https://doi.org/10.1016/S1058-2746(99)90076-9)
- [20] D.D. Ebaugh, P.W. McClure, A.R. Karduna, Effects of shoulder muscle fatigue caused by repetitive overhead activities on scapulothoracic and glenohumeral kinematics, *J. Electromyogr. Kinesiol.* (2006). <https://doi.org/10.1016/j.jelekin.2005.06.015>.
- [21] K.J. McQuade, J. Dawson, G.L. Smidt, Scapulothoracic muscle fatigue associated with alterations in scapulohumeral rhythm kinematics during maximum resistive shoulder elevation, *J. Orthop. Sports Phys. Ther.* (1998). <https://doi.org/10.2519/jospt.1998.28.2.74>
- [22] N.T. Tsai, P.W. McClure, A.R. Karduna, Effects of muscle fatigue on 3-dimensional scapular kinematics, *Arch. Phys. Med. Rehabil.* (2003). [https://doi.org/10.1016/S0003-9993\(03\)00127-8](https://doi.org/10.1016/S0003-9993(03)00127-8).
- [23] Optimal design of active-passive shoulder exoskeletons: a computational modeling of human-robot interaction Ali Nasr · Sydney Bell · JohnMcPhee Received: 19 May 2022 / Accepted: 31 October 2022. *Multibody System Dynamics* <https://doi.org/10.1007/s11044-022-09855-8>
- [24] Evaluation of a passive exoskeleton for static upper limb activities Kirsten Huysamena, Tim Boschb, Michiel de Loozeb, Konrad S. Stadlerc, Eveline Graf d, Leonard W. O’Sullivan a.
- [25] Romero, D., Stahre, J., Wuest, T., Noran, O., Bernus, P., Fast-Berglund, Å., Gorecky, D., 2016. Towards an operator 4.0 typology: a human-centric perspective on the fourth industrial revolution technologies. In: *International Conference on Computers and Industrial Engineering (CIE46) Proceedings*, Tianjin, China.
- [26] de Looze, M.P., Bosch, T., Krause, F., Stadler, K.S., O’Sullivan, L.W., 2016. Exoskeletons for industrial application and their potential effects on physical work load. *Ergonomics* 59 (5), 671–681.

- [27] Review on Design of Upper Limb Exoskeletons Muhammad Ahsan Gull 1,* , Shaoping Bai 1 and Thomas Bak. Received: 4 February 2020; Accepted: 13 March 2020; Published: 17 March 2020
- [28] Groshaw, P. Hardiman I Arm Test, Hardiman I Prototype, General Electric Rep; Technical report S-70-1019; General Electric Co.: Schenectady, NY, USA, 1969.
- [29] HUMAN/ROBOT INTERACTION VIA THE TRANSFER OF POWER AND INFORMATION SIGNALS H. Kazerooni Mechanical Engineering Department, University of Minnesota 111 Church Street SE, Minneapolis, MN 55455
- [30] The hybrid assistive limb (HAL) for Care Support successfully reduced lumbar load in repetitive lifting movements Kousei Miura, Hideki Kadone, Masao Koda, Tetsuya Abe, Hiroshi Kumagai, Katsuya Nagashima, Kentaro Mataka, Kengo Fujii, Hiroshi Noguchi, Toru Funayama, Hiroaki Kawamoto, Yoshiyuki Sankai, Masashi Yamazaki.
- [31] Soft Exoskeletons: Development, Requirements, and Challenges of the Last Decade Alan Francisco Pérez Vidal 1, Jesse Yoe Rumbo Morales 1,* , Gerardo Ortiz Torres 1 , Felipe de Jesús Sorcia Vázquez 1 , Alan Cruz Rojas 1, Jorge Aurelio Brizuela Mendoza 2 and Julio César Rodríguez Cerda 1.
- [32] Evaluation of a Novel Active Exoskeleton for Tasks at or Above Head Level Bernhard M. Otten , Robert Weidner , and Andreas Argubi-Wollesen. IEEE ROBOTICS AND AUTOMATION LETTERS, VOL. 3, NO. 3, JULY 2018
- [33] Considerations for Industrial Use: A Systematic Review of the Impact of Active and Passive Upper Limb Exoskeletons on Physical Exposures Tasha McFarland & Steven Fischer. <https://doi.org/10.1080/24725838.2019.1684399>
- [34] Procedia Engineering 41 (2012) 988 – 994 1877-7058 © 2012 Published by Elsevier Ltd. doi: 10.1016/j.proeng.2012.07.273 International Symposium on Robotics and Intelligent Sensors 2012 (IRIS 2012) Active Exoskeleton Control Systems: State of the Art Khairul Anama,b*, Adel Ali Al-Jumailyb.
- [35] Manna, S.K., Dubey, V.N.: Comparative study of actuation systems for portable upper limb exoskeletons. Medical Engineering and Physics 60, pp. 1-13 (2018).

- [36] Sanjuan, J.D., Castillo, A.D., Padilla, M.A., Quintero, M.C., Gutierrez, E.E., Sampayo, I.P., Hernandez, J.R., Rahman M.H.: Cable driven exoskeleton for upper-limb rehabilitation: A design review. *Robotics and Autonomous Systems* 126 103445 (2020).
- [37] Hu, F.Q., Watson, J.M., Payne, P.A., Page, M.: A Fast Opto-Pneumatic Converter for Pneumatic Actuation. *IEE Colloquium on Robot Actuators, Digest 1991/146*, pp. 10.1-2 (1991).
- [38] Tavakoli, M., Marques, L., de Almeida A.T.: A comparison study of pneumatic muscles and electrical motors. *ResearchGate* (2009).
- [39] Feasibility study of a passive pneumatic exoskeleton for upper limbs based on a McKibben artificial muscle Stefania Magnetti Gisolo¹, Giovanni Gerardo Muscolo, Maria Paterna, Carlo De Benedictis, Carlo Ferraresi.
- [40] Review on Research Progress of Hydraulic Powered Soft Actuator Hu Shi *, Kun Tan, Boyang Zhang and Wenqiao Liu
- [41] Rahman, T., et al.: A Simple Technique to Passively Gravity Balance Articulated Mechanisms. *Journal of Mechanical Design* 117(4), pp. 655-658 (1995).
- [42] Rahman, T., Sample, W., Jayakumar, S., King, M.M., Wee, J.Y., Seliktar, R., Alexander, M., Scavina, M., Clark, A.: Passive exoskeletons for assisting limb movement. *Journal of Rehabilitation Research and Development, JRRD*, Volume 43, number 5, pp. 583-590 (2006).
- [43] Work-related musculoskeletal disorders: the epidemiologic evidence and the debate Laura Punnett, David H. Wegman University of Massachusetts Lowell, One University Avenue, Lowell, MA 01854, USA
- [44] Evaluation of a passive exoskeleton for static upper limb activities Kirsten Huysamena, Tim Boschb, Michiel de Loozeb, Konrad S. Stadlerc, Eveline Grafd, Leonard W. O'Sullivan.
- [45] A Review on Design of Upper Limb Exoskeletons Muhammad Ahsan Gull ¹, Shaoping Bai ¹ and Thomas Bak.

- [46] Mechanical Designs of Active Upper-Limb Exoskeleton Robots State-of-the-Art and Design Difficulties R. A. R. C. Gopura, Student Member, IEEE, Kazuo Kiguchi, Member, IEEE
- [47] A Kinematic Model of the Shoulder Complex Obtained from a Wearable Detection System Jianfeng Li , Chunzhao Zhang, Mingjie Dong * and Qiang Cao
- [48] Hingtgen, B.; McGuire, J.R.; Wang, M.; Harris, G.F. An upper extremity kinematic model for evaluation of hemiparetic stroke. *J. Biomech.* 2006, 39, 681–688.
- [49] Klopčar, N.; Lenarčič, J. Bilateral and unilateral shoulder girdle kinematics during humeral elevation. *Clin. Biomech.* 2006, 21, 20–26.
- [50] Soft Exoskeletons: Development, Requirements, and Challenges of the Last Decade Alan Francisco Pérez Vidal, Jesse Yoe Rumbo Morales, Gerardo Ortiz Torres, Felipe de Jesús Sorcia Vázquez, Alan Cruz Rojas, Jorge Aurelio Brizuela Mendoza and Julio César Rodríguez Cerda.
- [51] DESIGN REQUIREMENTS OF A HAND EXOSKELETON ROBOTIC DEVICE Jamshed Iqbal³, Nikos G. Tsagarakis¹, Angelo E. Fiorilla^{2,3}, Darwin G. Caldwell¹ ¹Department of Advanced Robotics, Italian Institute of Technology (IIT), Genova, Italy ²Robotics, Brain and Cognitive Sciences Department, Italian Institute of Technology (IIT), Genova, Italy ³University of Genova, Italy.
- [52] Gupta S., Singla E, Agrawal A.: Wearable Exoskeletons: Generations, Design Challenges and Task Oriented Synthesis: Advances in Theory and Practice. ResearchGate (2016).
- [53] A Review on the Development of Pneumatic Artificial Muscle Actuators: Force Model and Application Bhaben Kalita, Alexander Leonessa and Santosha K. Dwivedy.
- [54] Andrea Manuello Bertetto. Muscoli a fluido. A. Manuello Bertetto, professore ordinario di Meccanica applicata alle macchine, Dipartimento di Ingegneria meccanica, Università degli Studi di Cagliari. readerservice.it n. 258
- [55] Study on mechanical behaviors of pneumatic artificial muscle Kanchana Crishan Wickramatunge, Thananchai Leephakpreeda School of Manufacturing Systems and

- Mechanical Engineering, Sirindhorn International Institute of Technology, Thammasat University, P.O. Box 22, Thammasat-Rangsit Post Office, Pathum-Thanni 12121, Thailand.
- [56] Modeling and control of a pneumatic artificial muscle manipulator joint – Part I: Modeling of a pneumatic artificial muscle manipulator joint with accounting for creep effect Tri Vo Minh, Bram Kamers, Herman Ramon, Hendrik Van Brussel Katholieke Universiteit Leuven, Faculty of Engineering, Mechanical Engineering, Celestijnenlaan 300B, B-3001 Leuven, Belgium
- [57] Braided thin McKibben muscles for musculoskeletal robots Gihyeok Na, Hiroyuki Nabae , Koichi Suzumori Department of Mechanical Engineering, Tokyo Institute of Technology, 2-12-1 Ookayama, Meguro-ku, Tokyo 152-8552, Japan.
- [58] Theoretical Comparison of McKibben-Type Artificial Muscle and Novel Straight-Fiber-Type Artificial Muscle Hiroki Tomori and Taro Nakamura Chuo University Kasuga 1-13-27, Bunkyo-ku, Tokyo 112-8551, Japan.
- [59] Fluidic Muscle DMSP/MAS FESTO
- [60] DOI:10.1109/SISY.2009.5291145Corpus ID: 1469464 Accurate position control of PAM actuator in Lab VIEW environment J. Sárosi, J. Gyeviki, +1 author P. Toman Published 23 October 2009 Engineering, Computer Science 2009 7th International Symposium on Intelligent Systems and Informatics
- [61] The Exo4Work shoulder exoskeleton effectively reduces muscle and joint loading during simulated occupational tasks above shoulder height Arthur van der Have, Marco Rossini, Carlos Rodriguez-Guerrero, Sam Van Rossom, Ilse Jonkers.
- [62] David A. Winter-Biomechanics and Motor Control of Human Movement-Wiley (2009)
- [63] Hošovský, A., Havran, M.: Hill's muscle model based modeling of pneumatic artificial muscle. Annals of DAAAM for 2011 & Proceedings of the 22nd International DAAAM Symposium, pp. 1005-1006 (2011).
- [64] Hill, A.V.: The heat of shortening and the dynamic constants of muscle. Proceedings of the Royal Society of London Series B-Biological Sciences, vol.126 (1938).

[65] <https://meccanicabicchi.com/>